

**Homoleptic Cyclic Trinuclear d^{10} Complexes: From Self-Association via Metallophilic and
Excimeric Bonding to the Breakage Thereof via Oxidative Addition, Dative Bonding,
Quadrupolar and Heterometal Bonding Interactions**

Rossana Galassi,^{*,a} Manal A. Rawashdeh-Omary,^b H. V. Rasika Dias,^c and Mohammad A. Omary^d

^a: *University of Camerino, School of Science and Technology, Via Sant'Agostino, 1, Camerino I-62032, Italy*

^b: *Department of Chemistry and Physics, Texas Woman's University, Denton, TX 76204, USA*

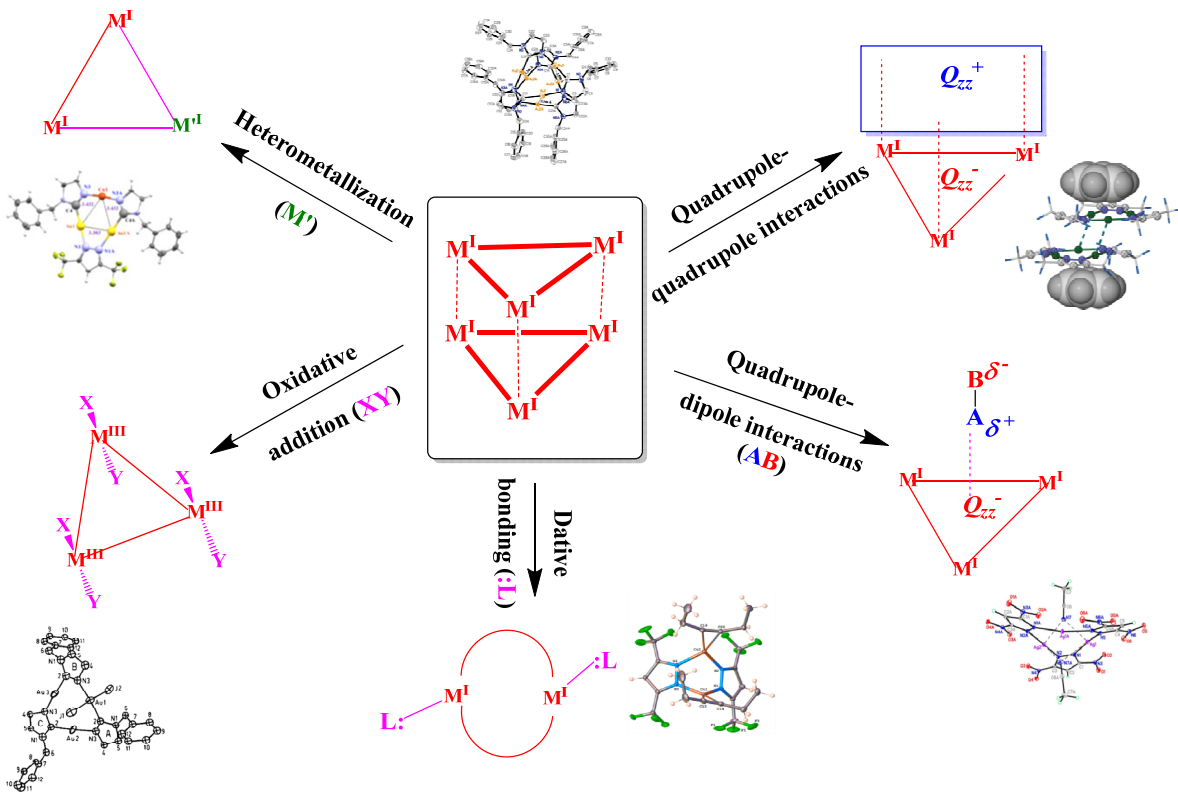
^c: *Department of Chemistry and Biochemistry, The University of Texas at Arlington, Arlington, TX 76019, USA*

^d: *Department of Chemistry, University of North Texas, Denton, TX 76203, USA*

**: Corresponding author. E-mail: rossana.galassi@unicam.it*

Abstract

Trinuclear coinage metals metallacycles, are obtained when two-coordinate metals are bonded to C, N or N, N anionic ligands of the proper symmetry to form cycles where metals alternate with bridging ligands. Cyclotrimers often exhibit semiplanar structures and mostly columnar or finite stacking in the solid state by means of metallophilic interactions. They show some peculiar properties with an impact on many different fields such as supramolecular architectures, luminescence, molecular recognition, host-guest chemistry, and acid-base chemistry. The comprehensive evaluation of the data shows that depending on the nature of the central metal and bridging ligand, there is a fine balance of the energy involved in the inter-trimer bond cleavages and the energy gained from the formation of new intermolecular electrostatic interactions, proceeding occasionally to the chemical extreme of redox process. In this review, a number of important developments are highlighted and systematically analyzed along with structural and computational data and chemical properties to rationalize and build a unifying leitmotif for this chemistry; focus is made on the authors' contributions in these areas.



Keywords: coinage metals, metallacycles, supramolecular arrangements, emissive properties, crystal structures, dipole-dipole dipole-quadrupole interactions, metallophilic bondings, theoretical calculations.

1. Introduction

Crystal structures of cyclic trinuclear complexes of the d^{10} monovalent coinage metals, described below as cyclotrimers, are fascinating for their elegant self-assembly, their supramolecular stackings based on non-classic chemical bonding, and for their remarkably-rich optoelectronic properties. Thorough understanding of the aforementioned phenomena has opened up an area of fertile and promising research for both fundamental scientific reasons and applications. The significance of this class of complexes embraces cross-sectional chemistry areas, including acid-base chemistry, metalloaromaticity, metallophilic bonding, supramolecular assemblies, M-M bonded (metal-metal bonded) excimers and exciplexes, and host/guest chemistry.¹⁻⁸ Moreover, this class of complexes are surprising for their fascinating luminescence properties and their sensitivity to multiple stimuli. For example, Balch reported that $\{\mu^{C,N}-(MeOC=NMe)Au\}_3$ ($MeOC=NMe = N$ -methyl-methoxy-carbeniate) exhibits “solvoluminescence”,³ in which a spontaneous yellow emission is observed upon contact with solvent following irradiation with long-wavelength UV light. Related cyclic Au^I trimers form deeply-colored charge-transfer stacks with nitro-substituted 9-fluorenones^{7b} while some undergo gold deposition reactions on standing in air leading to hourglass figures within the crystals.^{Error! Bookmark not defined.c} Fackler, Burini, and coworkers reported supramolecular stacks with visible luminescence that can be altered on interaction of nucleophilic imidazolate and/or carbeniate Au^I complexes with several types of electrophiles that include Tl^+ and Ag^+ cations,^{4a} a fluorinated cyclic trinuclear Hg^{II} neutral complex,^{4b} and organic Lewis acids or electron acceptors.^{4c} Aida *et al.* reported the design of trinuclear Au^I complexes that exhibit metallophilic interactions that lead to self-assembled dendritic “superhelical fibers”^{6a} and RGB phosphorescent organogels.^{6b} Gabbaï and coworkers reported the sensitization of room temperature phosphorescence of polycyclic aromatic upon interaction with $[o-C_6F_4Hg]_3$ ($o-C_6F_4 =$ ortho-tetrafluorophenylene),^{7a-c} a similar phenomenon has been reported by Omary and Fackler for the interaction of perfluoronaphthalene with an electron-rich trinuclear Au^I carbeniate complex^{8a} and by Rawashdeh-Omary *et al.* for an imidazolate congener thereof. Moreover, a variety of trinuclear Cu^I pyrazolates exhibit fascinating optical phenomena that include *luminescence thermochromism*, *luminescence solvatochromism*, *luminescence rigidochromism*, and *concentration luminochromism*.⁹

Since Vaughan synthesized the first $Au(I)$ cyclotrimer,¹⁰ a productive period of synthesis, and a reliable rationalization of the chemistry of these complexes, afforded to a new way to design these complexes and to the tuning of their properties by planning the choice of the ligands with proper steric and electronic demands, and by choosing the central coinage metals in the +1 oxidation state. Among the possible bridging ligands, pyrazoles or imidazoles were often chosen as versatile ligands for these metallacycle.¹¹ Pyrazoles are considered to be flexible ligands that can interact with the

coinage metals in several fashion^{11d}: neutral monodentate (**A**), anionic monodentate (**B**) or exo/endo (η^1 - η^1 / η^2) bidentate (**C** / **D**); see Figure 1.

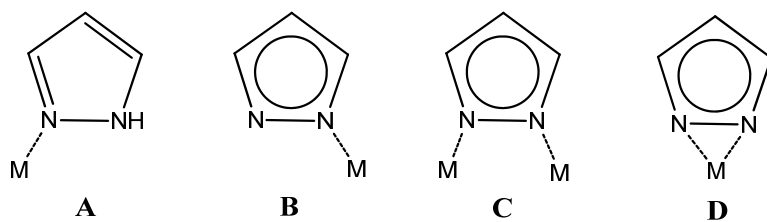


Figure 1. Common coordination modes of the pyrazole ligand and the corresponding anionic ligand.

In the bidentate mode, after deprotonation of the N-H group, pyrazoles are optimal bridging ligands to form metallacycles with different nuclearity such as: dimers, trimers, tetramers, hexamers, etc. -- depending on the substituents on the ligand and their overall steric hindrance (Figure 2). Substituents at 3- and 5- position modify the steric properties, whereas substituents at the 4- position can mainly influence the electronic properties. Polymers can also be obtained and examples with the coinage metals are reported in literature.¹²

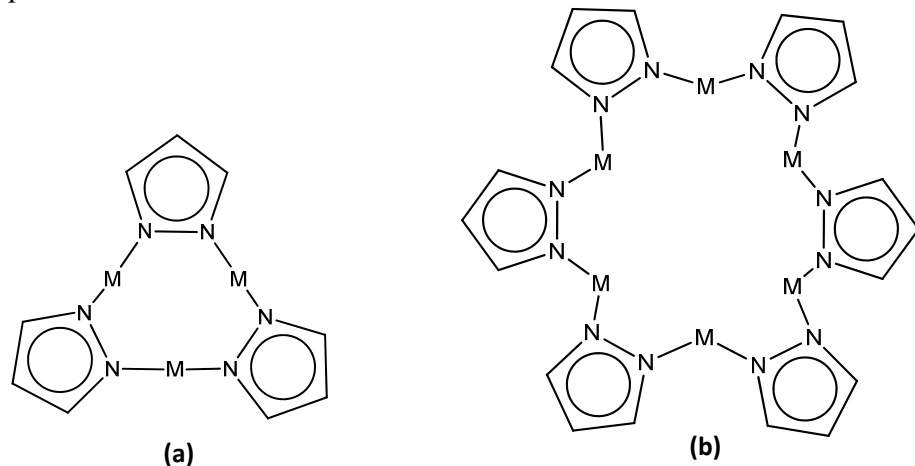


Figure 2. Two frameworks of pyrazolate metallacycles: trinuclear (a) and hexanuclear (b) metallacycles.

The imidazole is an aromatic heterocycle sterically and electronically comparable with the pyrazole. In the anionic form, imidazole can act as a monodentate ligand to give mononuclear complexes,¹³ while in the exo-bidentate coordination it can form polymers¹⁴ or metallacycles.^{8b,15}

Both type of exo-bidentate coordinations are possible as shown in Figure 3, involving N,N' or N^3,C^2 metal binding: the latter is typical in N-substituted imidazoles after deprotonation of the C^2 .

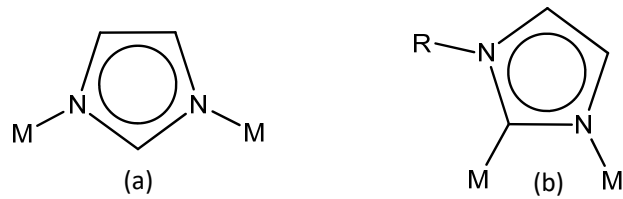


Figure 3. Possible exo-bidendate coordination modes of the imidazolates: (a) N,N' and (b) N^3,C^2

2. SELF-ASSEMBLY OF CYCLOTRIMERS SORTED BY THE COINAGE METAL CENTER

2.1. Self-Assembly of Trinuclear Copper(I) Complexes

The syntheses of copper(I) pyrazolates were first reported at the end of the 19th century¹⁶; however, the first structural characterized trinuclear copper(I) cyclic complex, such as $[\text{Cu}(\mu\text{-3,5-Ph}_2\text{Pz})]_3$ ($3,5\text{-Ph}_2\text{Pz}$ = 3,5-diphenyl-pyrazolate) has been reported one hundred years later and lastly.¹⁷ This complex was obtained as a minor product of the reaction of the 3,5-diphenyl-pyrazolate ligand $[3,5\text{-Ph}_2\text{Pz}]^-$, with CuCl and AgNO_3 , in equimolar amount, working under argon atmosphere to prevent the easy oxidation of Cu(I) and using CH_2Cl_2 as solvent. Another synthetic approach used molten substituted pyrazole with metal copper shot in the presence of limited amount of dioxygen. The reaction products depend on the substituents in the pyrazole ligand; a trimeric cyclic copper(I) compound was obtained when 3,4,5-trimethylpyrazole was used; the yield was low and the insoluble colorless complex $[\text{Cu}(\mu\text{-3,4,5-(CH}_3)_3\text{Pz})]_3$, ($3,4,5\text{-}(CH_3)_3\text{Pz}$ = 3,4,5- trimethyl-pyrazolyl-1H), was obtained in mixture with pale purple crystals of the copper(I/II) complex $\{[\text{Cu}(3\text{-CO}_2\text{-4,5-(CH}_3)_2\text{Pz})(3,4,5\text{-}(CH}_3)_3\text{Pz})]_2\text{Cu}\}$, ($3\text{-CO}_2\text{-4,5-(CH}_3)_2\text{Pz}$ = 3-carboxyl-4,5-dimethyl-pyrazolyl-1H).¹⁸ The synthesis is successful also with 3,5-dimethyl-pyrazole even though in this case the critical step is the purification; in fact, crystals of $[\text{Cu}(\mu\text{-3,5-(CH}_3)_2\text{Pz})]_3$, ($3,5\text{-}(CH_3)_2\text{Pz}$ = 3,5-dimethyl-pyrazolyl-1H, Figure 4), were manually separated from a reddish brown powder under a microscope. It appeared that the reddish powder was likely the polymer $[\text{Cu}(\text{Pz})]_n$.¹⁹ Further evidences of the importance of the substituents in the Pz ligand and of the synthesis mechanism, have been highlighted by Ardizzoia *et al.* whose obtained the $[\text{Cu}(\mu\text{-4-NO}_2\text{-3,5-(CH}_3)_2\text{Pz})]_3$, ($4\text{-NO}_2\text{-3,5-(CH}_3)_2\text{Pz}$ = 4-nitro-3,5-dimethyl-pyrazolyl-1H), in almost quantitative yield by reacting, in acetone solution, the 3,5-dimethyl-4-nitro-pyrazole with $[\text{Cu}(\text{CH}_3\text{CN})_4](\text{BF}_4)$ using triethylamine as base. A Cu(I) cyclotrimer with pyrazoles containing deactivating groups such as CF_3 , have been synthesized by

Dias.²⁰ The synthesis proceeds by reacting the pyrazole with an excess of Cu₂O in an inert atmosphere in benzene. The pyrazole is deprotonated by the oxide. The complex shows peculiar emissive properties depending upon the temperature, the solvent and the excitation wavelength.^{9a}

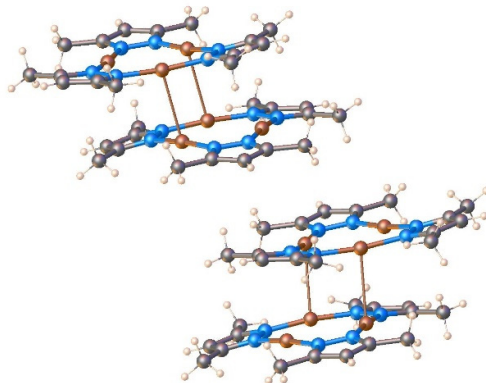


Figure 4: Stereoscopic view of $[\text{Cu}(\mu\text{-3,5-(CH}_3)_2\text{Pz})]_3$ showing the Cu···Cu interactions. **Reprinted** with permission from Ehlert, M. K.; Retting, S. J.; Storr, A.; Thompson, R. C.; Trotter, J. *Can. J. Chem.* **1990**, *68*, 1444.

Cu(I) pyrazolate cyclotrimers show essentially planar nine-membered M₃N₆ cycle with slight deviations from the planarity, except the complex $[\text{Cu}(\mu\text{-3,5-(Ph})_2\text{Pz})]_3$, (3,5-(Ph)₂Pz = 3,5-diphenylpyrazolyl-1H) showing a twisted ring with significant deviations from planarity.¹⁷ These derivatives show intra and inter-molecular Cu-Cu interactions. In fact, in the crystal lattice trimers can be paired through crystallographic inversion centers with two Cu atoms of a M₃N₆ cyclotrimer being positioned close to two Cu atoms of the second trimer unit.

Recently five trinuclear-based copper(I) pyrazolate polymers $\{\text{CuX}[\text{CuL}]_3 \cdot \text{solvent}\}_n$ (X = Cl, Br, I, SCN and solvent = MeCN) have been reported.²¹ The synthetic method used solvothermal reactions of 3,5-diethyl-4-(4-pyridyl)-pyrazole with CuX or CuX₂ (X = Cl, Br, I, and SCN) in DMF and aqueous ammonia basic solvents, even in a mixed acetonitrile-ethanol-H₂O solution. It was chosen the 3,5-diethyl-4-(4-pyridyl)-pyrazole because it combines the coordination features either the pyrazole and pyridyl ligands. The first forms cyclic trinuclear units with copper(I) centers while the latter extends trinuclear units by bridging a second metal center into a coordination polymer. Halide or pseudohalide anions can act as soft Lewis bases and interact with the coordinatively-unsaturated copper(I) centers of π -acid [Cu₃] moieties. These Lewis acid-base interactions lead to 1D double strand-chains, 2D supramolecular layers or 3D supramolecular frameworks, as shown in Figure 5.

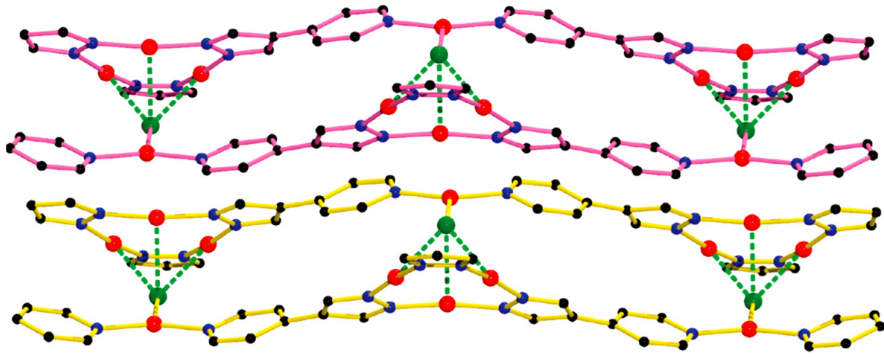
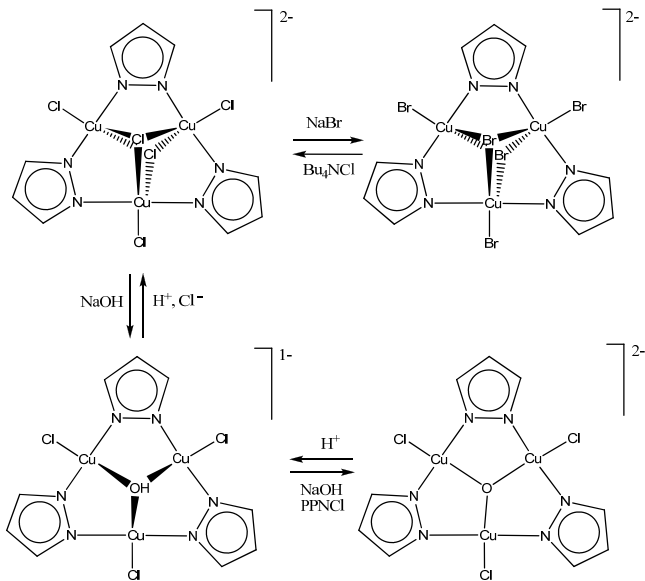


Figure 5: 1D supramolecular double-strand chain, showing the $[\text{Cu}_3] \cdots \text{Cl}$ interactions between adjacent single chains. (Reprinted with permission from Hou, L.; Shi, W.-J.; Wang, Y.-Y.; Wang, H.-H.; Cui, L.; Chen, P.-X.; Shi, Q.-Z. *Inorg. Chem.* **2011**, *50*, 261)

The face-to-face stacking of $\text{Cu}_2\text{I}_2(\text{NH}_3)_2$ in between two $[\text{Cu}_3]$ cores containing the ligand 4-(1-methyl-tetrazol-5-ylthio)-3,5-dimethyl-1H-pyrazole, was achieved by a direct self-assembly reaction of the anionic ligand and CuI in the presence of ammonia by a solvothermal method.²² The adduct is stabilized by the synergy of intermolecular $[\text{Cu}_3] \cdots \text{I}$ (π acid...base), $\text{Cu} \cdots \text{Cu}$ and $\text{N} \cdots \text{H}$ interactions, to form a Cu_8I_2 cluster for which the luminescence originates from the triplet state of Cu_8I_2 , $[\text{Cu}_3]\text{Cu}_2\text{I}_2[\text{Cu}_3]$, cluster-centered charge transfer (^3CC).

Copper(II) ions can also form trinuclear cyclic derivatives but in this case mono- or bi-capped complexes are obtained. The syntheses of these complexes having the $[\text{Cu}^{\text{II}}(\mu\text{-Pz})_3]$ framework depend on many factors. The complexes $[\text{But}_4\text{N}][\text{Cu}_3(\mu_3\text{-OH})(\mu\text{-Pz})_3\text{Cl}_3]$, $[\text{PPN}][\text{Cu}_3(\mu_3\text{-OH})(\mu\text{-Pz})_3\text{Cl}_3]$, $[\text{PPN}]_2[\text{Cu}_3(\mu_3\text{-O})(\mu\text{-Pz})_3\text{Cl}_3]$, $[\text{PPN}]_2[\text{Cu}_3(\mu_3\text{-Cl})_2(\mu\text{-Pz})_3\text{Cl}_3]$, $[\text{But}_4\text{N}]_2[\text{Cu}_3(\mu_3\text{-Cl})_2(\mu\text{-Pz})_3\text{Cl}_3]$, $[\text{But}_4\text{N}]_2[\text{Cu}_3(\mu_3\text{-Br})_2(\mu\text{-Pz})_3\text{Br}_3]$, (But₄N = tetrabutylammonium; PPN = bis(triphenylphosphoranylidene)ammonium, Pz = pyrazolyl-1H), were synthesized from equimolar mixtures of CuX_2 (X = Cl, Br) and PzH, these syntheses differ for a delicate equilibrium concerning the amounts of halide, the nature of the counterions, the pH and the solvent used.²³ Bridging and terminal chloride ions can be exchanged with bromides ions by reacting $[\text{But}_4\text{N}]_2[\text{Cu}_3(\mu_3\text{-Cl})_2(\mu\text{-Pz})_3\text{Cl}_3]$ with NaBr in dichloromethane solution, the reverse reaction occurs upon addition of Bu₄NCl to $[\text{Bu}_4\text{N}]_2[\text{Cu}_3(\mu_3\text{-Br})_2(\mu\text{-Pz})_3\text{Br}_3]$, (Scheme 1).²⁴



Scheme 1. Schematic view of the pH controlled halides metathesis equilibria

The complexes $[\text{Cu}_3(\mu_3\text{-OH})(\mu\text{-Cl})(\mu\text{-Pz})_3(\text{HPz})_2\text{Cl}]\cdot\text{solv}$ (HPz = pyrazole; $\text{solv} = \text{H}_2\text{O, THF}$) were instead synthesized by oxidation of the dimeric copper(I)-pyrazole complex $[\{\text{Cu}(\text{HPz})_2\text{Cl}\}]$ with molecular oxygen. Their reaction with pyridine yields the related $[\text{Cu}_3(\mu_3\text{-OH})(\mu\text{-Cl})(\mu\text{-Pz})_3(\text{py})_2\text{Cl}]\cdot\text{py}$ derivative.²⁵ Moreover $[\text{Cu}_3(\mu_3\text{-OH})(\mu\text{-Pz})_3(\text{MeCOO})_2(\text{HPz})]$ has been obtained by adding HPz to hydrated copper(II)acetate in ethanol (or other solvents) at room temperature without addition of hydroxide ions or other bases.²⁶

The spontaneous self-assembly of $[\text{Cu}^{\text{II}}(\mu\text{-4-R-Pz})_3]$ cycle cores occurs only when unsubstituted pyrazole or 4-substituted pyrazoles (4-R-PzH ; $\text{R} = \text{H, Cl, Br, I, Me, NO}_2$) are employed, while 3-, 3,5- and 3, 4, 5-substituted ones favor the synthesis of mononuclear or dinuclear copper(II) species.^{23b,25} The X-ray crystal structure determinations of trimer copper(II) pyrazolate complexes always show the presence of a corrugate nine-membered $[\text{Cu-N-N}]_3$ framework where the cyclotrimer can be mono- or bi-capped (Figure 6). In the mono-capped structures the Cu atoms show an approximate square-planar geometry, each metal centre is coordinated by two pyrazolato rings, a terminal L ligand (usually Cl or Br) and a $\mu_3\text{-X}$ bridging anion ($\text{X} = \text{O}^{2-}, \text{HO}^-$). In the bi-capped structures the Cu atoms have a distorted trigonal bipyramidal geometry, each metal centre is coordinated by two pyrazolate rings, a terminal L ligand (Cl or Br) and two $\mu_3\text{-X}$ bridging anions.

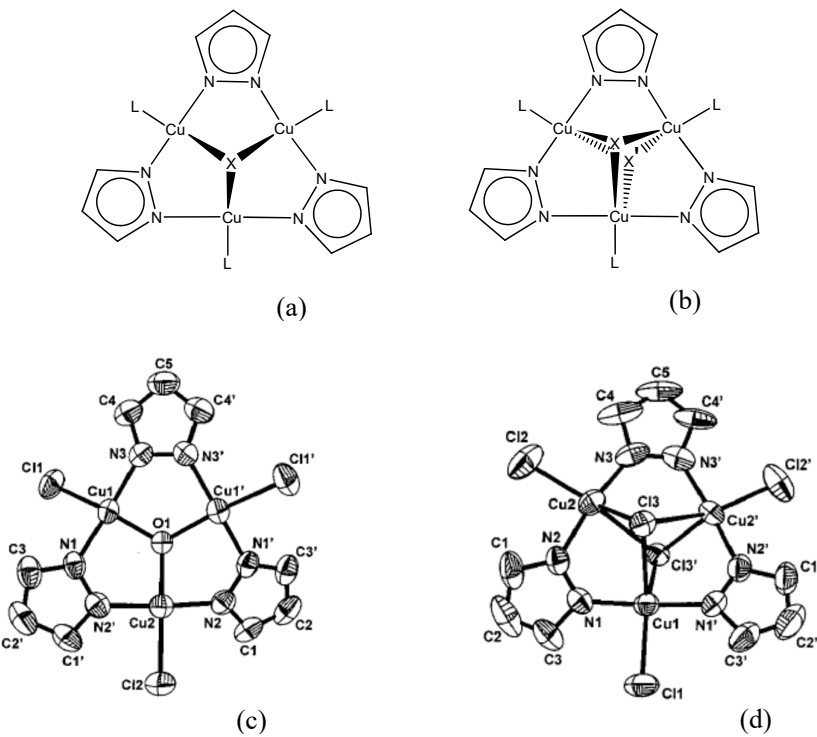


Figure 6. Top: Possible structures of the copper(II) cyclotrimer: (a) mono-capped and (b) bi-capped. Bottom: ORTEP plots of the trinuclear complexes $[\text{Cu}_3(\mu_3\text{-O})(\mu\text{-Pz})_3\text{Cl}_3]$ (c) and $[\text{Cu}_3(\mu_3\text{-Cl})_2(\mu\text{-Pz})_3\text{Cl}_3]$ (d) highlighting the two possible structures (a) and (b); (where Pz = pyrazolyl-1H). Reprinted and adapted with permission from Mezei, G.; Rivera-Carrillo, M.; Raptis, R. G. *Inorg. Chim. Acta*. 2004, 357, 3721 and Casarin, M.; Corvaja, C.; di Nicola, C.; Falcomer, D.; Franco, L.; Monari, M.; Pandolfo, L.; Pettinari, C.; Piccinelli, F.; Tagliatesta, P. *Inorg. Chem.* 2004, 43, 5865)

Dias *et al* have synthesized a series of mainly fluorinated trinuclear copper(I) derivatives^{9b} with pyrazoles having different combinations of -H, -CF₃, -Me, -Ph or -iPr groups at the 3,5-positions. The X-ray crystal structures of $\{[3\text{-(CF}_3\text{)Pz}]\text{Cu}\}_3$, $\{[3\text{-(CF}_3\text{),5-(Me)Pz}]\text{Cu}\}_3$, $\{[3\text{-(CF}_3\text{),5-(Ph)Pz}]\text{Cu}\}_3$, $\{[3,5\text{-(CF}_3\text{)}_2\text{Pz}]\text{Cu}\}_3$, and $\{[3,5\text{-(i-Pr)}_2\text{Pz}]\text{Cu}\}_3$, (where 3-(CF₃)Pz = 3-trifluoromethyl-pyrazolyl-1H, 3-(CF₃),5-(Me)Pz = 3-trifluoromethyl-5-methyl-pyrazolyl-1H, 3-(CF₃),5-(Ph)Pz = 3-trifluoromethyl-5-phenyl-pyrazolyl-1H; 3,5-(CF₃)₂Pz = 3,5-bis(trifluoromethyl)-pyrazolyl-1H), show the trinuclear nature of all the compounds with mostly planar cyclotrimers and linear coordination around the Cu(I) centers. It is interesting to note that the X-ray crystal structure of the $\{[3\text{-(CF}_3\text{)Pz}]\text{Cu}\}_3$ (Figure 7), shows an asymmetrically oriented pyrazolyl group; the substituents at the pyrazolyl group's 3- and 5-positions (H and CF₃) do not show a regular, alternating pattern, whilst the $\{[3\text{-(CF}_3\text{),5-(Ph)Pz}]\text{Cu}\}_3$ this alternation is observed.^{9b} $\{[3\text{-(CF}_3\text{)Pz}]\text{Cu}\}_3$ is the least air-

stable solid in this set of compounds. They have also reported a much more convenient way to purify $\{[3,5-(Me)_2Pz]Cu\}_3$ through vacuum sublimation (rather than manually separating the crystals).

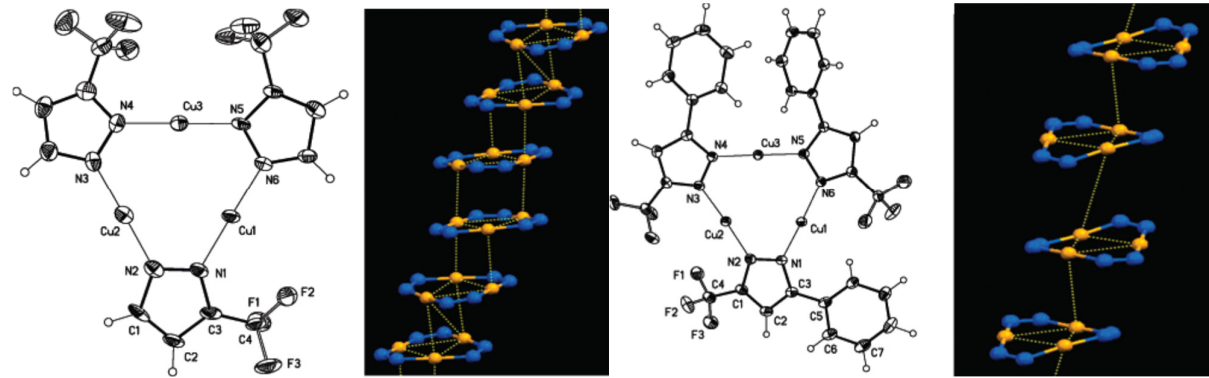


Figure 7. X-ray crystal structures of $\{[3-(CF_3)Pz]Cu\}_3$ (left) and $\{[3-(CF_3),5-(Ph)Pz]Cu\}_3$ (right) showing the labeling scheme of the molecular unit and the packing of the Cu_3N_6 cyclotrimer, (where $3-(CF_3)Pz = 3$ -trifluoromethyl-pyrazolyl-1H and $3-(CF_3),5-(Ph)Pz = 3$ -trifluoromethyl-5-phenyl-pyrazolyl-1H). Reprinted with permission from Dias, H. V. R.; Diyabalanage, H. V. K.; Eldabaja, M. G.; Elbjeirami, O.; Rawashdeh-Omary, M. A.; Omary, M. A. *J. Am. Chem. Soc.* **2005**, *127*, 7489.

In all the above mentioned compounds, both with fluorinated and non-fluorinated substituents, there are long inter-triangle contacts involving the copper atoms forming extended chains resulting in dimer of cyclotrimers (Figure 7). These $Cu \cdots Cu$ distances range from 2.94 to 3.84 Å. The intratrimer $Cu \cdots Cu$ separations within the copper triangles (“ $[Cu_3]$ ” units) range from 3.20 to 3.26 Å. These distances are much longer than the estimated sum of the van der Waals radii of two copper atoms (2.80 Å) or the Cu-Cu distance in the open-shell metallic copper (2.556 Å). Furthermore, the non-fluorinated $\{[3,5-(i-Pr)_2Pz]Cu\}_3$, where $3,5-(i-Pr)_2Pz = 3,5$ -diisopropylpyrazolyl-1H, as well as previously noted $\{[3,5-(Me)_2Pz]Cu\}_3$ form shorter inter-trimer $Cu \cdots Cu$ contacts leading to dimers of $[Cu_3]$ units, whereas the fluorinated analogues like $\{[3,5-(CF_3)_2Pz]Cu\}_3$ display significantly longer inter-trimer $Cu \cdots Cu$ separations and form columns of $[Cu_3]$ units. Similar pattern is observed with sterically similar but electronically different, $\{[3,4,5-(Me)_3Pz]Cu\}_3$ ²⁷ and $\{[3,5-(Me)_2,4-(NO_2)Pz]Cu\}_3$ ²⁸ systems. The $\{[3,4,5-(Me)_3Pz]Cu\}_3$ forms dimers of $[Cu_3]$ units, while $\{[3,5-(Me)_2,4-(NO_2)Pz]Cu\}_3$ forms chains of $[Cu_3]$ with longer inter-trimer $Cu \cdots Cu$ distances. Overall, these data seem to indicate that electron-withdrawing groups on pyrazolyl rings weaken the intercyclotrimer $Cu \cdots Cu$ contacts and favor long-range interactions in infinite chains of trimers instead of dimers of trimers. All the compounds show

bright luminescence upon exposure to UV radiation in the solid state with large Stokes Shifts, while the $\{[3,5-(CF_3)_2Pz]Cu\}_3$ shows solvachromism combined with thermochromism.

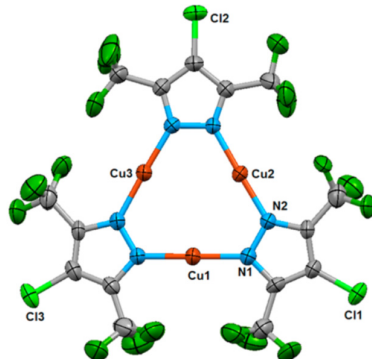


Figure 8. View down c axis of the molecular structure of complex $[\mu\text{-}(4\text{-Cl-3,5-(CF}_3)_2\text{Pz})\text{Cu}]_3$, (where 4-Cl-3,5-(CF₃)₂Pz = 4-chloro-3,5-bis(trifluoromethyl)-pyrazolyl-1H). Reprinted with permission from Hettiarachchi, C. V.; Rawashdeh-Omary, M. A.; Korir, D.; Kohistani, J.; Yousufuddin, M.; Dias, H. V. R. *Inorg. Chem.* **2013**, *52*, 13576

The presence of chloro or bromo substituents at 4-position of the 3,5-(CF₃)₂PzH does not affect the formation of semiplanar M₃N₆ cyclotrimer frameworks, but it does affect the packing in the solid state. In fact, unlike $\{[3,5-(CF_3)_2Pz]Cu\}_3$ which features zigzag chains with somewhat close intertrimer Cu···Cu contacts (closest at 3.232 Å), $\{[4\text{-Cl-3,5-(CF}_3)_2\text{Pz}]Cu\}_3$ does not have intertrimer copper atoms at a close distance (closest intertrimer Cu···Cu at 5.08 Å). However, it forms intertrimer interactions via Cu···Cl contacts.

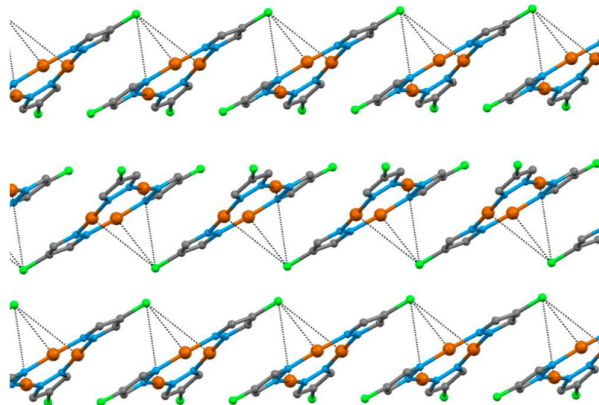


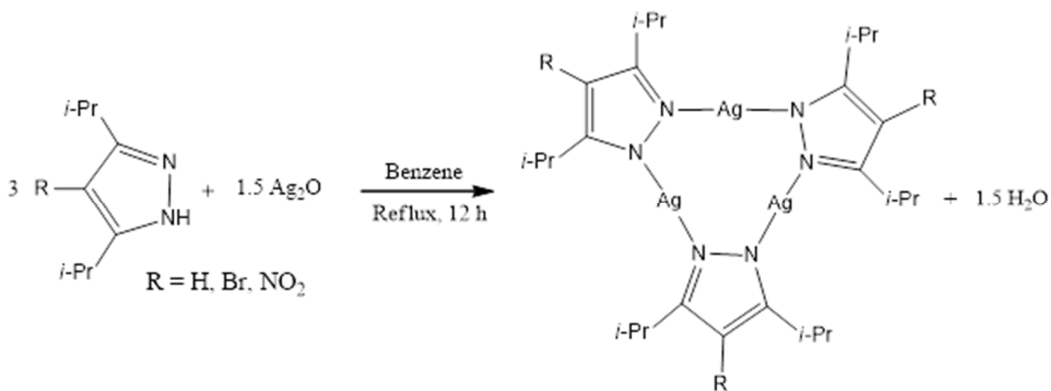
Figure 9. View showing intertrimer Cu···Cl separations leading to supra-molecular structure (CF₃ groups have been omitted for clarity in the bottom. Reprinted with permission from Hettiarachchi, C. V.; Rawashdeh-Omary, M. A.; Korir, D.; Kohistani, J.; Yousufuddin, M.; Dias, H. V. R. *Inorg. Chem.* **2013**, *52*, 13576

For example, as illustrated in Figure 9, one chlorine atom of each of the trinuclear $\{[4\text{-Cl-3,5-}(\text{CF}_3)_2\text{Pz}]\text{Cu}\}_3$ shows three such $\text{Cu}\cdots\text{Cl}$ separations at 3.60, 4.43, and 4.64 Å, so that it forms a distorted trigonal pyramid-like structure with the Cl atom at the vertex situated on one side of the ninemembered Cu_3N_6 metallacyclic or the triangular $[\text{Cu}_3]$ core. The other side of the $[\text{Cu}_3]$ core remains somewhat open, hence it is susceptible to interaction with guest molecules. These $\text{Cu}\cdots\text{Cl}$ intertrimer alignments give rise to an extended stair-step structural motif.

A large number of scientific contributions have been dedicated to the synthesis and spectroscopic characterization of copper(I) pyrazolate cyclotrimers. In contrast, only a small number of studies describes their possible applications. These compounds show properties covering a wide range of applications such as, for example, catalytic (e.g., peroxidative oxidation or dye photodegradation), magnetic (e.g., spin system frustration), MOF material for potential gas storage and separation (where MOF = Metal-Organic Framework), and solvent-mediated exchange as recently reported for $\text{Cu}_3(\mu^3\text{-OH})(\mu\text{-Pz})_3$ (where Pz = unsubstituted pyrazolate).²⁹

2.2. Self-Assembly of Trinuclear Silver(I) Complexes

The chemistry of pyrazolate and imidazolate silver cyclotrimer is less extensive respect to the copper ones and not many examples are reported in literature. The cyclotrimers are the most important and the first example, structurally characterized by power diffraction, is the complex $[\text{Ag}(\mu\text{-Pz})_3]$.^{12a} Several methods can be used to obtain trimeric, silver(I) pyrazolates. In 1988 Fackler and co-workers reported the synthesis of $[\text{Ag}(\mu\text{-3,5-(Ph)}_2\text{Pz})_3$ from CuCl and $[\text{3,5-(Ph)}_2\text{Pz}]\text{Na}$ in the presence of AgNO_3 or using $[\text{3,5-(Ph)}_2\text{Pz}]\text{Na}$ and $\text{Ag}(\text{THT})\text{NO}_3$, (THT = tetrahydrothiophene).^{17,30,31} Masciocchi *et al.* reported the synthesis of trimeric $[\text{Ag}(\mu\text{-Pz})_3]$ by removing PPh_3 from dimeric silver(I) pyrazolate, $\{(\text{PPh}_3)\text{Ag}[\text{Pz}]\}_2$ ^{12a} while the trimeric $\{\text{Ag}[\text{Pz}(\text{IN})]\}_3$ was synthesized by Ishida *et al.* by a reaction of $[\text{Pz}(\text{IN})]\text{H}$ = 3-pyrazolyl imino nitroxide], AgClO_4 , and 1,8-diazabicyclo[5.4.0]-7-undecene in acetonitrile.³²



Scheme 2. General procedure for the synthesis of the $[\text{Ag}(\mu\text{-}3,5\text{-(}i\text{-Pr}\text{)}_2,4\text{-(R)Pz})]_3$, where $\text{R} = \text{H}$, Br , NO_2 .

A very useful and convenient synthetic method to obtain silver **cyclotrimers** containing deactivated pyrazoles was developed by Dias.²⁰ This procedure is the same for the synthesis of trinuclear copper(I) complexes with fluorinated pyrazoles and the only difference consists, in the use of silver(I) oxide to deprotonate the pyrazole. Indeed, the complex $[\text{Ag}(\mu\text{-}3,5\text{-(CF}_3)_2\text{Pz})]_3$ was synthesized using a mixture of Ag_2O and 3,5-bis(trifluoromethyl)pyrazole in benzene or toluene at 50 – 60 °C for two days. The trinuclear product was isolated in very high yield. The synthetic route established for $[\text{Ag}(\mu\text{-}3,5\text{-(CF}_3)_2\text{Pz})]_3$ was then utilized for the preparation of other trimeric silver(I) complexes.³³ For example the compounds $[\text{Ag}(\mu\text{-}3,5\text{-(}i\text{-Pr}\text{)}_2\text{Pz})]_3$, $[\text{Ag}(\mu\text{-}3,5\text{-(}i\text{-Pr}\text{)}_2,4\text{-(Br)Pz})]_3$, and $[\text{Ag}(\mu\text{-}3,5\text{-(}i\text{-Pr}\text{)}_2,4\text{-(NO}_2\text{)Pz})]_3$ were synthesized according to Scheme 2. One year later Dias *et al.* reported the synthesis and the structural characterization of a new series of fluorinated silver **cyclotrimers**³⁴ such as: $[\text{Ag}(\mu\text{-}3\text{-(CF}_3)\text{Pz})]_3$, $[\text{Ag}(\mu\text{-}3\text{-(CF}_3),5\text{-(CH}_3)\text{Pz})]_3$, $[\text{Ag}(\mu\text{-}3\text{-(CF}_3),5\text{-(Ph)Pz})]_3$, $[\text{Ag}(\mu\text{-}3\text{-(CF}_3),5\text{-(}^t\text{Bu)\text{Pz}})]_3$, and $[\text{Ag}(\mu\text{-}3\text{-(C}_3\text{F}_7),5\text{-(}^t\text{Bu)\text{Pz}})]_3$. These **cyclotrimers** were obtained by treating the corresponding pyrazole with a slight excess of silver oxide. This method appears to be fairly general because it is possible to use a wide spectrum of pyrazoles such as the electron-rich $[\text{3,5-(}i\text{-Pr}\text{)}_2\text{Pz}]_3$, weakly coordinating $[\text{3,5-(CF}_3)_2\text{Pz}]_3$, and sterically demanding $[\text{3-(C}_3\text{F}_7),5\text{-(}^t\text{Bu)\text{Pz}}]_3$, (where $3\text{-(C}_3\text{F}_7),5\text{-(}^t\text{Bu)\text{Pz}} = 3\text{-heptafluoropropyl-5-tertbutyl-pyrazolyl-1H}$). Moreover, a very similar method was followed by Chi *et al.* to obtain $[\text{Ag}(\mu\text{-}3\text{-(}^t\text{Bu}),5\text{-(CF}_3)\text{Pz})]_3$ and $[\text{Ag}(\mu\text{-}3,5\text{-(}^t\text{Bu})_2\text{Pz})]_3$, (where $3\text{-(}^t\text{Bu),5\text{-(CF}_3)\text{Pz} = 3\text{-tertbutyl-5-trifluoromethyl-pyrazolyl-1H}$).³⁵

The X-ray data of the all silver **cyclotrimers** reported above show a trinuclear cyclic structure with essentially planar nine-membered Ag_3N_6 cycles and very often these derivatives show intra and inter-molecular Ag–Ag interactions. An example can be the complex $[\text{Ag}(\mu\text{-}3\text{-(CF}_3),5\text{-(CH}_3)\text{Pz})]_3$. In its crystal packing neighboring pairs of these trinuclear units are linked by two equal and relatively short $\text{Ag}\cdots\text{Ag}$ contacts (3.3553 Å) across a crystallographic inversion center. The dimer of trimers

interacts further with their neighbors via additional Ag···Ag links (3.4263 Å), forming extended stepladder-shaped columns (Figure 10).

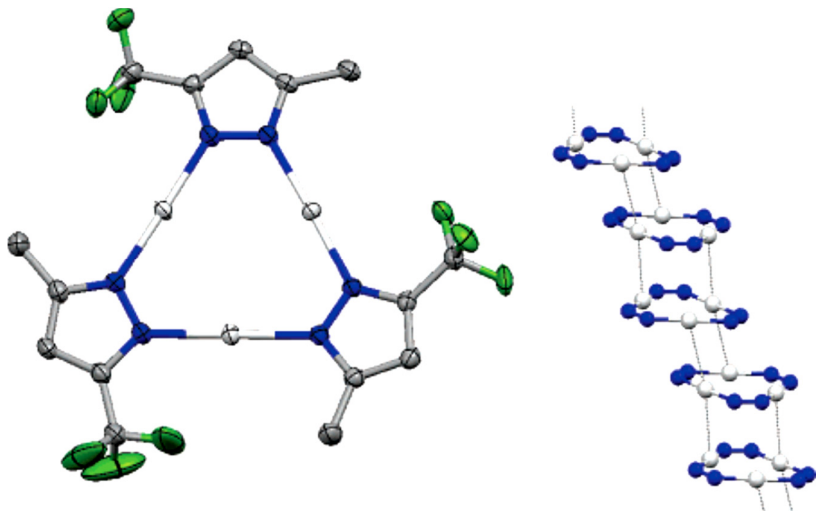


Figure 10. Molecular structure of $[\text{Ag}(\mu\text{-3-(CF}_3\text{),5-(CH}_3\text{)Pz})]_3$ (hydrogen atoms have been omitted for clarity) and the extended chains of $[\text{Ag}(\mu\text{-3-(CF}_3\text{),5-(CH}_3\text{)Pz})]_3$ formed via Ag···Ag contacts (all except nitrogen and silver atoms have been omitted for clarity, and 3-(CF₃),5-(CH₃)Pz = 3-trifluoromethyl-5-methyl-pyrazolyl-1H). Reprinted with permission from Dias, H. V. R.; Gamage, C. S. P.; Keltner, J.; Diyabalanage, H. V. K.; Omari, I.; Eyobo, Y.; Dias, N. R.; Roehr, N.; McKinney, L.; Poth, T. *Inorg. Chem.* **2007**, *46*, 2979.

Unlike the copper **cyclotrimers**, it is interesting to note that the presence of two bulky substituents on the pyrazolyl ring, such as in the complex $[\text{Ag}(\text{3-(C}_3\text{F}_7\text{),5-(}^{\text{'}}\text{Bu})\text{Pz})]_3$ gives the typical trinuclear unit (Figure 11). These trinuclear units pack in a staggered fashion (i. e., with a lateral slippage), forming zigzag chains that do not feature any intertrimer Ag···Ag contacts (the closest separation is at 5.376 Å). The nine-membered Ag₃N₆ **cyclotrimer** in $[\text{Ag}(\mu\text{-3-(C}_3\text{F}_7\text{),5-(}^{\text{'}}\text{Bu})\text{Pz})]_3$ shows also a significant deviation from planarity and it appears that this ring twisting is caused primarily by the inter**cyclotrimer** steric interactions of the two large substituents.

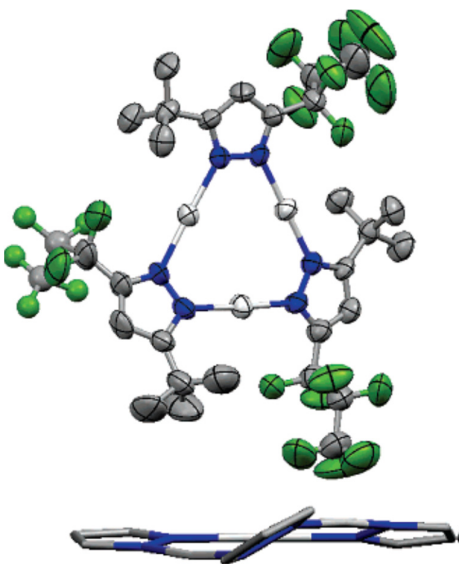
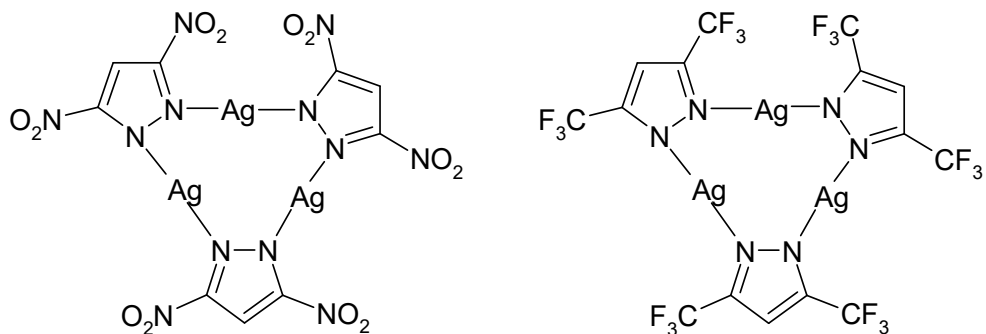


Figure 11. Molecular structure of $[\text{Ag}(\mu\text{-3-(C}_3\text{F}_7\text{)}, 5\text{-(}^{\text{'}}\text{Bu})\text{Pz})]_3$ (hydrogen atoms have been omitted for clarity) and a side view showing the twisted Ag_3N_6 core (pyrazolyl ring substituents have been omitted for clarity and $3\text{-(CF}_3\text{),5-(CH}_3\text{)Pz} = 3\text{-trifluoromethyl-5-methyl-pyrazolyl-1H}$). Reprinted with permission from Dias, H. V. R.; Gamage, C. S. P.; Keltner, J.; Diyabalanage, H. V. K.; Omari, I.; Eyobo, Y.; Dias, N. R.; Roehr, N.; McKinney, L.; Poth, T. *Inorg. Chem.* **2007**, *46*, 2979.



Scheme 3. Molecular structure of $[\text{Ag}(\mu\text{-3,5-(NO}_2\text{)}_2\text{Pz})]_3$ and $[\text{Ag}(\mu\text{-3,5-(CF}_3\text{)}_2\text{Pz})]_3$

Another silver(I) cyclotrimer has been obtained by using 3,5-dinitro-pyrazole as the bridging ligand. By reacting its sodium salt with AgBF_4 the **cyclotrimer** was obtained in good yield. The molecular structure is showed in Scheme 3, and is compared to that of the CF_3 analog.³⁶ The design of the synthesis of $[\text{Ag}(\mu\text{-3,5-(NO}_2\text{)}_2\text{Pz})]_3$, (where $3,5\text{-(NO}_2\text{)}_2\text{Pz} = 3,5\text{-dinitro-pyrazolyl-1H}$), was performed to obtain a **cyclotrimer** possessing very similar electronic and steric properties to $[\text{Ag}(\mu\text{-3-(C}_3\text{F}_7\text{)}, 5\text{-(}^{\text{'}}\text{Bu})\text{Pz})]_3$.

$\text{3,5-(CF}_3\text{)}_2\text{Pz}]\text{)}_3$, which chemistry and emissive properties were already known in literature.^{20,37} They have both strong electron withdrawing substituents on the pyrazole and in the same position with the NO_2 more electron withdrawing than CF_3 . Actually their behavior on the regards of nucleophilic molecules was mostly different as well as their emissive properties, as it is thorough described in a following section.

The $\{[4\text{-Cl-3,5-(CF}_3\text{)}_2\text{Pz}]\text{Ag}\}_3$ and $\{[4\text{-Br-3,5-(CF}_3\text{)}_2\text{Pz}]\text{Ag}\}_3$ are also known.³⁸ They do not form inter-trimer $\text{Ag}\cdots\text{Ag}$ contacts, but show inter-trimer $\text{Ag}\cdots\text{halogen}$ contacts. For example in $\{[4\text{-Cl-3,5-(CF}_3\text{)}_2\text{Pz}]\text{Ag}\}_3$, each $[\text{Ag}_3]$ core lies relatively close to two chlorine atoms of the neighboring trimers, so that it forms a distorted Cl_2Ag_3 trigonal bipyramidal like structure with the Cl atom at the vertex situated on both sides of the nine-membered Ag_3N_6 cyclotrimer. Overall, this arrangement leads to a 3D-network structure as illustrated in Figure 12 rather than chains. In addition, there are a number of intertrimer $\text{C}\cdots\text{F}$, $\text{N}\cdots\text{F}$, and $\text{F}\cdots\text{F}$ contacts. The 4-Br substituted analogue, $\{[4\text{-Br-3,5-(CF}_3\text{)}_2\text{Pz}]\text{Ag}\}_3$, also forms an extended structure similar to that observed for $\{[4\text{-Cl-3,5-(CF}_3\text{)}_2\text{Pz}]\text{Ag}\}_3$. It also has a Ag_3 core sheltered from both top and bottom by a heavier halide.

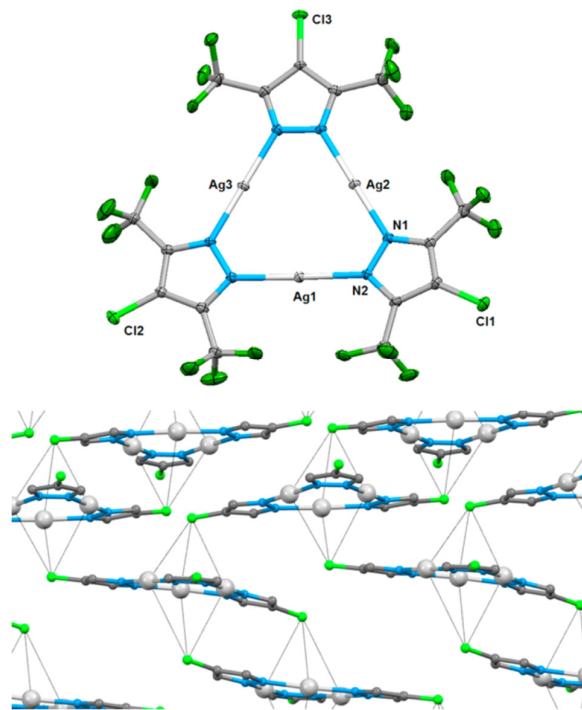
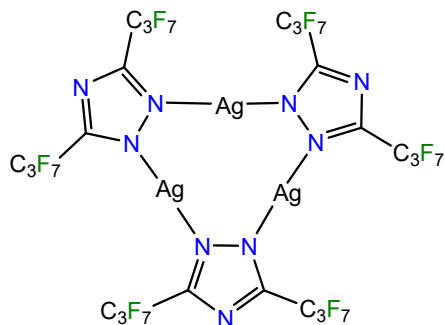


Figure 12. Molecular structure of $\{[4\text{-Cl-3,5-(CF}_3\text{)}_2\text{Pz}]\text{Ag}\}_3$ and a view showing intercyclotrimer $\text{Ag}\cdots\text{Cl}$ contacts leading to aggregates (CF_3 groups have been omitted for clarity in the bottom figure). Reprinted with permission from Hettiarachchi, C. V.; Rawashdeh-Omary, M. A.; Korir, D.; Kohistani, J.; Yousufuddin, M.; Dias, H. V. R. *Inorg. Chem.* 2013, 52, 13576.

In addition to pyrazolate and imidazolate, triazolate and carbeniate ligands also provide cyclotrimers of Ag(I). As concern the silver carbeniate cyclotrimer, the first example was prepared according to the reaction of o-tolyl-isocyanide-silver chloride and o-tolylisocyanide in the presence of KOH; the determination of the cyclotrimer nature was ascertained only by the molecular weight obtained by osmometric methods in benzene solutions.³⁹ The triazole Ag(I) cyclotrimer has been obtained in good yield from 3,5-bis(heptafluoropropyl)-1,2,4-triazole by reacting with Ag₂O.³⁷ Its reactivity on the regards of PPh₃ in the 1 : 1 mole ratio leads to the cleavage of the cyclotrimer and the formation of a dinuclear specie such as $\{[3,5-(C_3F_7)_2Tz]Ag(PPh_3)\}_2$.



Scheme 4. Molecular structure for the silver cyclotrimer with the 3,5-(heptafluoropropyl)-1,2,4-triazole.

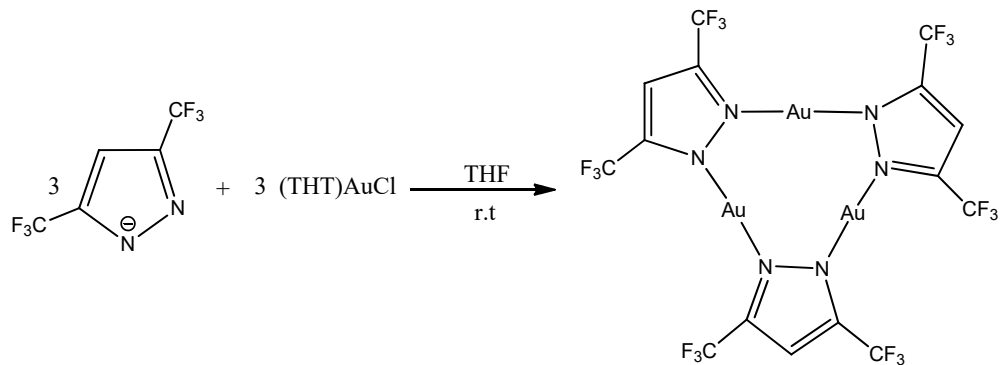
The triazole ligand is more nucleophilic than pyrazole and it contains an additional potential binding site for the metal, however its presence does not seem to affect the synthesis path. The acid-base chemistry of $\{[3,5-(C_3F_7)_2Tz]Ag\}_3$ shows new aspects when compared to the analog $\{[3,5-(CF_3)_2Pz]Ag\}_3$, as the flexible and electrophilic -C₃F₇ arms in the rigid core of the cyclotrimer behave as additional wrapping sites to interact with nucleophilic guests.^{37c}

2.3. Self-Assembly of Trinuclear Gold(I) Complexes

Pyrazolate gold(I) cyclotrimers are well known and they have the general formula [Au(μ-Pz)]₃ (Pz = pyrazolate or variously substituted pyrazolates). In these compounds the bidentate anion ligands bridging the gold atoms are obtained by deprotonation of the corresponding pyrazole ring with a base such as KOH, NaH or Et₃N. An example of a pyrazolate gold trimer synthesis, [Au(μ-3,5-(CF₃)₂Pz)]₃, is presented in Scheme 5.

The molecular structure of [Au(μ-3,5-(CF₃)₂Pz)]₃ was reported by Bonati *et al.* and it was the first gold(I) cyclotrimer with a N-Au-N environment, structurally characterized.^{40,41} The nine-membered ring is rather irregular and non-planar, with the Au-N average distance of 1.93(1) Å. The

M–N bond length values agree with the trend expected; the long intermolecular Au···Au distance of 3.998(2) Å rules out any interaction between the trinuclear units due to the bulky substituents on the pyrazolate rings.



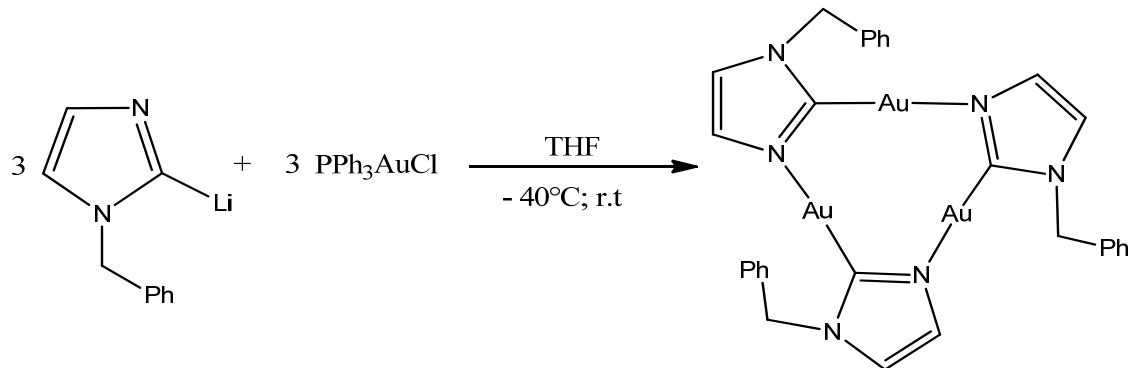
Scheme 5. Description of the synthesis of gold(I) cyclotrimer with the 3,5-bis(trifluoromethyl)-pyrazolyl-1H.

The substitution of the CF_3 groups in 3,5-positions with Ph groups has been reported for $[\text{Au}(\mu\text{-3,5-(Ph)}_2\text{Pz})]_3$.³¹ In this case, this substitution does not introduce big deviation and the nine-membered ring is regular and planar with long Au···Au distances $> 7.567\text{\AA}$ that exclude any intermolecular interaction. The substituents play a role in the self-assembly, and, surprisingly, also bulky groups can lead to stacking structures; when very long chain substituents are introduced in the 3,5 positions of the pyrazolate ring, columnar mesophases can be obtained.^{41,42} X-ray powder diffraction measurements have demonstrated that the supramolecular columnar arrangement is present in the crystalline solids as well as in the mesomorphic phase. The X-ray crystal structure of complex $[\text{Au}(\mu\text{-3,5-(4-MeOPh)}_2\text{Pz})]_3$, where 3,5-(4-MeOPh)₂Pz = 3,5-di[(4-methoxy)phenyl]-pyrazolyl-1H, which has an anisole unit on the pyrazolates, yields a unit cell that contains two independent trinuclear units.³⁹

The classic synthesis paths failed for the complexes $[\text{Au}(\mu\text{-Pz})]_3$, and $[\text{Au}(\mu\text{-4-(Me)Pz})]_3$.⁵ Only long time crystallization of $[\text{Au}(\mu\text{-Pz})]_3$ yielded well-shaped prismatic single crystals suitable for the X-ray diffraction. The molecular structure of $[\text{Au}(\mu\text{-Pz})]_3$ consists of the usual nine-membered ring with Au–N distances and N–Au–N angles in the range of 1.992(6)–2.014(6) Å and 176.9(3)–178.9(3), respectively. Intramolecular aurophilic gold-gold interactions are present with Au···Au distances 3.372(1)–3.401(1) Å.

A family of trinuclear gold(I) complexes, having a C–Au–N environment, was described in which the bridging ligand between gold atoms is an alkyl-2-imidazolate anion (alkyl group = CH_3 or CH_2Ph).^{15b} A typical reaction is carried out at -40°C in THF solution using Vaughan's method¹⁰

(Scheme 6), but in this case the crude brown solid was extracted overnight at room temperature with hexane.



Scheme 6. Description of the synthesis of the **gold(I) cyclotrimer** with 1-benzylimidazole

By following the reaction Scheme 6, some imidazolate based cyclotrimers can be obtained with high yield $[\text{Au}(\mu\text{-N}^3, \text{C}^2\text{-bzim})]_3$ and $[\text{Au}(\mu\text{-N}^3, \text{C}^2\text{-meim})]_3$ (bzim = 1-benzyl-2-imidazolate and meim = 1-methyl-2-imidazolate). Recently the crystal structure of $[\text{Au}(\mu\text{-N}^3, \text{C}^2\text{-bzim})]_3$ has been reported.^{8b} With this ligand dimer of trimer units by a semi-prismatic conformation with one long (3.558 Å) and two short (3.346 Å) intercyclotrimeric intergold distances were obtained (Figure 13).

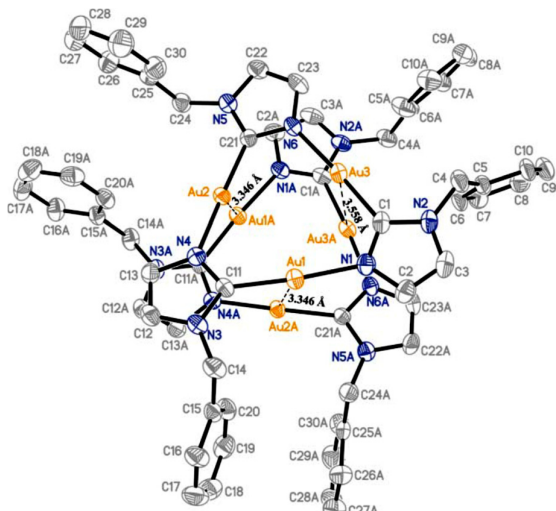


Figure 13. Crystal structure of $[\text{Au}(\mu\text{-N}^3, \text{C}^2\text{-bzim})]_3$ showing a dimer-of-trimer repeat unit.

Among the C-Au-N trinuclear derivatives, **carbeniate gold(I) cyclotrimers** have shown unprecedented properties for this class of metallacycles. The first example of carbeniate derivative was made by Bonati et al.⁴³ and it corresponds to the formula $[\mu\text{-C}_2\text{N}(\text{Me-N=C-OC}_6\text{H}_{11})\text{Au}]_3$, where $(\text{Me-N=C-OC}_6\text{H}_{11} = \text{N-methyl-O-cyclohexyl-carbeniate})$. A series of carbeniate **cyclotrimers** can be obtained by mixing the relative isonitriles $\text{R-N}\equiv\text{C}$ with Ph_3PAuCl , THTAuCl (THT = tetrahydrothiophene) or

Me₂SAuCl in a KOH solution of R'-OH to obtain the relative $[\mu\text{-C,N(R-N=C-OR')}_3\text{Au}]_3$. These trimers show features such as solvchromism,^{3a} π basic properties^{4a} or, as recently published, acting as molecular nanowire.⁴⁴

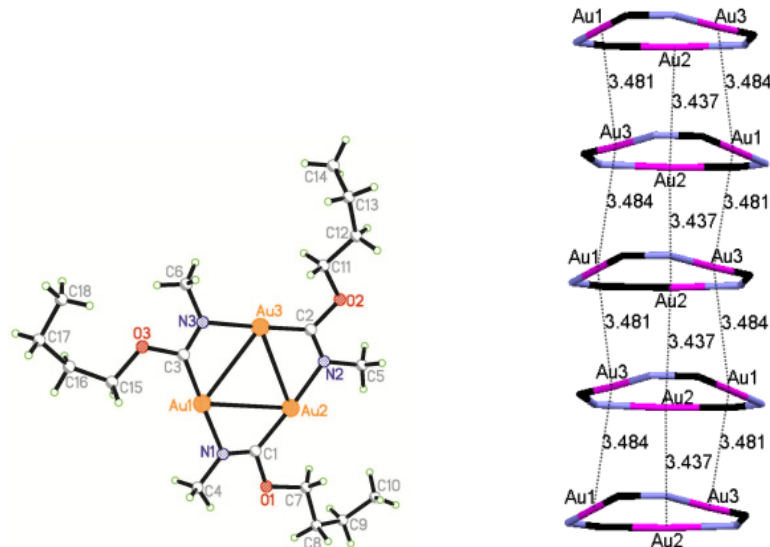


Figure 14. Crystal structure of $[\text{Au}_3(\text{Me-N=C-O}^n\text{Bu})_3]_3$ (left). Molecule stacking orientation. (Pink = Au, blue = N, black = C.) (right); where $\text{Me-N=C-O}^n\text{Bu} = \text{N-methyl-O-(n-butyl)-carbeniate}$. Reprinted with permission from McDougald, R. N.; Chilukuri, B.; Jia, H.; Perez, M. R.; Rabaâ, H.; Wang, X.; Nesterov, V. N.; Cundari, T. R.; Gnade, B. E.; Omary, M. A. *Inorg. Chem.* **2014**, *53*, 7485.

By reacting the 3,5-isopropyl-1,2,4-triazolate ligand with gold(I) precursors, a new cyclotrimer was obtained showing in the crystal structure dimer of cyclotrimer units. This result was already observed for other cyclotrimers already mentioned, but in this case the conformation of the hexanuclear unit exhibits reversible interconversion between C₂ and D₃ effective symmetries upon change of temperature in the solid crystal state or the concentration in solution.⁴⁵

The change of temperature causes a thermal contraction at R.T. vs 95K with a change of the crystal density from 2.209 vs 2.342 g/cm³ and the cell volume 6300.15 vs 5943.22 Å³. This rearrangement affects in special way the intercyclotrimer Au-Au distances, showing a distortion of the stacking going from 3.46, 3.42, and 3.42 Å to 3.19, 3.55 and 3.55 Å going from R. T. to 95K. This compound exhibits phosphorescence excimeric emissions which depends on the temperature, a high energy emission with a strong ligand character in the UV region, one centered at 650 nm (LE1) and the other 750 nm (LE2) when the temperature is < 180K while at T > 180K only the emission at 750 dominates. These results perfectly agree the thermal conformational change of the crystal symmetries as by increasing the temperature the number of bands is reduced by the increase of the symmetry from C₂ to D₃.

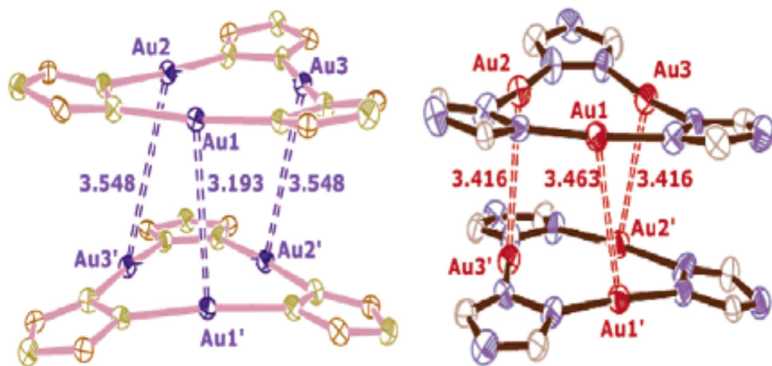


Figure 15. Dimer of cyclotrimer prismatic units of $[\text{Au}(3,5\text{-}(\text{iPr})_2\text{-}1,2,4\text{-tz})]_3$ at 95K (left) and room temperature (right) via three intermolecular Au(I)-Au(I) aurophilic bondings; 3,5-(iPr)₂-1,2,4-tz = 3,5-diisopropyl-1,2,4-triazolyl-1H. Reprinted with permission from Yang, C.; Messerschmidt, M.; Coppens, P.; Omary, M. A. *Inorg. Chem.* **2006**, *45*, 6592.

3. BREAKAGE OF CYCLOTRIMER SELF-ASSEMBLY BY OXIDATIVE ADDITION

Mixed-valence Au(I)/Au(III) trinuclear complexes represent the main oxidative addition products; these products do not self-assemble via intercyclotrimer aurophilic interactions due to the axial addition modes of the two ligands from the AB oxidative addition reagent. Very little work has been done on the oxidative addition of Ag(I) and Cu(I) complexes so this section is largely limited to Au(I) complexes.

Trimeric pyrazolate and imidazolate gold(I) complexes can undergo oxidative-addition reactions of halogens at the metal centers giving mixed-valence $\text{Au}_2^{\text{I}}/\text{Au}^{\text{III}}$ cyclotrimers.⁴⁶ There is evidence that electronic more than steric factors may influence the reactivity of the gold atoms in these compounds. In fact, except for complex $[\text{Au}(\mu\text{-C}(\text{OMe})=\text{N}(\text{Me})]_3$ (with a carbeniate ligand such as $\text{C}(\text{OMe})=\text{NMe}$ = N-methyl-methoxy-carbeniate), only one metal center appears to be oxidized to give mixed-valence $\text{Au}_2^{\text{I}}/\text{Au}^{\text{III}}$ cyclotrimers. Surprisingly, *aqua regia* also fails to give complexes beyond the $\text{Au}_2^{\text{I}}/\text{Au}^{\text{III}}$ oxidation state for the pyrazolates. Thus an unusual stability of the $d^{10}d^{10}d^8$ configuration for the trinuclear gold complexes is observed. The electronic communication between the gold atoms may be the origin of this effect. The oxidation of the first gold atom may improve the π -acceptor ability of the two ligands coordinated to it so that they decrease sufficient electron density from the remaining two Au^{I} atoms and prevent their oxidation. However, this hypothesis is not supported by crystallographic data. No changes in the gold-ligand bond lengths are observed. When complex $[\text{Au}(\mu\text{-}3,5\text{-}(\text{Ph})_2\text{Pz})]_3$ is reacted with aqua regia halogenation at the 4-position of the

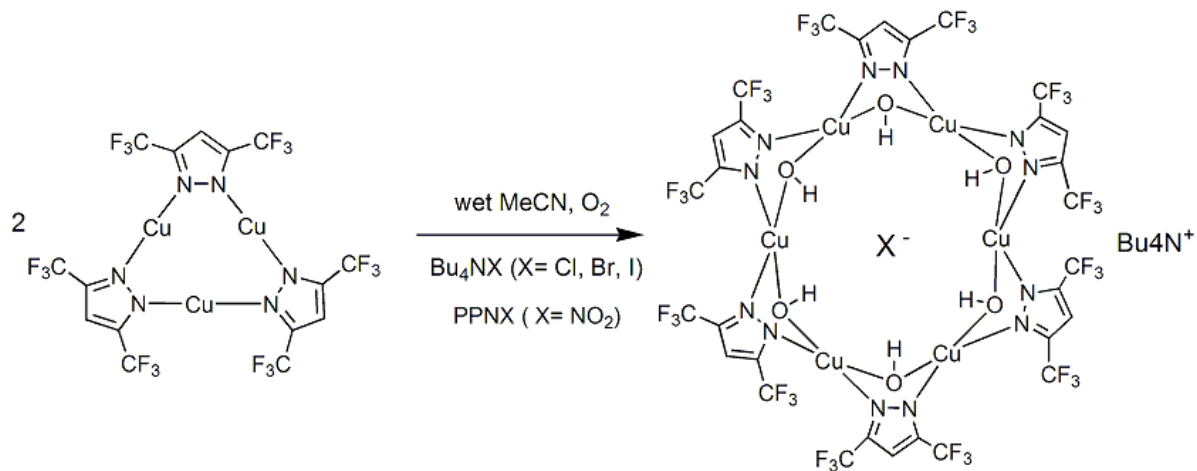
pyrazolate rings occurs causing the formation of $[\text{Au}(\mu\text{-3,5-(Ph)}_2\text{4-(Cl)Pz})]_3\text{Cl}_2$. The crystal structure of this complex shows that there is no statistically significant difference between the $\text{Au}^{\text{I}}\text{-N}$ and the $\text{Au}^{\text{III}}\text{-N}$ bond lengths, which range from 1.98(3) to 2.05(2) Å, just as it had been seen in the structure of $[\text{Au}(\mu\text{-3,5-(Ph)}_2\text{Pz})]_3\text{Cl}_2$.^{46c}

Complex $[\text{Au}(\mu\text{-C(OMe)}=\text{N(Me)})]_3$ seems to be unique in the family of the gold(I) **cyclotrimers**, in fact, it is the only one that gives the stepwise addition of halogens, resulting in the formation of either mixed-valent or completely oxidized gold **cyclotrimer**. The X-ray structures of these derivatives were reported,^{46g} many years later after their synthesis.^{46a}

Oxidative-addition with halogens was also investigated for complex $[\text{Au}(\mu\text{-N}^3,\text{C}^2\text{-bzim})]_3$. This substrate behaves similarly to most of the gold(I) **cyclotrimers** since it adds iodine at only one gold center to yield $[\text{Au}(\mu\text{-N}^3,\text{C}^2\text{-bzim})]_3\text{I}_2$.⁴⁷ It consists of discrete trinuclear complexes with the gold atoms bridged by three 1-benzylimidazolate groups. The coordination about $\text{Au}(2)$ and $\text{Au}(3)$ is nearly linear, while $\text{Au}(1)$ has nearly a square planar arrangement. The Au-C , Au-N , and Au-I bond lengths are similar to those found in the analogous carbeniate derivatives.

A different behavior of complex $[\text{Au}(\mu\text{-N}^3,\text{C}^2\text{-bzim})]_3$ was observed when it was reacted with other reagents capable of oxidative-addition such as alkyl or acyl halides. In these cases the products were characterized by X-ray crystal structure^{46d,f} or by ^{197}Au Mössbauer investigation.⁴⁷ Moreover, an oxidation was observed when complex $[\text{Au}(\mu\text{-N}^3,\text{C}^2\text{-bzim})]_3$ reacted with Me_3SiI ($\text{Au}^{\text{I}}/\text{Au}^{\text{III}}$) or SOCl_2 (Au^{III}_3).^{46d,47}

The oxidation of Cu(I) metal centres in the $[\text{Cu}(\mu\text{-3,5-CF}_3)_2\text{Pz}]_3$ by the oxygen of air led to an original behavior. When this latter is left in a wet and aerated acetonitrile solution in presence of an halide source such as Ph_3PAuCl or $[\text{Bu}_4\text{N}][\text{Cl}]$, $[\text{Bu}_4\text{N}][\text{Br}]$, $[\text{Bu}_4\text{N}][\text{I}]$, or $[\text{PPN}][\text{NO}_2]$ the corresponding halide centered hexanuclear copper(II) metallacycle such as $[\text{trans-Cu}_6(\mu\text{-OH})_6(\mu\text{-3,5-(CF}_3)_2\text{Pz})_6\supset\text{X}]$ ($\text{X} = \text{anion}$) was obtained.⁴⁸ Further investigations showed that the anions does not have any role in templating the formation of the hexanuclear framework, while by changing the substituents of the pyrazole, using dry condition or the cyclic polymerization affording to the hexanuclear cycle was not observed.



Scheme 7. Description of the synthesis of the hexanuclear copper(II) pyrazolate metallacycle

The X-ray diffraction structural determinations for the Cu(II) metallacycles showed a core containing a hexanuclear copper(II) ring bridged by six hydroxyl groups and six pyrazolate ligands. In Figure 16 the crystal structure of the metallacycles with the bromide or iodide anions in the centre of the cavity. The average Cu-X bond distance is 3.069 Å in [trans-Cu₆(μ-OH)₆(μ-3,5-(CF₃)₂Pz)₆⊜X] where X = Cl and the counterion is (Ph₃P)₂Au⁺, 3.0717 Å where X = Cl and the counterion is Bu₄N, 3.074 Å where X = Br and the counterion is Bu₄N, and 3.096 Å where X = I and the counterion is Bu₄N. These bond distances are significantly longer than the covalent ones of 2.38, 2.43, and 2.77 Å, reflecting the primarily ionic interactions between the halide and copper ions.

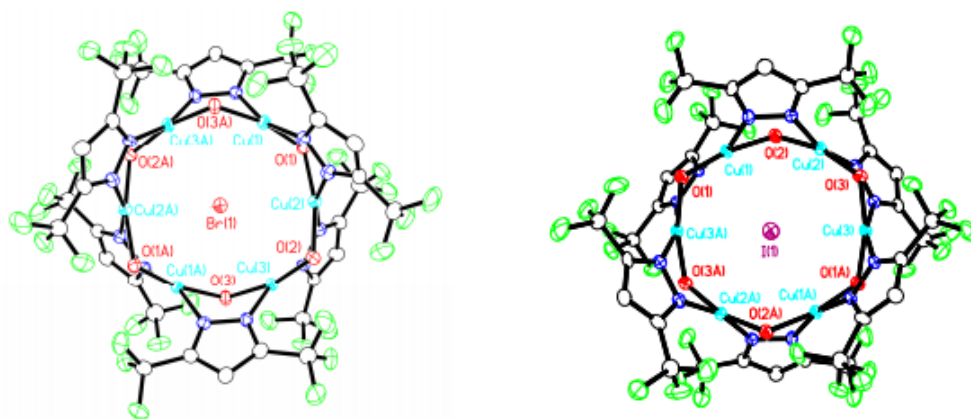


Figure 16. Front view of the bromide and iodide centered copper(II) metallacycles. Reprinted with permission from Mohamed, A. A.; Burini, A.; Galassi, R.; Paglialunga, D.; Galán-Mascarós, J.-R.; Dunbar, K. R.; Fackler, J. P., Jr. *Inorg. Chem.* **2007**, *46*, 2348.

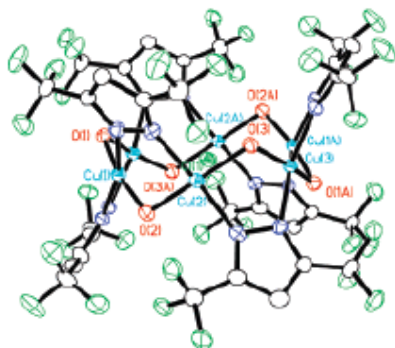
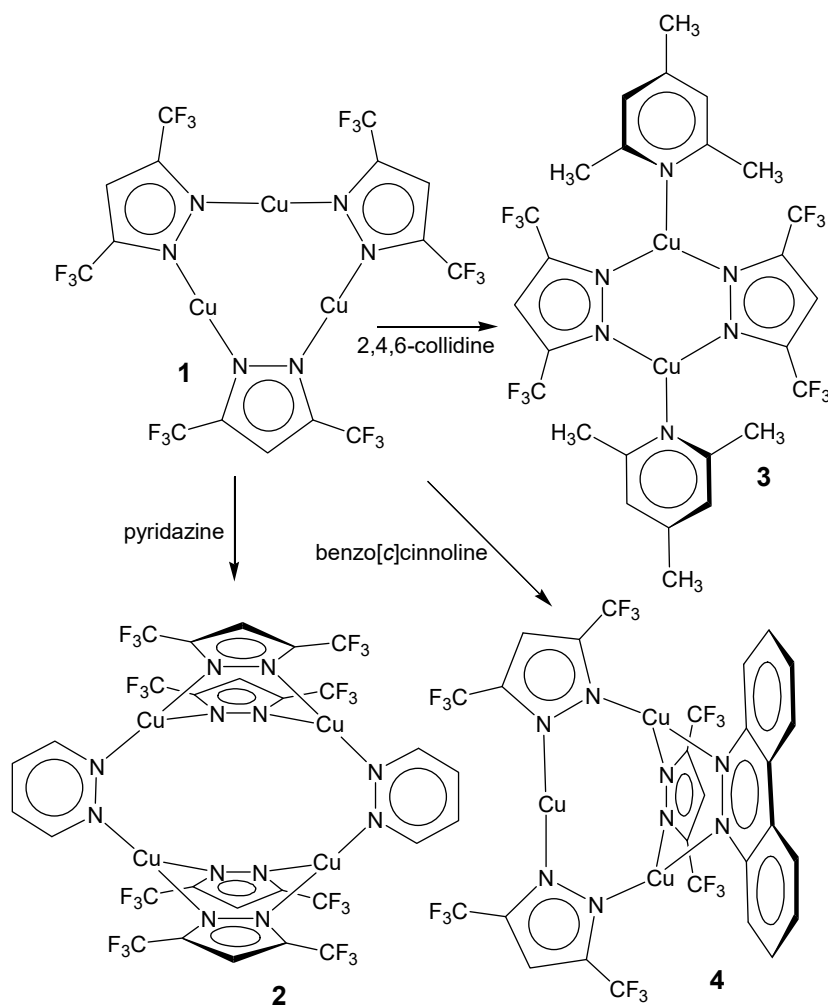


Figure 17. Side view of the hexanuclear copper(II) metallacycle where is visible the plane of the six copper atoms (pale blue) and the trans configuration of the 6 hydroxyl groups (red). Reprinted with permission from Mohamed, A. A.; Ricci, S.; Burini, A.; Galassi, R.; Santini, C.; Chiarella, G. M.; Melgarejo, D. Y.; Fackler, J. P., Jr. *Inorg. Chem.* **2011**, *50*, 1014.

These metallacycles behave as hosts for spherical, bent anions by accommodate them in the cavity, with a certain degree of selectivity with a better affinity for chloride, bromide instead to iodide. The anion recognition occurs by electrostatic interactions and hydrogen bonding.

4. BREAKAGE OF CYCLOTRIMER SELF-ASSEMBLY BY DATIVE BONDING

The trinuclear metal pyrazolates are excellent precursors to obtain different types of metal pyrazolate aggregates like dinuclear and tetranuclear adducts. This can be achieved by the break-up of trinuclear systems using appropriate Lewis bases. For example, the reaction of $\{[3,5-(CF_3)_2Pz]Cu\}_3$ with 2,4,6-collidine has resulted in dinuclear complex $\{[3,5-(CF_3)_2Pz]Cu(2,4,6\text{-collidine})\}_2$ (**2**, Scheme 8).



Scheme 8. View of the sysnthesis of $\{[3,5-(CF_3)_2Pz]Cu\}_3$ with 2,4,6-collidine, benzo[c]collidine and pyridazine

It features a planar Cu(μ -N-N)₂Cu unit with a Cu-Cu separation of 3.3940 Å.⁴⁹ The reaction of $\{[3,5-(CF_3)_2Pz]Cu\}_3$ with the bidentate nitrogen ligand pyridazine (C₄H₄N₂) however has resulted in a tetranuclear species $[\{[3,5-(CF_3)_2Pz\}_4Cu_4(C_4H_4N_2)_2]$ (3). This molecule has a *para*-cyclophane core. The pyridazine molecules act as bridging ligands for dinuclear copper pyrazolate “ $\{[3,5-(CF_3)_2Pz]Cu\}_2$ ” fragments. Unlike the example described earlier with 2,4,6-collidine, the Cu(μ -N-N)₂Cu moieties in $[\{[3,5-(CF_3)_2Pz\}_4Cu_4(C_4H_4N_2)_2]$ adopts a boat conformation. Although benzo[c]cinnoline is structurally similar to pyridazine, the reaction with copper(I) pyrazolate $\{[3,5-(CF_3)_2Pz]Cu\}_3$ under the conditions utilized with 2,4,6-collidine has not resulted in the break up of

the trinuclear system. It has produced a molecule with a Y-shaped framework $[\{3,5-(CF_3)_2PzCu\}_3(C_{12}H_8N_2)]$ (4).

The reaction between silver(I) pyrazolate $\{[3,5-(CF_3)_2Pz]Ag\}_3$ and 2,4,6-collidine and pyridazine have also been reported. The reaction with pyridazine produces a tetranuclear $[\{3,5-(CF_3)_2Pz\}_4Ag_4(C_4H_4N_2)_2]$ with a *para*-cyclophane framework. The *para*-cyclophane core consists of four silver and twelve nitrogen atoms (Figure 18). However, in contrast to the copper analog, the pyrazolyl moieties (rather than the pyridazines) act as bridges that link the two six membered $Ag(\mu-N-N)Ag$ fragments. The reaction of $\{[3,5-(CF_3)_2Pz]Ag\}_3$ with 2,4,6-collidine has afforded a dinuclear $\{[3,5-(CF_3)_2Pz]Ag(2,4,6\text{-collidine})\}_2$. It features a six-membered $Ag(\mu-N-N)Ag$ unit in a half-boat conformation. The intramolecular $Ag\cdots Ag$ distance is 3.5618(6) Å. Note that analogous $\{[3,5-(CF_3)_2Pz]Cu(2,4,6\text{-collidine})\}_2$ has a planar $Cu(\mu-N-N)Cu$ core. The copper and silver collidine adducts $\{[3,5-(CF_3)_2Pz]M(2,4,6\text{-collidine})\}_2$ are blue emitters.

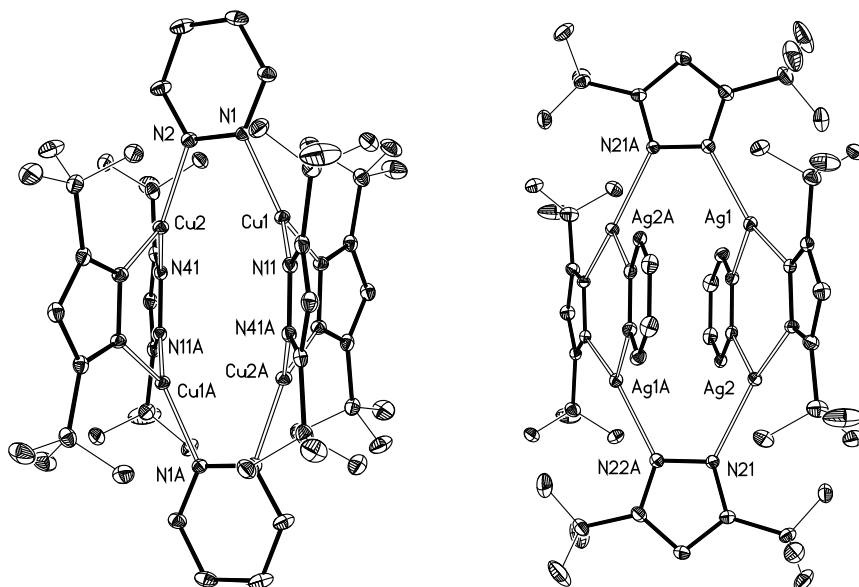


Figure 18. Molecular structures of $[\{3,5-(CF_3)_2Pz\}_4Cu_4(C_4H_4N_2)_2]$ (left) and $[\{3,5-(CF_3)_2Pz\}_4Ag_4(C_4H_4N_2)_2]$ (right), where $C_4H_4N_2 = 2,4,6\text{-collidine}$.

The copper(I) and silver(I) complexes of highly fluorinated triazolate ligand $[3,5-(C_3F_7)_2Tz]^-$ ($\{[3,5-(C_3F_7)_2Tz]Cu\}_3$ ($[Cu_3]'$) and $\{[3,5-(C_3F_7)_2Tz]Ag\}_3$ ($[Ag_3]'$), where $3,5-(C_3F_7)_2Tz = 3,5\text{-di(heptafluoropropyl)-1,2,4-triazolyl-1H}$, react with PPh_3 affording dinuclear species, $\{[3,5-(C_3F_7)_2Tz]Cu(PPh_3)\}_2$ and $\{[3,5-(C_3F_7)_2Tz]Ag(PPh_3)\}_2$ in excellent yields. These complexes have

trigonal planar metal sites (Figure 19) and feature a six-membered $M(\mu\text{-N-N})_2M$ core with a boat conformation.

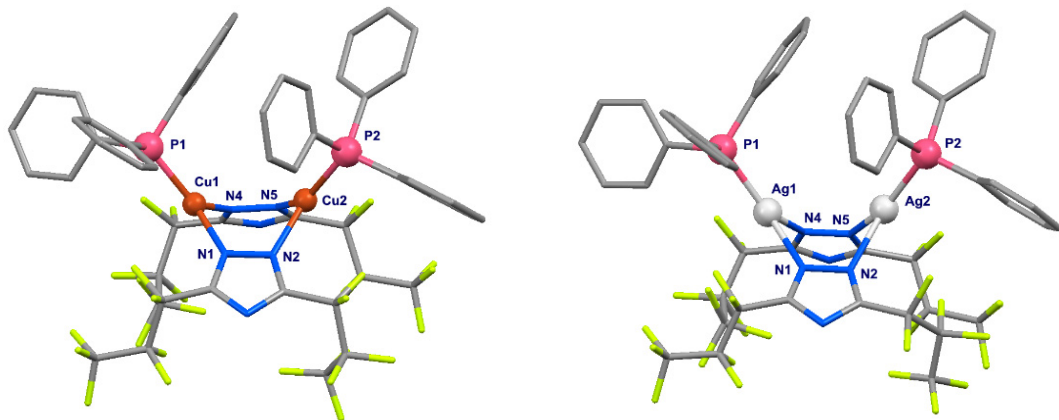
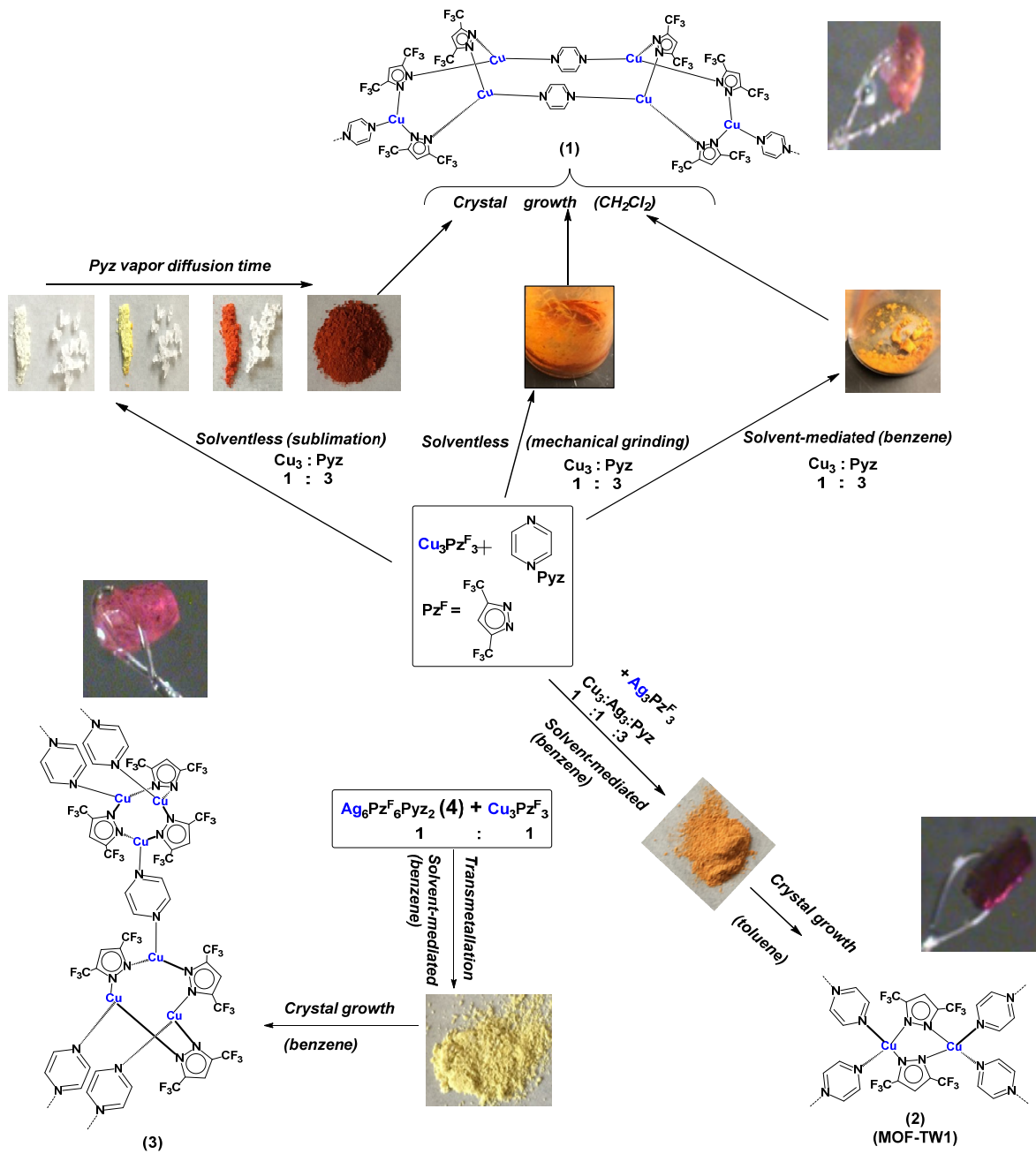
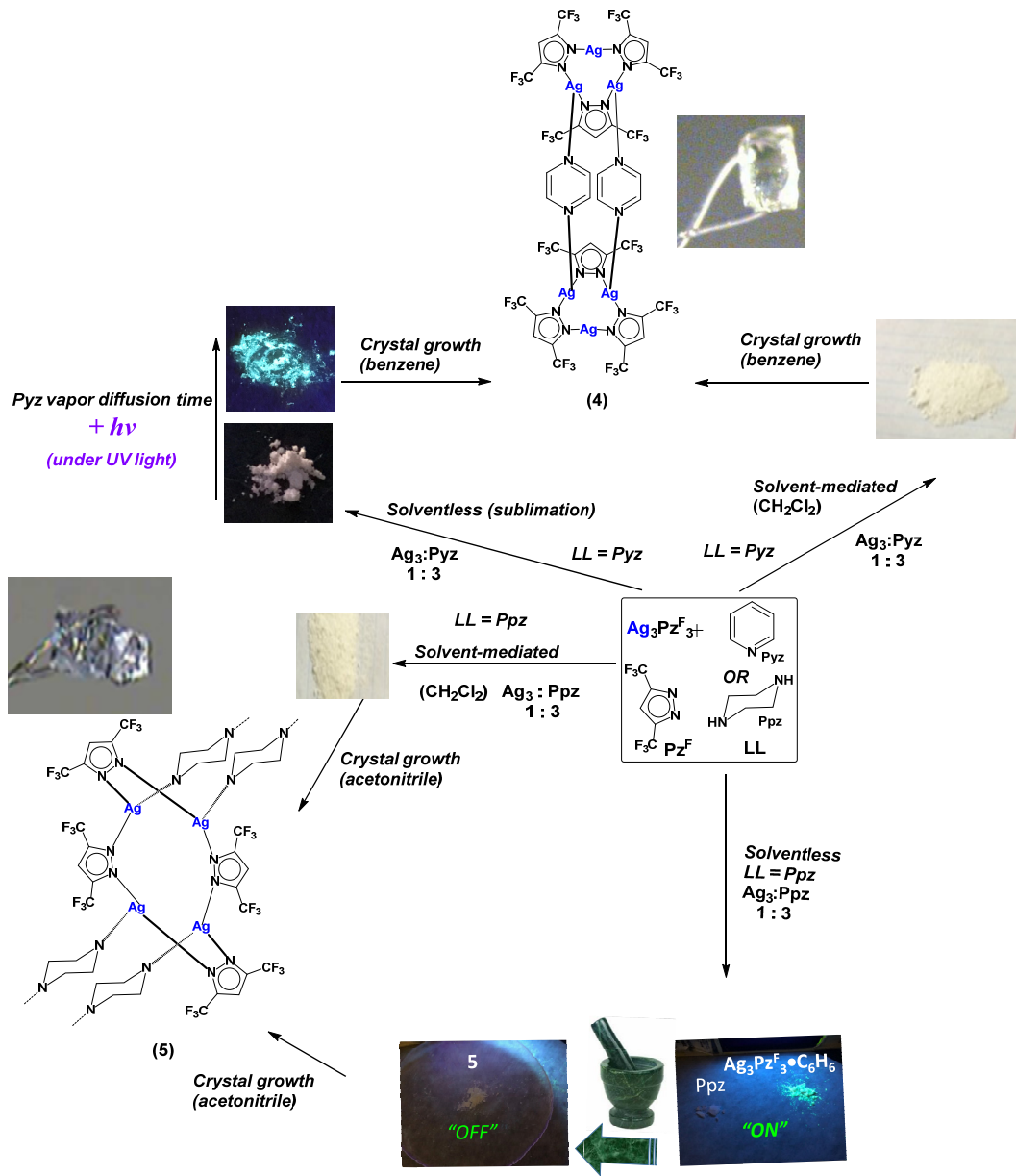


Figure 19. Molecular structures of $\{[3,5-(C_3F_7)_2Tz]Cu(PPh_3)\}_2$ (left) and $\{[3,5-(C_3F_7)_2Tz]Ag(PPh_3)\}_2$ (right), where the $3,5-(C_3F_7)_2Tz = 3,5\text{-di(heptafluoropropyl)-1,2,4-triazolyl-1H}$. Reprinted with permission from Almotawa, R. M., Aljomaih, G.; Trujillo, D. V. ; Nesterov, V. N.; Rawashdeh-Omary; M. A. *Inorg. Chem.* **2018**, *57*, 9962-9976

The cyclic trinuclear copper(I) and silver(I) pyrazolates $\{[3,5-(CF_3)_2Pz]Cu\}_3$ and $\{[3,5-(CF_3)_2Pz]Ag\}_3$ react with a small molar excess of 1,4-pyrazine (Pyz) or 1,4-piperazine (Ppz) (with respect to a 3 : 1 mixing stoichiometry with $\{[3,5-(CF_3)_2Pz]M\}_3$, where $M = Cu$ or Ag , or 2 : 1 with $[Cu(MeCN)_4]BF_4$ reactions) in benzene/toluene/dichloromethane by solvent-mediated transformations.⁵⁰ However, for these reactions also solventless methods can be applied⁵¹ with the same mixing stoichiometries entailed mechanical grinding as well as simply exposing the solid metal precursor to the ambient vapor pressure of the Pyz volatile solid (whereas Ppz is not volatile so its solventless reactions are investigated only via mechanical grinding). According to these different procedures different products were obtained, following crystal growth from dichloromethane, benzene, toluene, or acetonitrile by slow evaporation. Moreover, mechanical grinding was seen to switch on emissions (scheme 10); the trigger of this phenomenon is not known but it was already observed for copper cyclotrimers, such as for $[Cu_3]$ with ethyl-4'-benzoate-3,5-dimethylpyrazolate and MBPz = methyl-4'-benzoate-3,5-dimethylpyrazolate as bridging ligands.⁵² In schemes 9 and 10, schematic views of all the products and the reaction schemes, whereas Figures 20 and 21 show representative examples of two crystallographic products.



Scheme 9. Chemical transformations by using of 1,4-pyrazine (Pyz) to either link adjacent Cu₃ cycles and conserve the metal framework of the precursors (e.g., Figure 20) or link adjacent Cu₂ cores obtained by breaking of the triangular metal backbone to attain new frameworks. **Reprinted with permission from Almotawa, R. M., Aljomaih, G.; Trujillo, D. V. ; Nesterov, V. N.; Rawashdeh-Omary; M. A. *Inorg. Chem.* 2018, 57, 9962-9976**



Scheme 10. Chemical transformations by using of 1,4-pyrazine (Pyz) or 1,4-piperazine (Ppz) to link between two $[\text{Ag}_3]$ cycles and conserve the metal framework of the precursors or link adjacent Ag_2 cores obtained by the breaking of the triangular metal backbone. Reprinted with permission from Almotawa, R. M., Aljomaih, G.; Trujillo, D. V. ; Nesterov, V. N.; Rawashdeh-Omary; M. A. *Inorg. Chem.* **2018**, *57*, 9962-9976

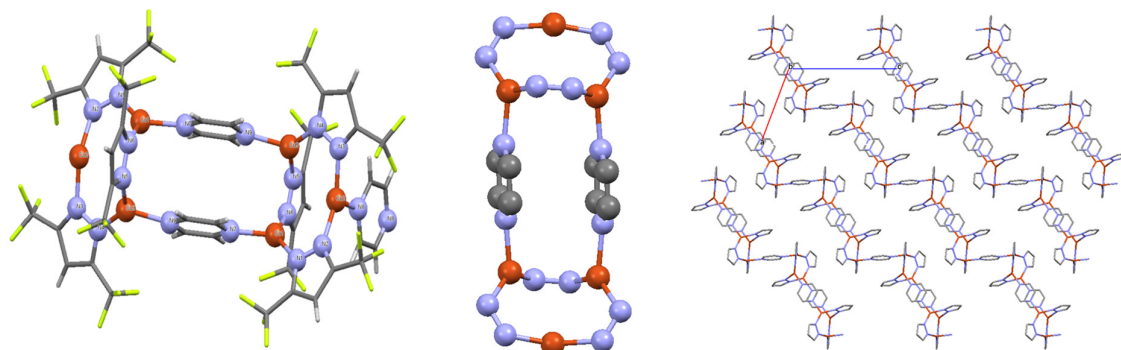


Figure 20. Molecular and packing structures of $\{\text{Cu}_6[3,5-(\text{CF}_3)_2\text{Pz}]_6(\text{Pyz})_3 \cdot \text{CH}_2\text{Cl}_2\}_\infty$ (1· CH_2Cl_2 in Scheme 9). Reprinted with permission from Almotawa, R. M., Aljomaih, G.; Trujillo, D. V. ; Nesterov, V. N.; Rawashdeh-Omary; M. A. *Inorg. Chem.* **2018**, *57*, 9962-9976

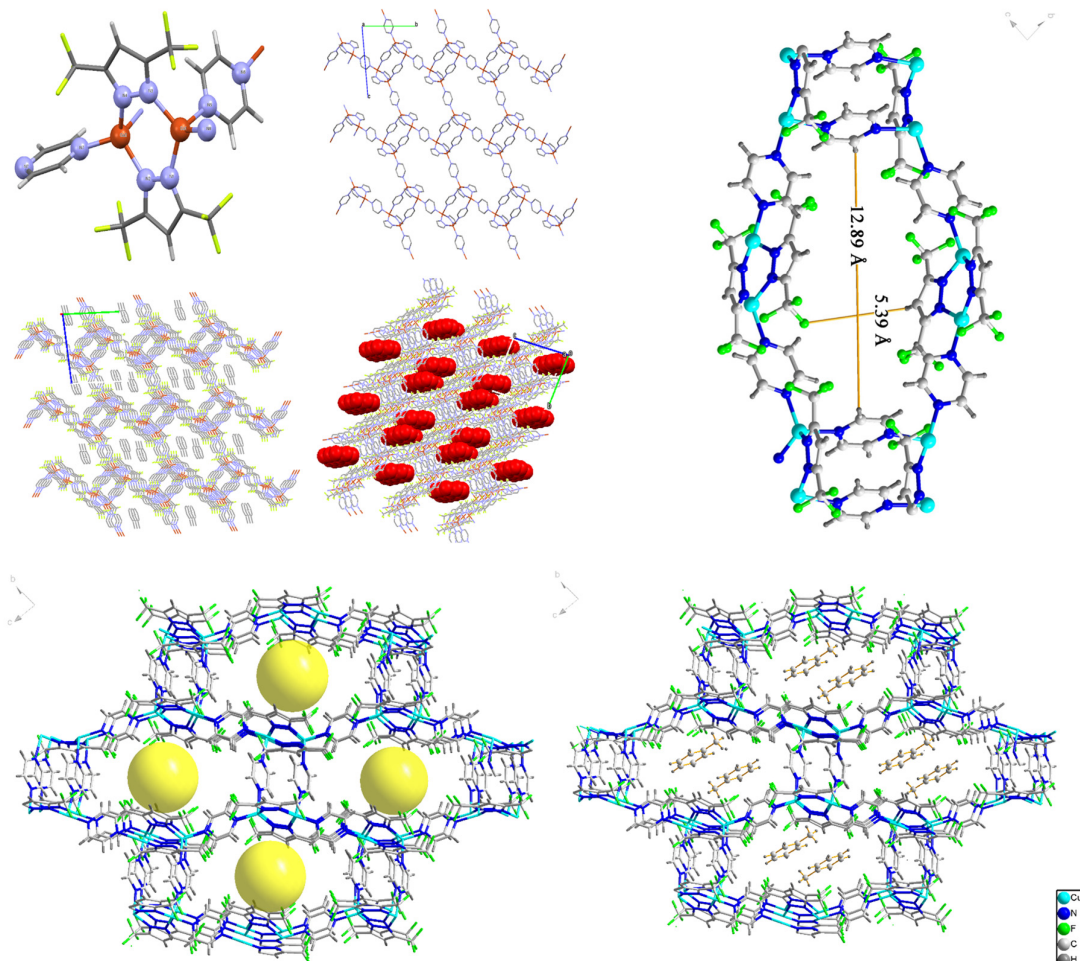


Figure 21. (a) Molecular and packing structures of $\{\text{Cu}_2[3,5-(\text{CF}_3)_2\text{Pz}]\}_2(\text{Pyz})_2 \cdot \text{toluene}\}_\infty$ (2·toluene = MOF-TW1 in Scheme 9) including pore representation of solvent-accessible regions. The total potential solvent-accessible volume is 416.4 \AA^3 (27.10% of the unit cell volume), surface area is $1278 \text{ m}^2/\text{g}$, and the pore size is $13.9 \text{ \AA} \times 5.4 \text{ \AA}$ for the parallelogram-shaped channels. Reprinted with permission from Almotawa, R. M., Aljomaih, G.; Trujillo, D. V. ; Nesterov, V. N.; Rawashdeh-Omary; M. A. *Inorg. Chem.* **2018**, *57*, 9962-9976

Another example of breaking the cyclotrimer self-assembly occurs by the addition of 2,3-hexyne to $\{[3,5-(CF_3)_2Pz]Cu\}_3$.⁵³ The strong interaction of the triple bonds with the copper moieties yields products with different nuclearity where the $[Cu_3]$ backbone is broken to generate $Cu_2(\mu-[3,5-(CF_3)_2Pz])_2(EtC\equiv CEt)_2$ or $Cu_4(\mu-[3,5-(CF_3)_2Pz])_4(EtC\equiv CEt)_2$ depending on mole ratio of the reactants. The Raman shift of the $\bar{\nu} C\equiv C$ vibrations of $Cu_2(\mu-[3,5-(CF_3)_2Pz])_2(EtC\equiv CEt)_2$ upon interaction with copper atoms exhibits a redshift of about 210 cm^{-1} compared to the free alkyne, which is typical for η^2 -bound Cu(I)-alkynes. On the contrary the ^1H NMR signals of the ethyl groups do not show large difference from the free alkyne marking the role of the triple bond on the coordination. The coordination of the triple bond was definitely showed in the solid state by the X-ray crystal structure determination (Figure 22).

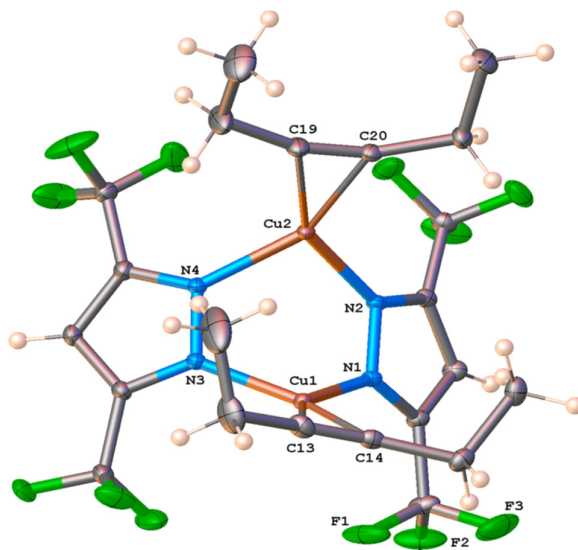


Figure 22. Molecular structure of $Cu_2(\mu-[3,5-(CF_3)_2Pz])_2(EtC\equiv CEt)_2$. Reprinted with permission from Parasar, D. Almotawa, R. M.; Jayaratna, N. B.; Ceylan, Y. S.; Cundari, T. R., Omary, M. A.; Dias H. V. R. *Organometallics* **2018**, *37*, 4105-4118

Interestingly, the reaction of $\{[3,5-(CF_3)_2Pz]Cu\}_3$ with 3-hexyne in a 2 : 3 molar ratio affords a different product in 84% yield, which was identified by several methods as $Cu_4(\mu-[3,5-(CF_3)_2Pz])_4(\mu-EtC\equiv CEt)_2$ (Figure 23). It shows a much larger reduction in $\bar{\nu} C\equiv C$ vibration compared to the free alkyne and has a formally 4e-donor alkyne. The $\{[3,5-(CF_3)_2Pz]Cu\}_3$ also reacts with $Me_3SiC\equiv CSiMe_3$, affording dinuclear $Cu_2(\mu-[3,5-(CF_3)_2Pz])_2(Me_3SiC\equiv CSiMe_3)_2$, which is an excellent volatile chemical vapor deposition (CVD) precursor for copper.

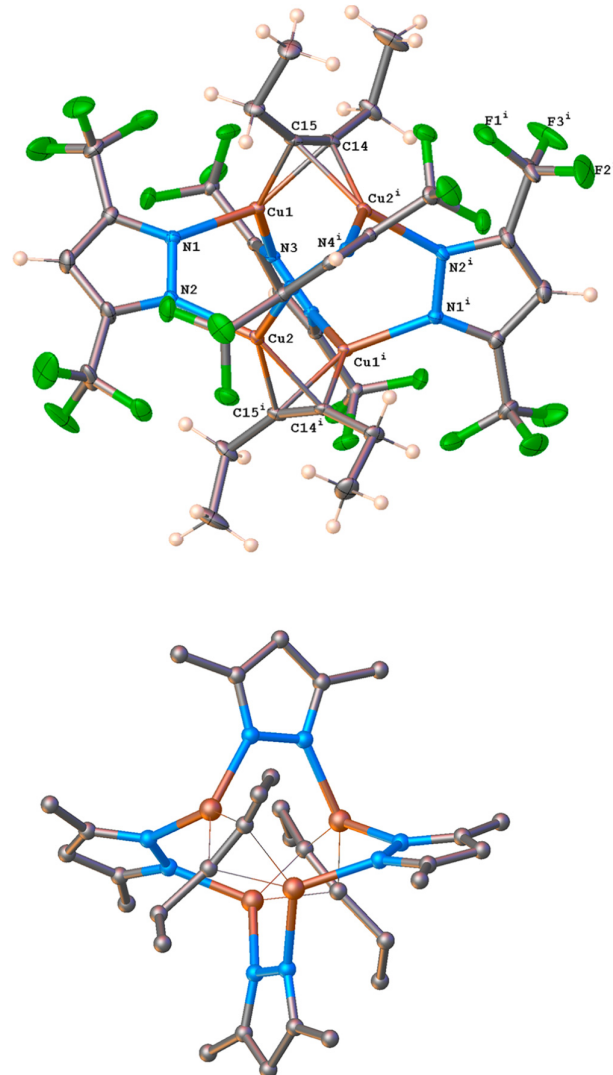


Figure 23. ORTEP diagram of $\text{Cu}_4(\mu\text{-[3,5-(CF}_3\text{)}_2\text{Pz]})_4(\mu\text{-EtC}\equiv\text{CEt})_2$ (top) and a view showing the Cu_4N_8 core (bottom; hydrogen and fluorine atoms have been omitted for clarity). Reprinted with permission from Parasar, D. Almotawa, R. M.; Jayaratna, N. B.; Ceylan, Y. S.; Cundari, T. R., Omary, M. A.; Dias H. V. R. *Organometallics* **2018**, *37*, 4105-4118.

5. BREAKAGE OF CYCLOTIMER SELF-ASSEMBLY BY CHEMISORPTIVE DIPOLE-QUADRUPOLE INTERACTIONS

The influence of the ligand in the π -acid or π -base properties of Ag(I) cyclotrimers were studied by comparing the chemistry of two similar π -acid silver(I) compounds: the $[\text{Ag(3,5-(CF}_3\text{)}_2\text{Pz})_3]$ and the $[\text{Ag(3,5-(NO}_2\text{)}_2\text{Pz})_3]$.^{36,37} The crystal structure of $[\text{Ag(3,5-(NO}_2\text{)}_2\text{Pz})_3]$ shows a non-planar nine-membered cyclotrimer with a deviation of the planarity of 0.1793 Å and with a N1–Ag1–N5 angle

of $165.36(4)^\circ$ (Figure 24). The **cyclotrimer** shows a strong interaction with two CH_3CN molecules, which ones point toward the centre of the **cyclotrimer** from opposite side, with distances of $\text{N}-\text{Ag}(2)$ of 2.590 Å and 2.647 Å. In the crystal packing there are no evidence of stacking dimer of trimer units by argentophilic bonds, while very weak intermolecular $\text{C}-\text{H}\cdots\text{O}$ hydrogen bonds link trimer and solvent molecules in the crystal, forming a network.

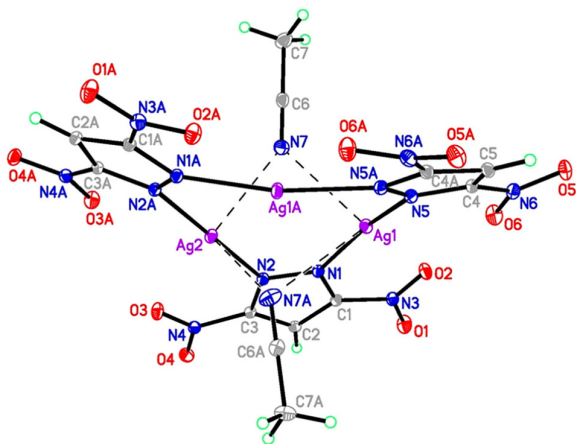


Figure 24. General view of $[\text{Ag}(3,5-(\text{NO}_2)_2\text{Pz})]_3 \cdot 2\text{CH}_3\text{CN}$ with two CH_3CN solvent molecules interacting with the Ag atoms. **Reprinted with permission from Galassi, R.; Ricci, S.; Burini, A.; Macchioni, A.; Rocchigiani, L.; Marmottini, F.; Tekarli, S. M.; Nesterov, V. N., Omary, M. A. *Inorg. Chem.*, 2013, 52, 14124.**

The treatment of $[\text{Ag}(3,5-(\text{NO}_2)_2\text{Pz})]_3$ with a base such as NH_3 and its solubilization in hot THF leads to the capture of Ag(I) centres and the formation of $[\text{Ag}(\text{NH}_3)_2]^+$ complex ions, the consequent breakage of the cyclotrimer and the following rearrangements in still a trinuclear system but with additional bridging pyrazolate ligand in a propeller like structure (Figure 25).

The structure of $\{[\text{3,5-(CF}_3)_2\text{Pz}]\text{Ag}\}_3$ shows the same **cyclotrimer** arrangement, a more planar conformation of the nine-membered Ag_3N_6 cycle, but an arrangements of molecules in the crystal lattice which consists of dimer of trimers units with intermolecular Ag-Ag distances are around 3.307 Å, much shorter than those recorded in the intramolecular Ag-Ag bond lengths of 3.44 and 3.54 Å. Both complexes stacks with naphthalene in a 1:1 mole ration even though only in the case of $\{[\text{3,5-(CF}_3)_2\text{Pz}]\text{Ag}\}_3$ a crystal structure was reported.⁵⁴ Actually in this last case the sensitizing of the naphthalene phosphorescence in the 1:1 adduct was also reported as an external heavy effect of silver,

underlying the intimate bonding between the electron poor silver(I) pyrazolate and the organic aromatic molecule.

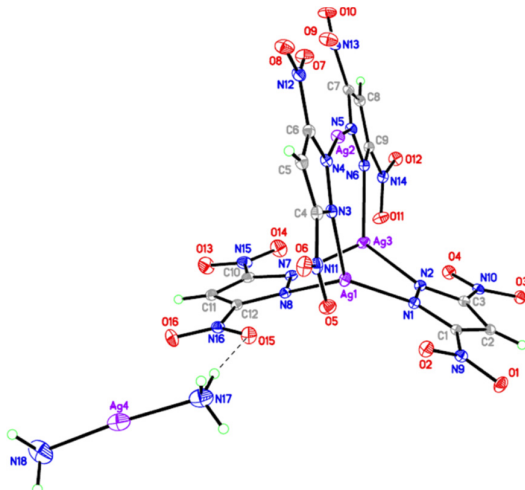


Figure 25. General view of the propeller like structure of the trinuclear Ag(I) compound obtained by the reaction of the silver trimer $[\text{Ag}(3,5-(\text{NO}_2)_2\text{Pz})]_3$ and ammonia in THF. [Reprinted with permission from Galassi, R.; Ricci, S.; Burini, A.; Macchioni, A.; Rocchigiani, L.; Marmottini, F.; Tekarli, S. M.; Nesterov, V. N., Omary, M. A. *Inorg. Chem.*, 2013, 52, 14124.](#)

Even though the base structure of both Ag(I) **cyclotrimers** contains the classic Ag_3N_6 framework and they show similar pi acid properties in the regards of naphthalene, the most evident discontinuance in the properties of these two compounds regards the emissive properties. The $[\text{Ag}(3,5-(\text{NO}_2)_2\text{Pz})]_3$ and also its naphthalene complex do not show any remarkable emissive properties in the solid state both at room temperature and cryogenic temperatures. However the exposition at room temperature of solid $[\text{Ag}(3,5-(\text{NO}_2)_2\text{Pz})]_3$ to vapors of acetone, acetonitrile, acetylacetone, ammonia, pyridine, triethylamine, dimethylsulfide, tetrahydrothiophene affords to a reversible chemisorption while the analog $\{[3,5-(\text{CF}_3)_2\text{Pz}]\text{Ag}\}_3$ does not. The chemisorption is selective in the regard of those above mentioned molecules while CO, THF, alcohols and dimethyl and diethyl ethers do not interact with the $[\text{Ag}(3,5-(\text{NO}_2)_2\text{Pz})]_3$. moreover the mole ratio of the final adduct varies, ranging to 1 : 1 (acetone); 1 : 2 (acetonitrile, dimethylsulfide) till to 1 : 3 in the case of ammonia, pyridine and THT. In addition, by TGA analyses it was found that the range of temperature for the weight loss for the adducts where 50 - 200 °C higher than the boiling points of the pure liquid compounds. Another evidence of a strong chemisorption mechanism. The presence of mesopores in the microcrystalline structure was ruled out by BET surface measurements and, so far, the only

plausible explanation to this different behavior came from computational calculations. The B3LYP/CEP-31G(d) theoretical treatment used the CO and acetonitrile interactions with $[\text{Ag}(3,5-(\text{NO}_2)_2\text{Pz})]_3$ as models representing the two limiting cases for small molecules exhibiting weak versus strong interactions according to the experimental data. In computation of the adsorption of two CO molecules to $[\text{Ag}(3,5-(\text{NO}_2)_2\text{Pz})]_3$, the B3LYP/CEP-31G(d) results show a vanishingly weak binding energy of $1.4 \text{ kcal mol}^{-1}$. The binding energy for one trimer $[\text{Ag}(3,5-(\text{NO}_2)_2\text{Pz})]_3$ molecule to one and two CH_3CN molecules was 8.5 and $15.9 \text{ kcal mol}^{-1}$, respectively. Using the M06 functional binding energy of $26.9 \text{ kcal mol}^{-1}$ for the $1\cdot 2\text{CH}_3\text{CN}$ binary adduct was calculated. Therefore, the M06/CEP-31G(d) results for the $1\cdot 2\text{CH}_3\text{CN}$ binary adduct are in agreement with the experimental data both qualitatively and quantitatively, with the latter being manifested by the binding energy representing chemisorption instead of physisorption, consistent with the BET surface area and TGA data reported. Additional insights on the associated nature of attractive forces based on Molecular Electrostatic Potential (MEP) computations are showed in Figure 26.

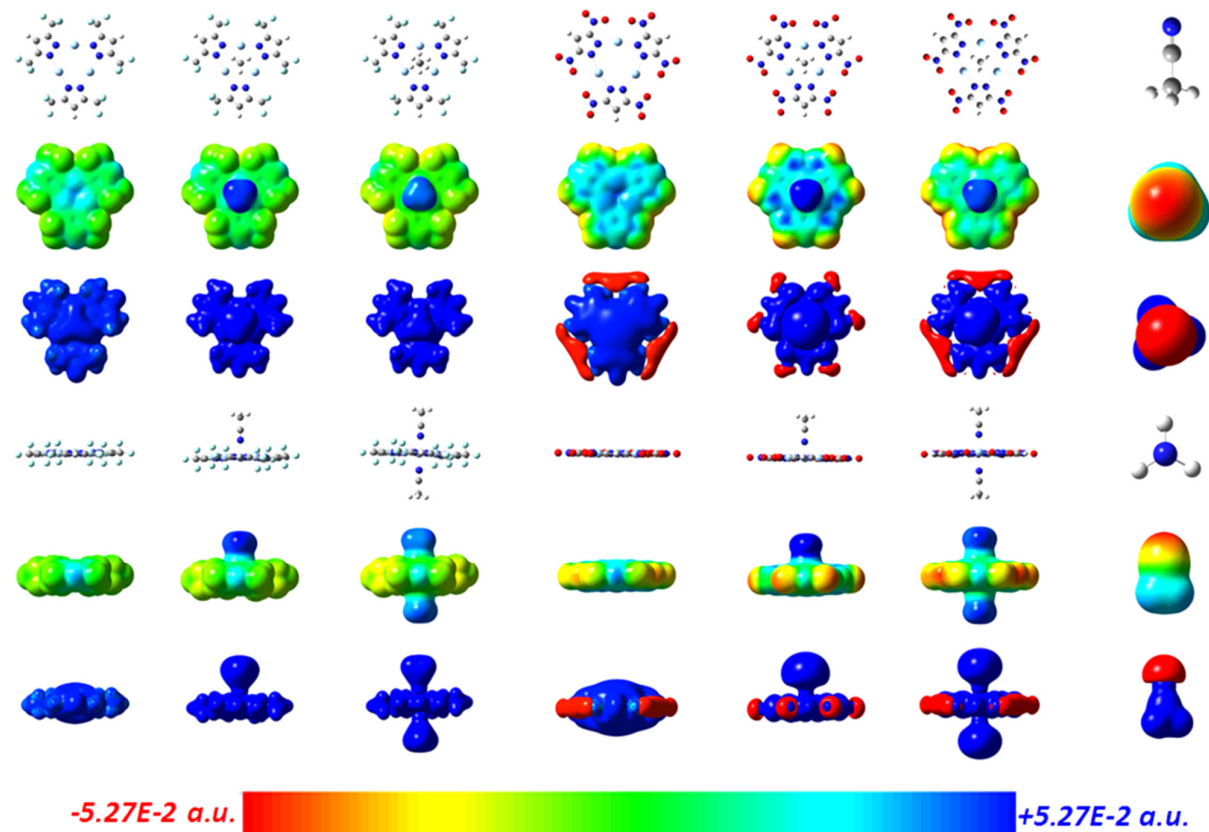


Figure 26. Illustration of quadrupole-dipole interactions involving the $[\text{Ag}(3,5-(\text{CF}_3)_2\text{Pz})]_3$ or $[\text{Ag}(3,5-(\text{NO}_2)_2\text{Pz})]_3$ trimers and acetonitrile using M06/CEP-31G(d). MEP surfaces are plotted in two manners, either mapped on electron density surfaces (rainbow plots with the color scale shown;

isodensity = 0.0004) or positive (blue) and negative (red) regions in space (range = ± 2.2 au; isodensity = 0.02). Atomic color code in the molecular structures: Ag, light-blue, larger spheres; C, gray; N, blue; O, red; H, white; F, light-blue, smaller spheres. Reprinted with permission from Galassi, R.; Ricci, S.; Burini, A.; Macchioni, A.; Rocchigiani, L.; Marmottini, F.; Tekarli, S. M.; Nesterov, V. N.; Omary, M. A. *Inorg. Chem.*, **2013**, *52*, 14124.

Although the 3-fold rotation in the $[\text{Ag}(3,5-(\text{NO}_2)_2\text{Pz})]_3$ model (D_{3h} effective symmetry) precludes dipole, the molecule is strongly quadrupolar with a rather strong π -acidic behavior at the center of the nine-membered macrometallocyclic ring and normal regions thereof in both sides. Therefore, these strongly electron-deficient regions are available to significant quadrupole–dipole interactions with the Lewis-basic acetonitrile molecule. Thus, strong quadrupole–dipole interactions exist between the $[\text{Ag}(3,5-(\text{NO}_2)_2\text{Pz})]_3$ cyclotrimer, on the one hand, and the lone pair of acetonitrile ($\mu = 3.92$ D), on the other hand, as depicted in Figure 20. For $[\text{Ag}(3,5-(\text{CF}_3)_2\text{Pz})]_3$, binding energies of 8.3 and 16.0 kcal mol^{-1} were found for one and two acetonitrile molecules, respectively, using B3LYP/CEP-31G(d), while analogous values using M06/CEP-31G(d) were 13.7 and 30.6 kcal mol^{-1} , respectively. These values are rather similar to the binding energies of $[\text{Ag}(3,5-(\text{NO}_2)_2\text{Pz})]_3$ to one and two acetonitrile molecules. However, the non-vanishing quadrupole moment tensors are significantly lower than the analogous values for trimer $[\text{Ag}(3,5-(\text{NO}_2)_2\text{Pz})]_3$. MEP plots also manifest a rather strong π -acidic behavior of this $[\text{Ag}(3,5-(\text{CF}_3)_2\text{Pz})]_3$ cyclotrimer, suggesting that it should exhibit somewhat less strong quadrupole–dipole interactions with acetonitrile. However, the MEP surfaces show greater polarizability for the model of $[\text{Ag}(3,5-(\text{NO}_2)_2\text{Pz})]_3$, suggested by the blue and turquoise MEP regions in the metallocyclic ring surface as opposed to the turquoise and green regions for the model of $[\text{Ag}(3,5-(\text{CF}_3)_2\text{Pz})]_3$. Thus, both the Q_{zz} quadrupole moment tensor values and MEP surfaces offer evidence in support of the experimental finding regarding isolation of an acetonitrile adduct with $[\text{Ag}(3,5-(\text{NO}_2)_2\text{Pz})]_3$ but not $[\text{Ag}(3,5-(\text{CF}_3)_2\text{Pz})]_3$. Moreover, by using M06/CEP-31G(d), the binding energy of $\{[\text{Ag}(3,5-(\text{CF}_3)_2\text{Pz})]_3\}_2$ is found to be 31.4 kcal mol^{-1} . This represents clear evidence of rather strong argentophilic bonding in the $\{[\text{Ag}(3,5-(\text{CF}_3)_2\text{Pz})]_3\}_2$ dimer-of-trimer, and the optimized structure is remarkably similar to the experimental crystal structure. The conclusive hypothesis is that such strong argentophilic bonding interactions in $\{[\text{Ag}(3,5-(\text{CF}_3)_2\text{Pz})]_3\}_2$ would not allow dissociation of trimers to form adducts with 1 or 2 equiv of acetonitrile molecules given that the dimer-of-trimer dissociation energy is almost twice that of the monosolvated model.

6. BREAKAGE OF CYCLOTRIMER SELF-ASSEMBLY BY QUADRUPOLE-QUADRUPOLE STACKING INTERACTIONS

An important characteristic of **these cyclotrimers** is their very interesting π -acid/ π -base properties leading to the formation of extended supramolecular structures with cations, and organic or organometallic molecules.^{4a-c,54} Omary *et al.* demonstrated, by theoretical calculations, that the π -acidity or the π -basicity depends by three factors: type of metal, type of ligand and nature of the substituents on the ligands.⁵⁵ Figure 26 shows a summary of these three factors.

For example the $[M(\mu\text{-}3,5\text{-(CF}_3)_2\text{Pz})_3]$ ($M = \text{Ag or Au}$) compounds form charge-transfer complexes with arenes in the solid-state (Figure 27).^{34,46a,d,53}

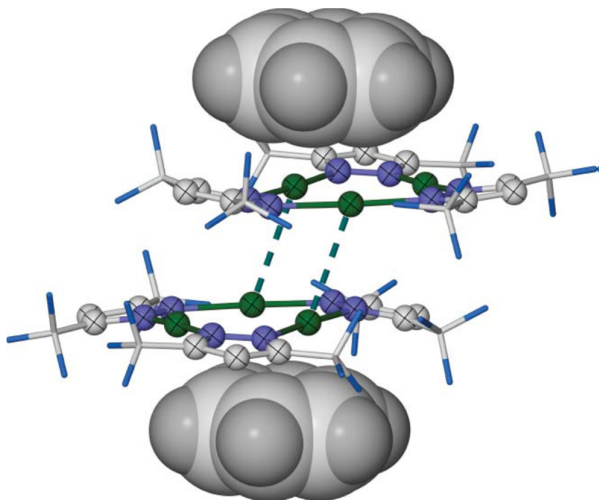


Figure 27. Structure of $[\text{Ag}(\mu\text{-}3,5\text{-(CF}_3)_2\text{Pz})_3] \cdot \text{C}_6\text{H}_6$, showing the dimerization of the cluster through two intermolecular argentophilic interactions, and the formation of a charge transfer complex with the benzene solvent. **Reprinted with permission from Dias, H. V. R.; Gamage, C. S. P.; Keltner, J.; Diyabalanage, H. V. K.; Omari, I.; Eyobo, Y.; Dias, N. R.; Roehr, N.; McKinney, L.; Poth, T. *Inorg. Chem.* 2007, **46**, 2979.**

These adducts have stacked structures, with either isolated or dimer $[M(\mu\text{-}3,5\text{-(CF}_3)_2\text{Pz})_3]$ units sandwiched between arene ligands (where $M = \text{Au, Ag and Cu}$). This is a consequence of the strongly electron withdrawing trifluoromethyl substituents on the pyrazole ligands, which convert what would normally be a π -basic metal cluster into a π -acid one. DFT calculations confirmed the electropositivity of the cluster surface, with the silver cluster as the most electron-deficient of the three coinage metal

compounds. On the contrary, DFT calculations^{54,4b} showed, that trinuclear gold(I) complexes with imidazolate or N-substituted imidazolates as bridging ligands, have strong π -basic properties with the donor regions located at the center of the nine-membered ring, so they can interact with cations^{4a,46a} and neutral organic^{4c} or organometallic acceptor^{4b} to give supramolecular π -acid/ π -basic complexes with extended structures and in some case with interesting luminescence properties.

The most π -acid $\{[3,5-(CF_3)_2Pz]Ag\}_3$, $[Ag_3]$ (among Cu, Ag, and Au analogs), shows the largest variety of compounds with π -bases, with aggregation pattern depends on the solvent and the arene and the stoichiometry.⁵⁶ Figure 28 shows four variations of such adducts formed between $\{[3,5-(CF_3)_2Pz]Ag\}_3$ and benzene or mesitylene (Mes). The chemistry reported by Gabbaï and co-workers using a group 12, trinuclear d¹⁰ π -acid $\{[o-C_6F_4]Hg\}_3$ is also noteworthy as readily forms one-dimensional organometallic polymers containing arene donors like benzene, naphthalene, and pyrene. As Rawashdeh-Omary et al demonstrated, $\{[3,5-(CF_3)_2Pz]Ag\}_3$ is a good sensor for some of the volatile arenes like benzene. The $\{[3,5-(CF_3)_2Pz]Ag\}_3$ complex of naphthalene is also known and has been to demonstrate the heavy atom effect of $\{[3,5-(CF_3)_2Pz]Ag\}_3$ to enhance the room temperature phosphorescence of naphthalene.

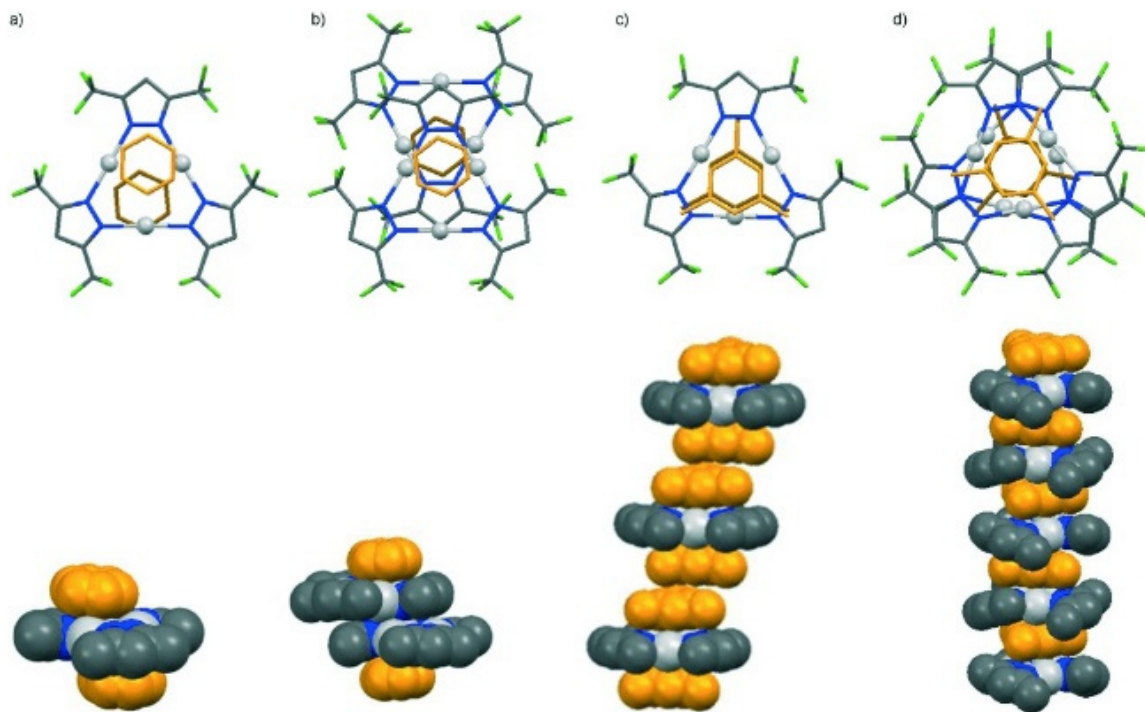


Figure 28. Few examples of π -acid/ π -base adducts of $[Ag(\mu-3,5-(CF_3)_2Pz)]_3$ with benzene and mesitylene (Mes). a) $[(C_6H_6)([Ag_3])(C_6H_6)]$ and b) $[(C_6H_6)([Ag_3])_2(C_6H_6)]$, c) $[(Mes)([Ag_3])(Mes)]$ and d) a portion of the supramolecular chain $\{(Mes)([Ag_3])(Mes)\}_\infty$. Reprinted with permission from Dias, H. V. R.; Gamage C. S. P. *Angew Chem* **2007**, 119, 2242-2244.

The related $\{[3,5-(CF_3)_2Pz]Cu\}_3$, $[Cu_3]$, and $\{[3,5-(CF_3)_2Pz]Au\}_3$, $[Au_3]$, also form π -acid/ π -base adducts, but the reports are fewer compared to the silver analog. Dias and co-workers recently reported benzene [Bz], mesitylene [Mes] and naphthalene [Nap] adducts of $\{[3,5-(CF_3)_2Pz]Cu\}_3$. They form columnar structures of the type $\{[Bz][Cu_3]_2\}_\infty$, $\{[Mes][Cu_3]\}_\infty$ and $\{[Nap][Cu_3]\}_\infty$ in the solid state, and are luminescent. The $\{[Au_3]_2[toluene]\}_\infty$ adduct in which toluene is sandwiched between dimer-of-trimer units of the fluorinated Au complex is an example of this type involving gold, which is the least π -acidic system of the coinage metal family (Figure 29).

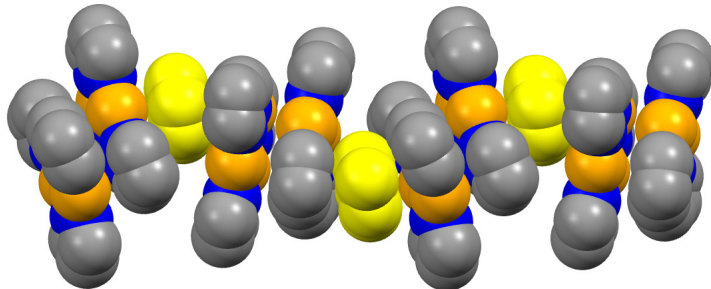


Figure 29. A view of the adduct formed between $\{[3,5-(CF_3)_2Pz]Au\}_3$ and toluene (only selected atoms are shown; toluene molecule is in yellow). Reprinted with permission from Dias, H.V. R.; Gamage C. S. P. *Angew Chem* **2007**, 119, 2242-2244.

Quite interestingly, it is also possible to use *non-planar* fullerenes in this μ -acid/ μ -base chemistry.⁵⁷ For example, C_{60} reacts with $[Ag_3]$ in 1 : 4 molar ratio to produce $\{C_{60}[Ag_3]_4\}_\infty$ as an air stable, crystalline solid. The related $[Cu_3]$ and $[Au_3]$ also afford analogues materials with C_{60} . The $[M_3]$ moieties adopt a concave conformation to accommodate curved surfaces of C_{60} . The $C_{60}[M_3]_4$ units pack as shown in Figure 30 to form a 3D-structure of the type $\{C_{60}[M_3]_4\}_\infty$ with tetrahedral symmetry.

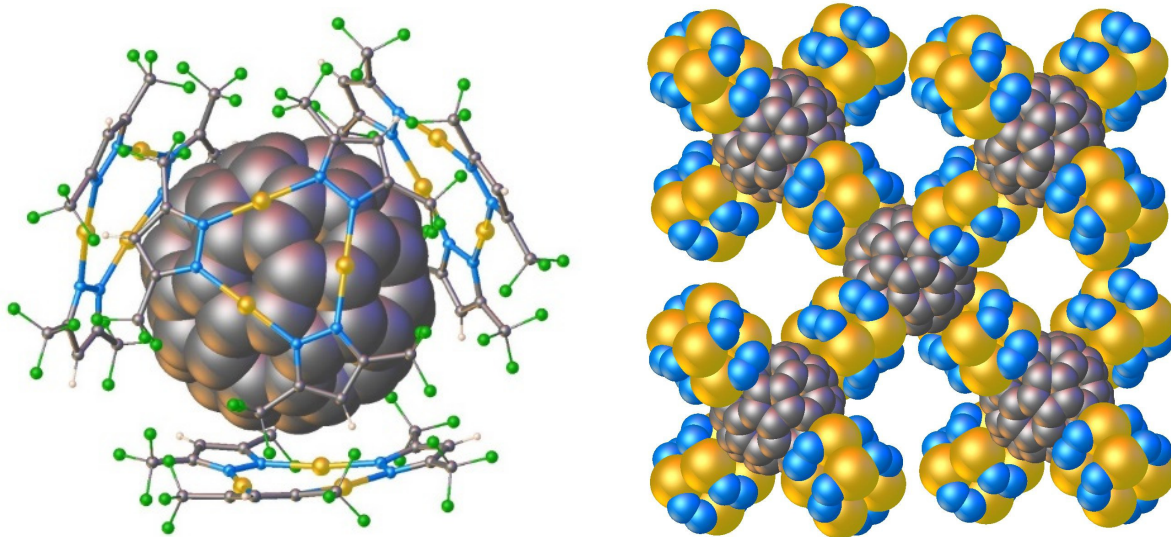


Figure 30. X-ray structure of $\{C_{60}[Au_3]_4\}_\infty$ showing the basic stoichiometry and tetrahedrally encapsulated C_{60} by four $[Au_3]$ (left). $\{C_{60}[Cu_3]_4\}_\infty$ and $\{C_{60}[Ag_3]_4\}_\infty$ analogs are isomorphous. A view of the supramolecular structure of $\{C_{60}[Au_3]_4\}_\infty$ (right, carbon, fluorine and hydrogen atoms of pyrazolyl moieties have been omitted for clarity). Reprinted with permission from Jayaratna, NB; Olmstead, MM, Kharisov, BI; Dias, HV. *Inorg Chem.* **2016**, *55*, 8277-80.

The $[M_3]$ units in these $\{C_{60}[M_3]_4\}_\infty$ appears as slightly twisted, trigonal prismatic dimers of trimers with three close metallophilic $M \cdots M$ interactions (Figure 30). The intercyclotrimer $M \cdots M$ distances of $\{C_{60}[M_3]_4\}_\infty$ for Cu, Ag, and Au adducts are 3.1580(17), 3.2046(7), and 3.2631(7) Å, respectively. These separations are well within Bondi's van der Waals radii sums (i.e., 3.32 and 3.44 Å for Au and Ag) while the Cu \cdots Cu contacts in $\{C_{60}[Cu_3]_4\}_\infty$ are slightly longer (cf. 2.80 Å).

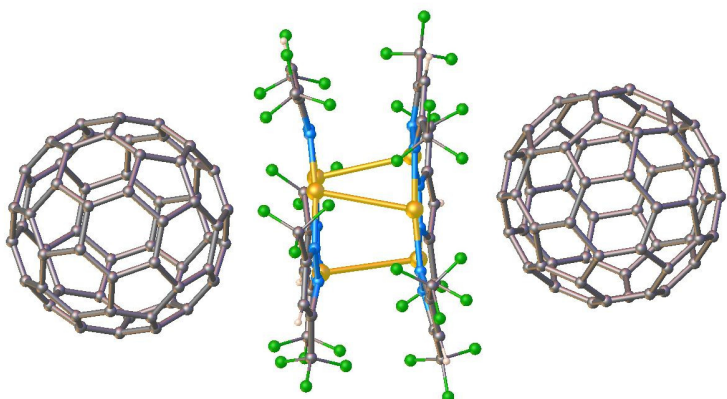


Figure 31. A view showing C_{60} sandwiched $[Au_3]_2$ with three inter-trimer $Au \cdots Au$ contacts. Reprinted with permission from Jayaratna, NB; Olmstead, MM, Kharisov, BI; Dias, HV. *Inorg Chem.* **2016**, *55*, 8277-80.

The π -acid / π -base complexes are not limited to pyrazolates. Copper(I) and silver(I) complexes of highly fluorinated triazolate ligand $[3,5-(C_3F_7)_2Tz]^-$ ($\{[3,5-(C_3F_7)_2Tz]Cu\}_3$ ($[Cu_3]'$) and $\{[3,5-(C_3F_7)_2Tz]Ag\}_3$ ($[Ag_3]'$)) also form sandwiched molecules with toluene [Tol], and they are of the type $[Tol][M_3]'$ [Tol] (Figure 32) forming extended columns.⁵⁸ Metal-carbon distances of these adducts point to rather tight interactions. The $[Cu_3]'$ and [Tol] centroids of $[Tol][Cu_3]'$ [Tol] are separated by 3.27 and 3.42 Å while the centroid-to-centroid distances observed in $[Tol][Ag_3]'$ [Tol] are 3.20 and 3.34 Å. These closest $M\cdots C(tol)$ and [Tol] to $[M_3]$ distances, taken together with larger covalent radius of Ag^I point to much tighter μ -acid/base interaction in the silver adduct (compared to that of copper), which is not surprising based on the expected acidity of the trinuclear systems. It is also possible to isolate compounds like $[Cu_3]'$ (THF)₂ with Cu-THF bonds involving $\{[3,5-(C_3F_7)_2Tz]Cu\}_3$.

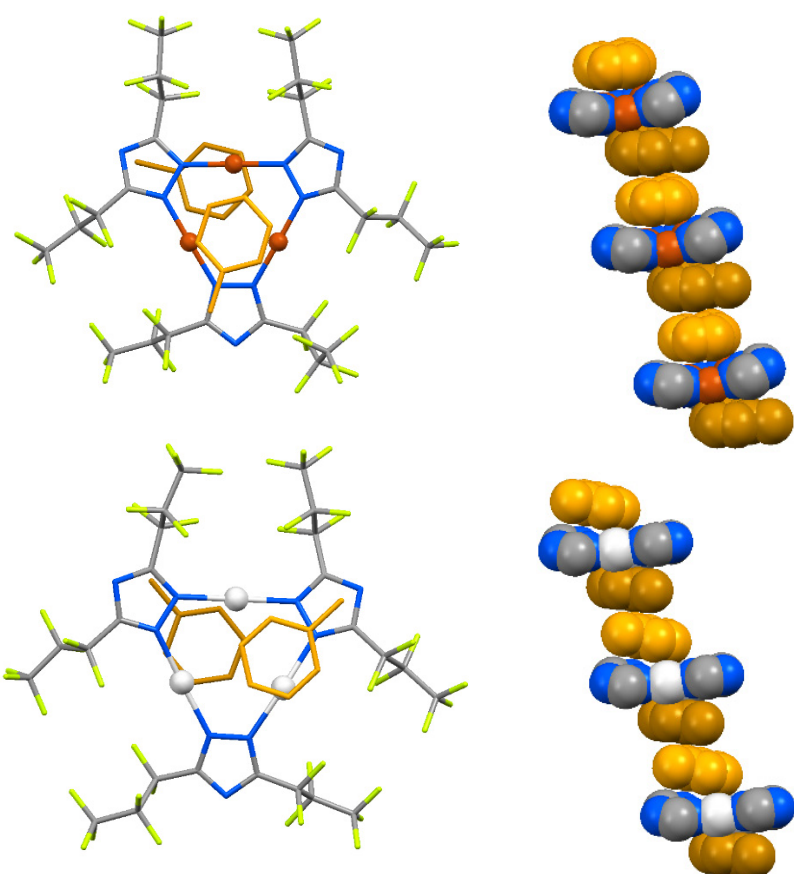
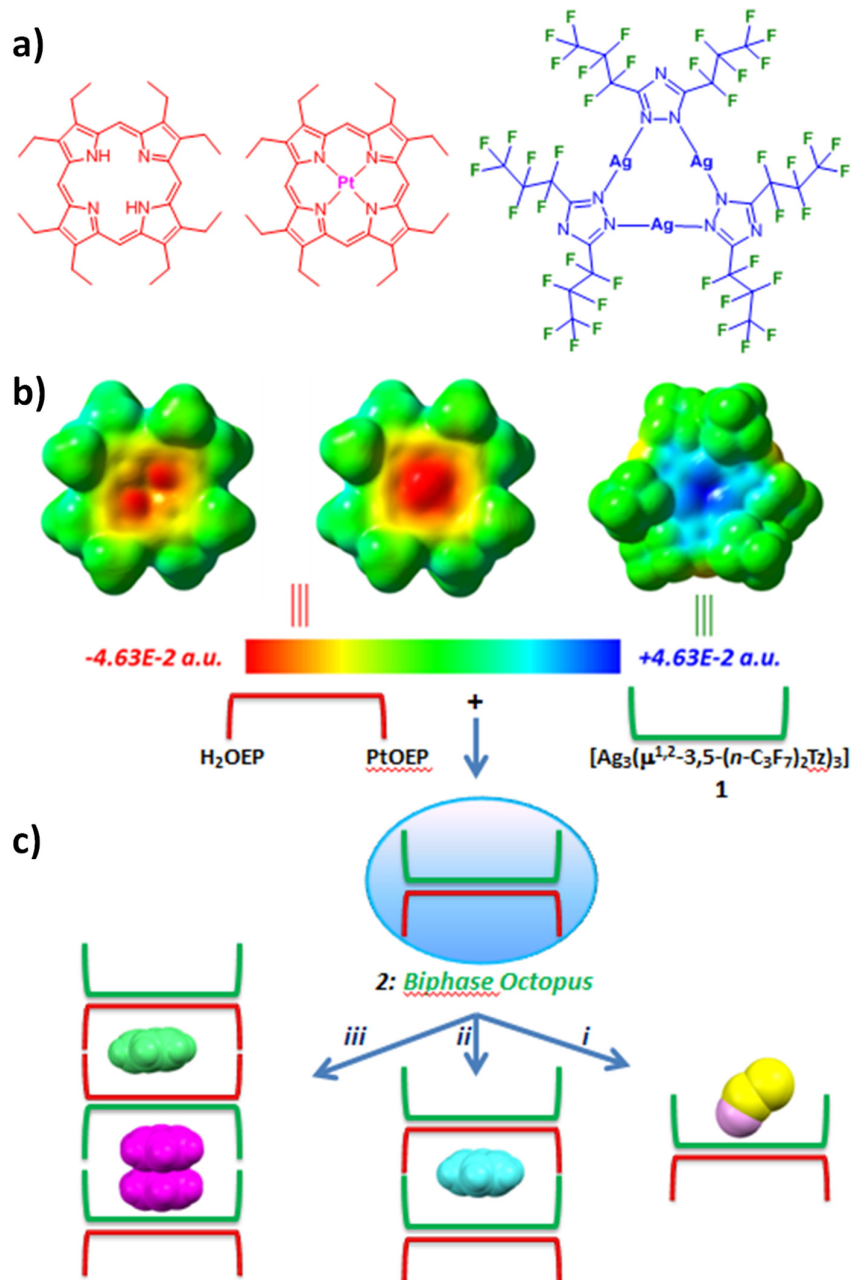


Figure 32. Molecular structures of $[(toluene)\{[3,5-(C_3F_7)_2Tz]Cu\}_3(toluene)]$, $[Tol][Cu_3]'$ [Tol] (top) and $[(toluene)\{[3,5-(C_3F_7)_2Tz]Ag\}_3(toluene)]$, $[Tol][Ag_3]'$ [Tol] (bottom). Extended structures of $[Tol][Cu_3]'$ [Tol] and $[Tol][Ag_3]'$ [Tol] are given on the left side of each molecule. Reprinted with permission from Dias, HV; Singh, S; Campana, CF. *Inorg Chem.* **2008**, *47*, 3943-5.

A final example related to stacking involves the strong quadrupolar interaction of the rather strong octopus π -acid $\{[3,5-(n\text{-C}_3\text{F}_7)_2\text{Tz}]\text{Ag}\}_3$ with π -bases of both apo- and Pt(II) porphyrin molecules, as shown in Scheme 10 and Figure 33.⁵⁹



Scheme 10. a) Molecular structure and b) molecular electrostatic potential (MEP) of H₂OEP, PtOEP and $\{[3,5-(n\text{-C}_3\text{F}_7)_2\text{Tz}]\text{Ag}\}_3$ (**1**); OEP = 2,3,7,8,12,13,17,18-octaethyl-21H,23H-porphine. c) Double-octopus assembly **2** formation by quadrupole-quadrupole interactions and guest inclusion by a semi-linear non-aromatic guest (i), an aromatic monomer guest alone (ii), or both an aromatic π -dimer and aromatic monomer. Reprinted with permission from Yang, C.; Arvapally, R. K.; Tekarli, S.; Gustavo, A.; Salazar, M.; Elbjeirami, O.; Wang, X.; Omary, M. A. *Angew Chem. Int. Ed.* **2015**, 54, 4842.

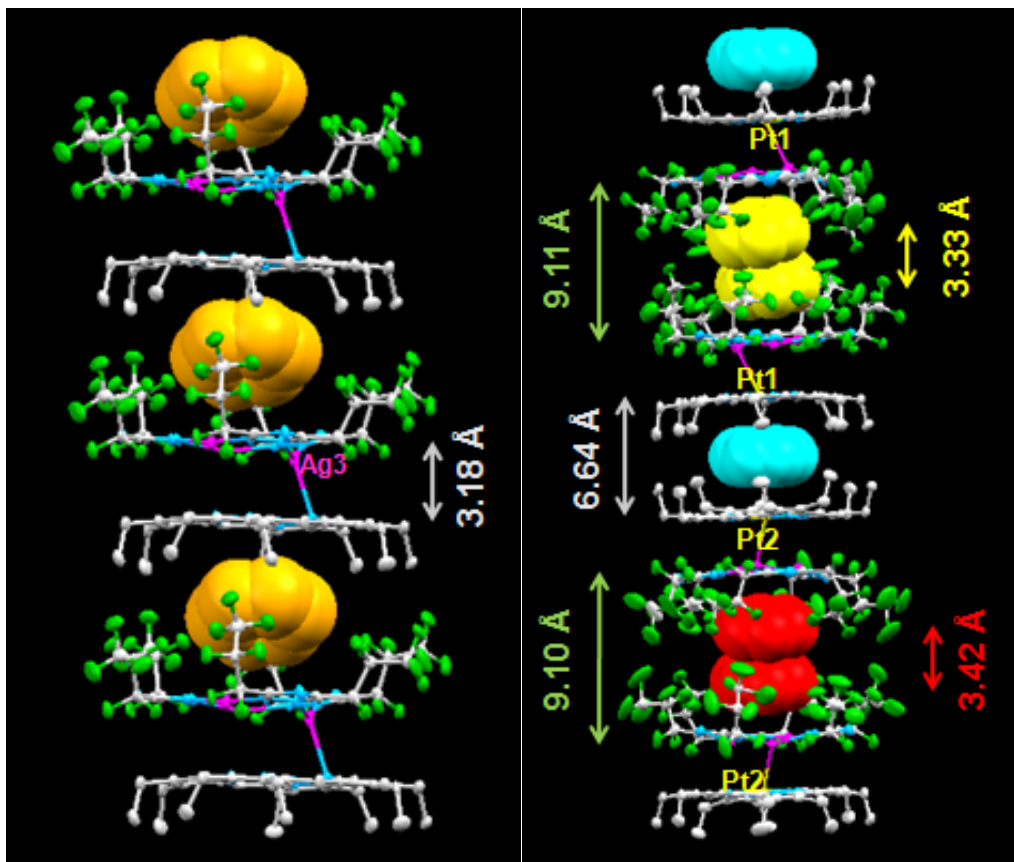


Figure 33. Supramolecular stacking diagrams in crystals of $[1 \cdot \text{H}_2\text{OEP}] \cdot \text{C}_6\text{H}_6$ and $[1 \cdot \text{PtOEP}] \cdot (\text{C}_6\text{H}_6)_{1.5}$ (OEP = 2,3,7,8,12,13,17,18-octaethyl-21H,23H-porphine). Crystallographically-independent benzene molecules are illustrated via space-filling models. Reprinted with permission from Yang, C.; Arvapally; R. K.; Tekarli; S.; Gustavo, A.; Salazar, M.; Elbejirami, O.; Wang, X.; Omary, M. A. *Angew Chem. Int. Ed.* **2015**, *54*, 4842.

7. BREAKAGE OF CYCLOTRIMER SELF-ASSEMBLY BY HETEROMETAL BONDING ATTRACTIONS.

7.1 Self-Assembly by Metallophilic Attraction between Gold(I) and Silver(I).

The existence in some extent of stacking in solution of trinuclear metallocyclic products has already been revealed by mean of PGSE measurements.⁶⁰ Mixing methylene solutions of π -basic cyclic trinuclear compounds of Au(I), such as $[(\text{carb})\text{Au}]_3$ or $[(\text{bzim})\text{Au}]_3$, where carb = N-methyl-methoxy-carbeniate and bzim = 1-benzylimidazole, with methylene solutions of π -acid cyclic trinuclear compounds of Ag(I) or Cu(I), the breaking of the π - π stacking affords to heterobimetallic compounds

of the type Au_2Ag , Ag_2Au or Au_2Cu and AuCu_2 , depending on the stoichiometric ratio of the starting **cyclotrimers**. In the solid state, these latter show the formation of dimer of **cyclotrimers** with very short intermolecular metal-metal bond length.

In the reaction of **gold(I) carbeniate or 1-beyzimidazolate cyclotrimers** with the silver(I) pyrazolate $[\text{Ag}(\mu\text{-3,5-Ph}_2\text{Pz})]_3$, the formation of crystalline products consisting of mixed-ligand, mixed-metal dimeric products $[\text{Au}(\text{carb})\text{Ag}_2(\mu\text{-3,5-Ph}_2\text{Pz})_2]$, $[\text{Au}_2(\text{carb})_2\text{Ag}(\mu\text{-3,5-Ph}_2\text{Pz})]\text{CH}_2\text{Cl}_2$, $[\text{Au}(\text{bzim})_2\text{Ag}_2(\mu\text{-3,5-Ph}_2\text{Pz})]$, and $[\text{Au}_2(\text{bzim})_2\text{Ag}(\mu\text{-3,5-Ph}_2\text{Pz})]$ were observed.⁶¹ They have been characterized by elemental analysis and ^1H NMR and ESI mass spectrometry in addition to the X-ray crystal structures. The breaking of the homonuclear **cyclotrimer** stacking results in a new **heteronuclear cyclotrimer** stacking with very short metal-metal **distance**. The crystalline products were not the expected acid-base adducts but rearranged dimeric, trinuclear products. Thus $[\text{Ag}(\mu\text{-3,5-Ph}_2\text{Pz})]_3$ behaves differently from the π -acid complex $[\text{Hg}(\text{C}_6\text{F}_4)]_3$ which forms exclusively stacking products. It is suspected that the lability of the M-N bond (M) Au, Ag in these complexes results in the subsequent cleavage of the cyclic complexes to produce the product statistically expected from the stoichiometry of materials used. The heterobimetallic dimer of **cyclotrimers** exhibits Au-Ag distance ranging within 3.08 and 3.40 Å.

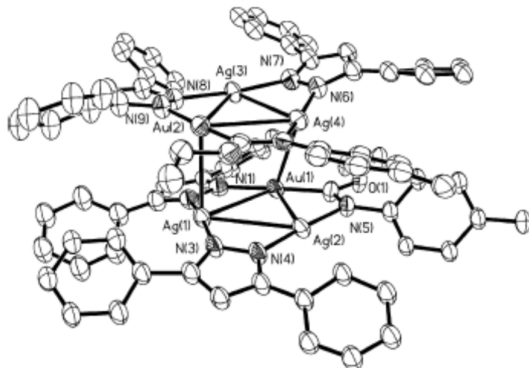
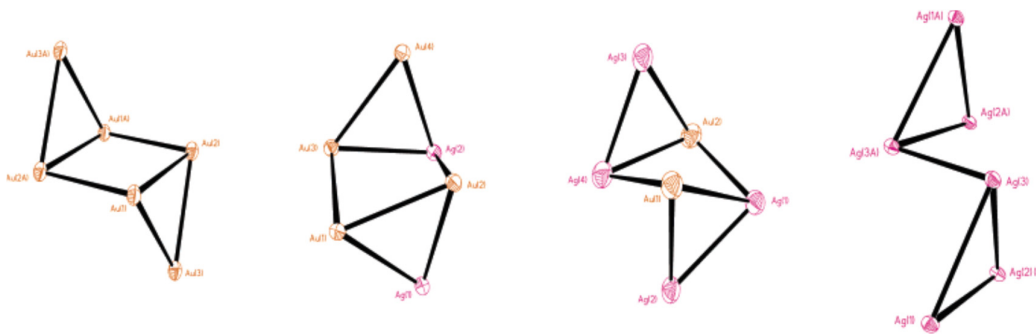


Figure 34. ORTEP diagram for a dimer-of-trimer unit of $[\text{Au}(\text{carb})\text{Ag}_2(\mu\text{-3,5-Ph}_2\text{Pz})_2]_2$. **Reprinted** with permission from Mohamed A. A., Galassi, R.; Papa, F. Burini, A., Fackler, J. P. Jr. *Inorg. Chem.* **2006**, 45, 7770–7776

Most of the metal frameworks adopted in the crystal structures of these compounds are similar to those reported for the parent Au(I) or Ag(I) trimers, but in some cases the puckering of the metal metal interaction differs largely affording to distorted metal frameworks such as those reported in Scheme 11 depending on the type of the metal arrangement.



Scheme 11. Intermetallic Arrangements of the metal atoms in the dimers of gold(I) carbeniate cyclotrimers (first from left side), $[\text{Au}_2(\text{carb})_2\text{Ag}(\mu\text{-3,5-Ph}_2\text{Pz})]_2\text{CH}_2\text{Cl}_2$ (second from left side), $[\text{Au}(\text{carb})\text{Ag}_2(\mu\text{-3,5-Ph}_2\text{Pz})]$ (third from the left side) and the starting $\text{Ag}(\text{I})$ 3,5-diphenyl-pyrazolate cyclotrimer (last from left side); carb = N-methyl-methoxy-carbeniate and 3,5-Ph₂Pz = 3,5-diphenyl-pyrazolyl-1H. Reprinted with permission from Mohamed A. A., Galassi, R.; Papa, F. Burini, A., Fackler, J. P. Jr. *Inorg. Chem.* **2006**, *45*, 7770–7776

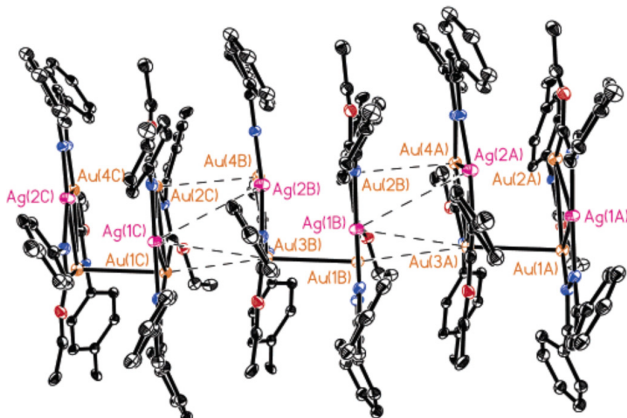
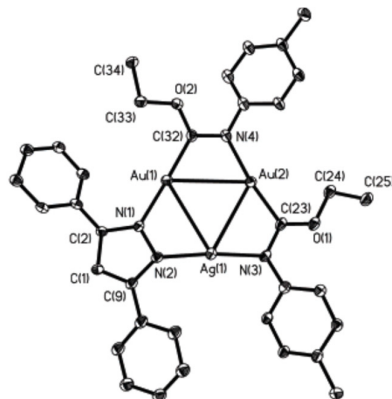


Figure 35. ORTEP diagram of an asymmetric unit of $[[\text{Au}_2(\text{carb})_2\text{Ag}(\mu\text{-3,5-Ph}_2\text{Pz})]_2$ (top) and whole of the metal metal interactions in the packing of the dimer of cyclotrimers (bottom). Reprinted with permission from Mohamed A. A., Galassi, R.; Papa, F. Burini, A., Fackler, J. P. Jr. *Inorg. Chem.* **2006**, *45*, 7770–7776

7.2 Self-Assembly by Metallocophilic Attraction or Polar-Covalent Bonding between Gold(I) and Copper(I).

The reaction of the π -basic gold(I) with 1-benzylimidazolate cyclotrimer, $[\text{Au}(\text{bzim})]_3$, with the π -acid $[(3,5-(\text{CF}_3)_2\text{Pz})\text{Cu}]_3$ confirmed the interaction of these trimers in solution according to their acid-base properties. Reactions of π -basic $[\text{Au}(\mu-\text{C}^2,\text{N}^3-\text{bzim})]_3$, $[\text{Au}(\mu-\text{C}^2,\text{N}^3-\text{etim})]_3$, or $[\text{Au}(\mu-\text{C}^2,\text{N}^3-\text{meim})]_3$, where etim = 1-ethylimidazolyl-2yl; meim = 1-methyl-imidazolyl-2yl and bzim = 1-benzylimidazolyl-2yl, with π -acidic $[\text{Cu}(\mu-3,5-(\text{CF}_3)_2\text{Pz})]_3$ in dichloromethane under ambient conditions attain new heterobimetallic complexes of the type Au_2Cu and Cu_2Au depending on the nature of the substituents in the imidazolate ligand as well as the metal framework.⁶² Noteworthy, solely in a case, when the $[\text{Au}(\text{bzim})]_3$ and $[\text{Cu}(\mu-3,5-(\text{CF}_3)_2\text{Pz})]_3$ were mixed in 1 : 1 ratio a π - π stacking product was obtained in addition to the Au_2Cu product which results to be stable in the solid state and in solution. Apart the π - π stacking product, all the compounds show peculiar emissive features. In Figure 36 the ORTEP plot of the crystal structure for the complex obtained by the reaction of $[\text{Au}(\text{bzim})]_3$ and $[\text{Cu}(\mu-3,5-(\text{CF}_3)_2\text{Pz})]_3$ in 2 : 1 mole ratio shows the mixed metal framework and the exchange of the ligands indeed, as the pyrazolate $[3,5-(\text{CF}_3)_2\text{Pz}]^-$, is bridging the two gold atoms through the nitrogen atoms, while the bzim are bridging the gold atoms with the Carbon atoms, and the copper atom with the nitrogen atoms.

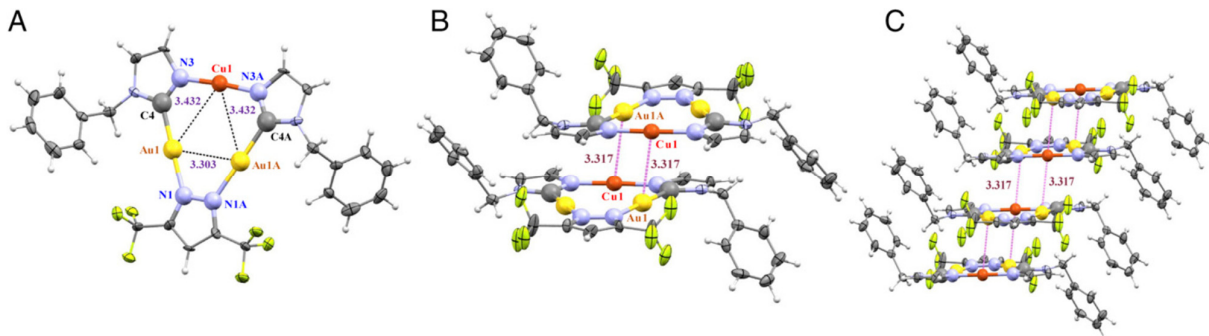


Figure 36. (A) ORTEP plot for the crystal structure for one molecule of complex 1. (B) Dimer-of-cyclotrimer formation found in the stacking of $[(\text{bzim})_2(\mu-3,5-(\text{CF}_3)_2\text{Pz})\text{Au}_2\text{Cu}]$. (C) Fragment of crystal packing of $[(\text{bzim})_2(\mu-3,5-(\text{CF}_3)_2\text{Pz})\text{Au}_2\text{Cu}]$ along the b axis.

The reaction between coinage metals cyclotrimers may afford π - π stacking products where the starting cyclotrimer framework are conserved, as well as simultaneous metal atoms and bridging ligand exchange, as observed in this last case. The nature of the final product is affected by the mole ratio of the trimers in the solution and the yields of the products are quite high. The stability of these

compounds in the solid state and the intensity of the phosphorescence of the solids are impressive. In a special case, when the imidazole contains the ethyl group as substituent, the quantum yield on the emission is near to the unit, while the spectral profiles are relatively simple for $[(\text{etim})_2(3,5-(\text{CF}_3)_2\text{Pz})\text{Au}_2\text{Cu}]$ crystalline powder showing a single emission in the green region with a peak maximum at 510 nm for the broad, unstructured band and a single excitation feature at 330 nm that is independent of temperature or excitation wavelength. These are assignable to $\text{T}_1 \rightarrow \text{S}_0$ phosphorescence emission and $\text{S}_0 \rightarrow \text{T}_1$ spin-forbidden excitation, respectively, whereas the rise in the blue edge of the excitation spectrum is the $\text{S}_0 \rightarrow \text{S}_1$ spin-allowed absorption given the microsecond lifetimes (6–7 μs) and the higher-energy solution absorption at $\lambda_{\text{max}} \leq 300 \text{ nm}$.

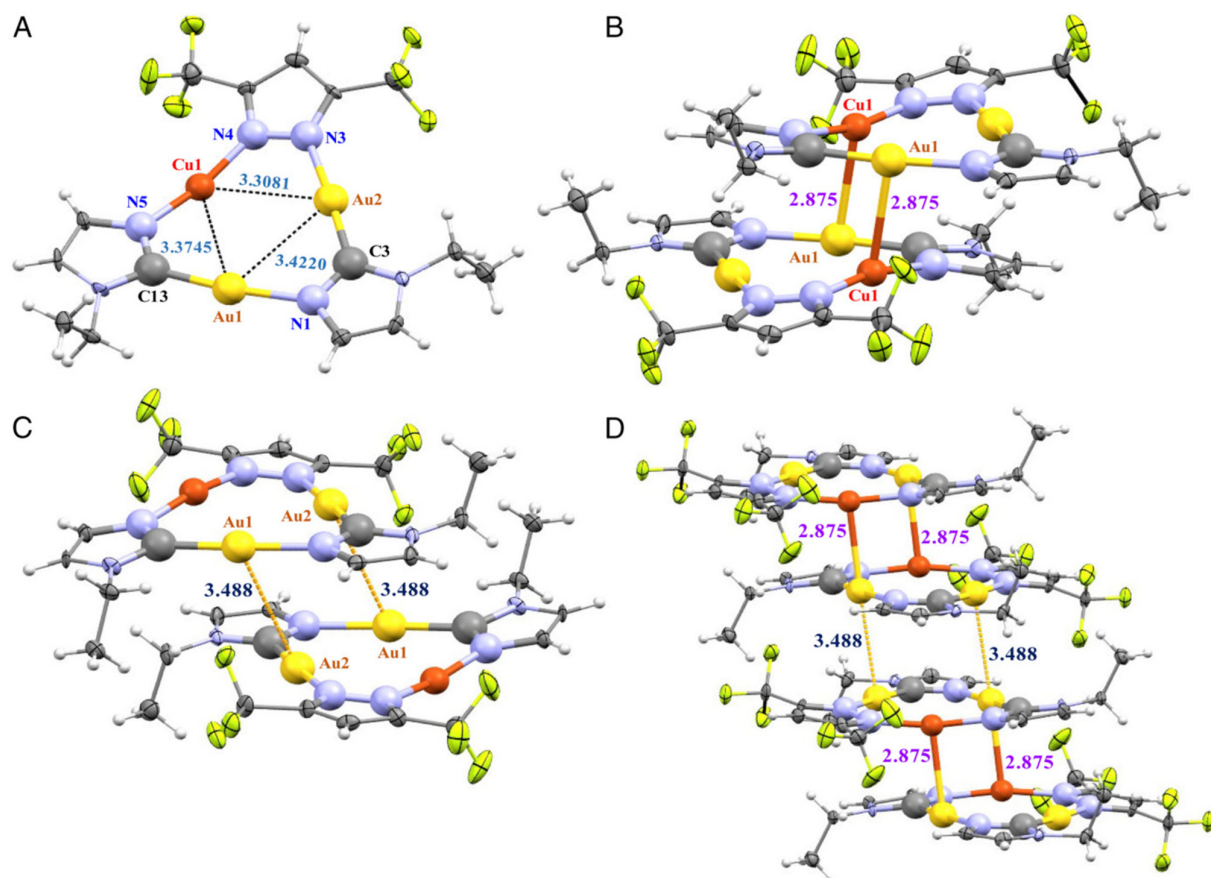


Figure 37. (A) ORTEP plot for the crystal structure for half the molecule, representing each monomer-of-cyclotrimer unit, $[(\text{etim})_2(3,5-(\text{CF}_3)_2\text{Pz})\text{Au}_2\text{Cu}]$. (B) Crystal structure for one full molecule of the cyclotrimer $[(\text{etim})_2(3,5-(\text{CF}_3)_2\text{Pz})\text{Au}_2\text{Cu}]$. (C) A fragment of the crystal packing along the a axis. (D) Extended crystal packing of the cyclotrimer $[(\text{etim})_2(3,5-(\text{CF}_3)_2\text{Pz})\text{Au}_2\text{Cu}]$ molecules along the a axis; $\text{etim} = 1\text{-ethyl-imidazolyl-2yl}$.

The structure of **cyclotrimer** $[(\text{etim})_2(3,5-(\text{CF}_3)_2\text{Pz})\text{Au}_2\text{Cu}]$ is shown in Figure 37 and it shows the principal evidence of an unprecedented ligand-unassisted short distance of $2.8750(8)$ Å between the two crystallographically equivalent Cu(1) atoms with their next-neighbor two crystallographically congruent Au(1) atoms in the adjacent cyclotrimers, as shown in the crystal structure of compound **cyclotrimer** $[(\text{etim})_2(3,5-(\text{CF}_3)_2\text{Pz})\text{Au}_2\text{Cu}]$ (Fig. 37 B and D). This is the shortest intermolecular distance ever reported between any two d^{10} centers so as to deem it as a “metal–metal bond” instead of a metal metal interaction. The affinity of copper to gold is manifest by a rather significant under deviation from linearity in the N(4)-Cu(1)-N(5) angles of $167.5(2)^\circ$ in the two adjacent cyclotrimers to effect attractive shortening of the two Cu(1)–Au(1) ligand-unassisted covalent bonds. The attractive deviation from linearity can be used to substantiate the involvement of the $3d\pi$ - $5d\pi$ component of the Cu(I)–Au(I) (or d^{10} – d^{10}) bonding claimed for the Cu(1)–Au(1) ligand-unassisted polar-covalent bonds **in** $[(\text{etim})_2(3,5-(\text{CF}_3)_2\text{Pz})\text{Au}_2\text{Cu}]$ crystals in addition to the $3d\sigma$ – $5d\sigma$ component. The discussion of unassisted polar covalent bonds for Cu-Au in this compound is supported by theoretical calculations with a calculated value for the BE of $12,000$ – $15,000$ cm^{−1} corresponding to 34 – 43 kcal/mol. These Au-Cu BE values are commensurate with the bond energies of *bona fide* single M–M covalent bonds such as those in Cotton’s classical d^1 – d^1 or d^9 – d^9 ground-state species.⁶³

8. PROPERTIES AND POTENTIAL APPLICATIONS OF COINAGE METALLACYCLES

8.1 Luminescence Properties

In these recent years the pyrazolate and imidazolate **cyclotrimers** have garnered a considerable interest in particular for their fascinating properties and potential applications. For example several $[\text{M}_3(\mu-\text{Pz}^{\text{R}})_3]$ are luminescent as single crystals or thin films, upon irradiation with UV-light.^{9b,44} Figure MM shows an example with the same R (CF₃) but different M (Cu, Ag, or Au), giving rise to multiple remarkable emissions for each complex upon temperature variation. The lowest-energy emission trend followed the relative triplet energy of the three monovalent coinage metals, which are then subject to similar excimeric stabilization upon photoexcitation.

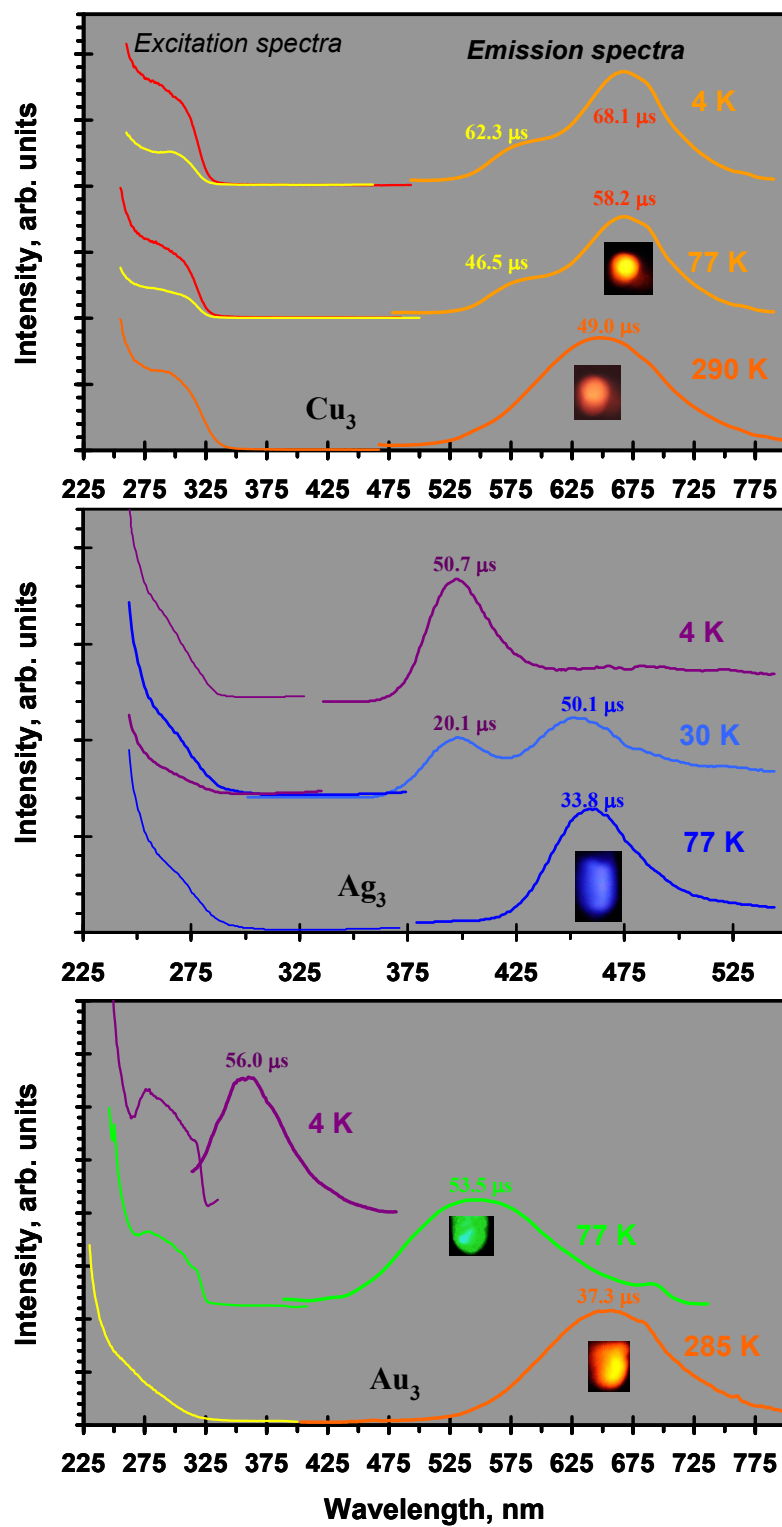


Figure 38. Temperature-dependent photoluminescence spectra for single crystals of $[M_3]$ (i.e., $[M(\mu\text{-}3,5\text{-(CF}_3)_2\text{Pz})_3]$ with $M = \text{Cu, Ag or Au}$). Reproduced with permission from Dias, H. V. R.; Diyabalanage, H. V. K.; Eldabaja, M. G.; Elbjeirami, O.; Rawashdeh-Omary, M. A.; Omary, M. A. *J. Am. Chem. Soc.* **2005**, *127*, 7489.

As another example for the same metal (M) but different R groups, the emission spectra of different trinuclear copper(I) compounds $[\text{Cu}(\mu\text{-3-(R),5-(R')Pz})_3]$ vary substantially, allowing compounds emitting red, yellow, green, or blue light making an appropriate choice of the ligands.^{9b} Another striking feature in the solid state luminescence data in Figure 38 is the “luminescence thermochromism” for which the most dramatic changes are for $[\text{Cu}(\mu\text{-3,5-(i-Pr)}_2\text{Pz})_3]$, in which cooling from room temperature to 77 K changes the emission color from orange ($\lambda_{\text{max}} = 662 \text{ nm}$) to green ($\lambda_{\text{max}} = 562 \text{ nm}$) while at intermediate temperatures, the sample’s emission appears yellow.

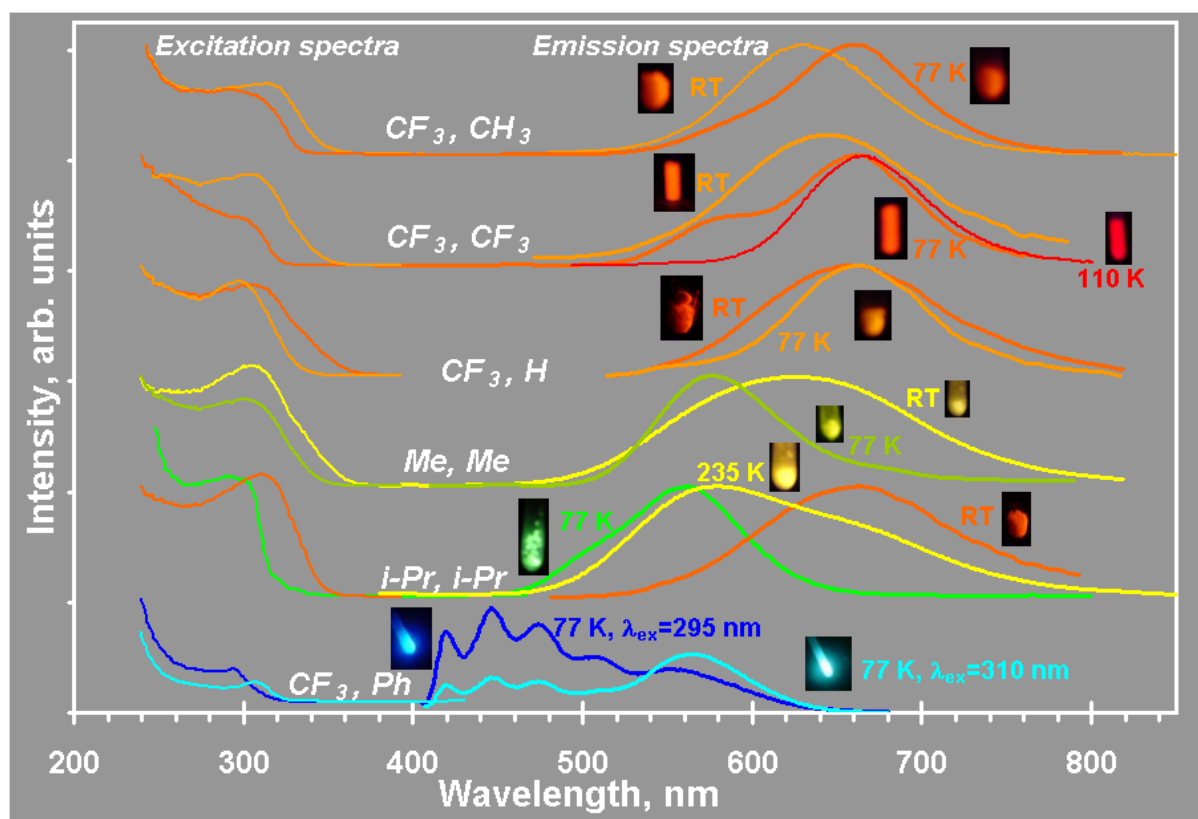


Figure 39. Luminescence spectra for single crystals of trinuclear $[\text{Cu}(\mu\text{-3-(R),5-(R')Pz})_3]$ complexes. The compounds are identified by the R and R' substituents. Reproduced with permission from Dias, H. V. R.; Diyabalanage, H. V. K.; Eldabaja, M. G.; Elbjeirami, O.; Rawashdeh-Omary, M. A.; Omary, M. A. *J. Am. Chem. Soc.* **2005**, *127*, 7489.

The luminescence is also sensitive to solvents and to different concentration. A detailed study has been performed on frozen solution of the copper(I) cyclotrimer $[\text{Cu}(\mu\text{-3,5-(CF}_3)_2\text{Pz})_3]$ (Figure 39).^{9a} The changes in the luminescence energies in different solvents are related to both the extent of

excited-state association of $[\text{Cu}(\mu\text{-3,5-(CF}_3)_2\text{Pz})]_3$ and the different electronic structure of various $\{[\text{Cu}(\mu\text{-3,5-(CF}_3)_2\text{Pz})]_3\text{: solvent}\}$ complexes.

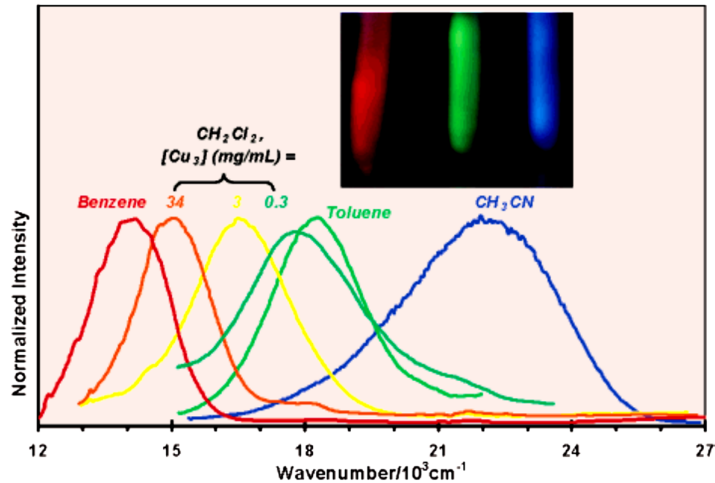


Figure 40. Representative emission spectra of frozen solutions (77 K) of $[\text{Cu}(\mu\text{-3,5-(CF}_3)_2\text{Pz})]_3$ versus solvents and concentrations. [Reproduced with permission from Dias, H. V. R.; Diyabalanage, H. V. K.; Eldabaja, M. G.; Elbeirami, O.; Rawashdeh-Omary, M. A.; Omary, M. A. *J. Am. Chem. Soc.* **2005**, 127, 7489.](#)

The cyclotrimer $[\text{Au}(3,5-i\text{-Pr}_2\text{Tz})]_3$, where $3,5-i\text{-Pr}_2\text{Tz} = 3,5\text{-diisopropyl-1,2,4-triazolyl-1H}$, exhibits remarkable changes in the luminescence color upon temperature change in the solid state or concentration adjustment in fluid solution, owing to a change in symmetry from three-fold to two-fold in the dimer-of-trimer aggregate, whereas a dissociated monomer of cyclotrimer has quenched luminescence (Figure 41).⁴⁵

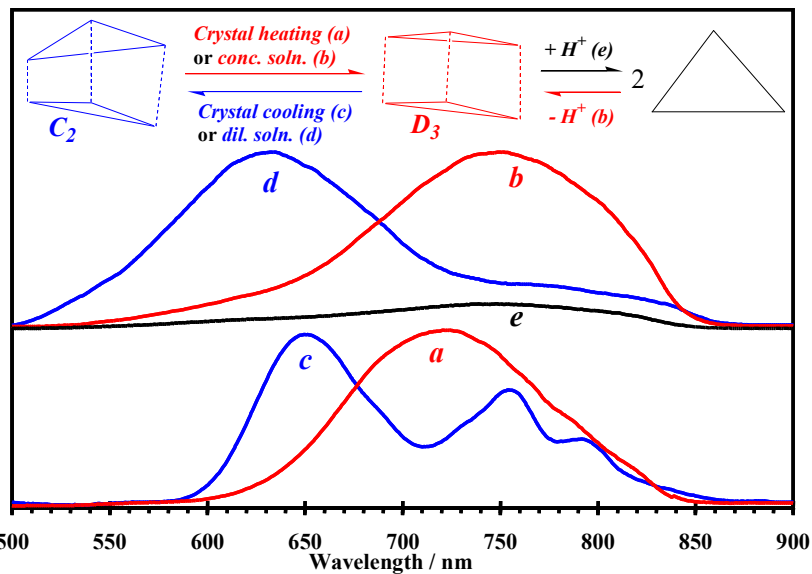


Figure 41. Luminescence spectral changes for $[\text{Au}(3,5\text{-}i\text{-Pr}_2\text{Tz})]_3$ upon temperature change in the solid state or concentration adjustment in fluid solution (dichloromethane). Adding the organic acid resorcinol leads to quenching of the fluid solution luminescence, presumably due to the dissociation of the dimer-of-trimer aggregate into a non-luminescent monomer-of-trimer complex. **Reproduced with permission from Yang, C.; Messerschmidt, M.; Coppens, P.; Omary, M. A. *Inorg. Chem.* 2006, 45, 6592.**

Besides the polar-covalent vs metallophilic bonding significance of the work by Omary, Galassi, and co-workers on heterobimetallic complexes,⁶² the symmetry reduction in those complexes versus their homometallic analogues was found to lead to a remarkable increase in the solution extinction coefficient and the solid-state photoluminescence quantum yield, the latter attaining near-unity (97%) for the complex $[(\text{meim})_2(3,5\text{-}(\text{CF}_3)_2\text{Pz})\text{Au}_2\text{Cu}]$; Table 1 summarizes these spectral results.

Table 1: Photophysical parameters for homometallic vs heterobimetallic complexes.^a

Complex	$\epsilon (\text{M}^{-1}\text{cm}^{-1})$	$\Phi_{\text{PL}} (\%)$
$[\text{Au}(\mu\text{-C}^2, \text{N}^3\text{-MeIm})]_3$	4,800	56.88 ± 3.58
$\text{Au}(\mu\text{-C}^2, \text{N}^3\text{-BzIm})]_3$	7,880	N/A
$[\text{Cu}(\mu\text{-3,5-(CF}_3)_2\text{Pz})]_3$	2,600	82.17 ± 0.16
$[\text{Au}_2(\mu\text{-C}^2, \text{N}^3\text{-BzIm})_2\text{Cu}(\mu\text{-3,5-(CF}_3)_2\text{Pz})]$	11,560	85.16 ± 1.57
$[\text{Au}_2(\mu\text{-C}^2, \text{N}^3\text{-MeIm})_2\text{Cu}(\mu\text{-3,5-(CF}_3)_2\text{Pz})]$	20,590	97.13 ± 0.80

[Au(μ -C ² ,N ³ -MeIm)Cu ₂ (μ -3,5-(CF ₃) ₂ Pz) ₂]	2,850	17.51 \pm 0.25
{Au(μ -C ² ,N ³ -BzIm)} ₃ {Cu(μ -3,5-(CF ₃) ₂ Pz)} ₃	N/A	N/A
[Au ₄ (μ -C ² ,N ³ -EtIm) ₄ Cu ₂ (μ -3,5-(CF ₃) ₂ Pz) ₂]	17,260	90.31 \pm 0.70
[Au(μ -C ² ,N ³ -EtIm)] ₃	3,950	N/A

^a: Notation: ε = solution extinction coefficient. Φ_{PL} = solid-state photoluminescence quantum yield.

Metallophilic bondings play a central role on the emission bands of gold complexes and in the construction of supramolecular architectures. One example that highlights the importance of the intermolecular aurophilic interactions on the luminescence properties in trimeric gold(I) pyrazolates has been reported by Raptis et al.⁵ The solid samples of [Au(μ -Pz)]₃ and [Au(μ -4-(Me)Pz)]₃ emit under UV irradiation at ambient temperature, red luminescence with maxima at 626 and 631 nm, respectively. On the other hand, [Au(μ -3-(Me),5-(Ph)Pz)]₃ does not luminesce under the same conditions and no Au \cdots Au intertrimer contacts are present in the crystal structure. This implies that the luminescence of [Au(μ -Pz)]₃ and [Au(μ -4-(Me)Pz)]₃ arises from the intermolecular aurophilic interactions.

A potential application for the **coinage metals cyclotrimers** with luminescence properties is for emitting materials in molecular electronic devices, especially complexes with fluorinated ligands because fluorination increases their volatility, thus facilitating thin-film fabrication. Besides the luminescence being from the trimers themselves, as shown in the above examples, an interesting example pertained to lighting up other molecules complexed to the trimer. This is illustrated by the “lighting up” of Pt-OEP in air upon complexation with {[3,5-(*n*-C₃F₇)₂Tz]Ag}₃, as shown in Figure 42.

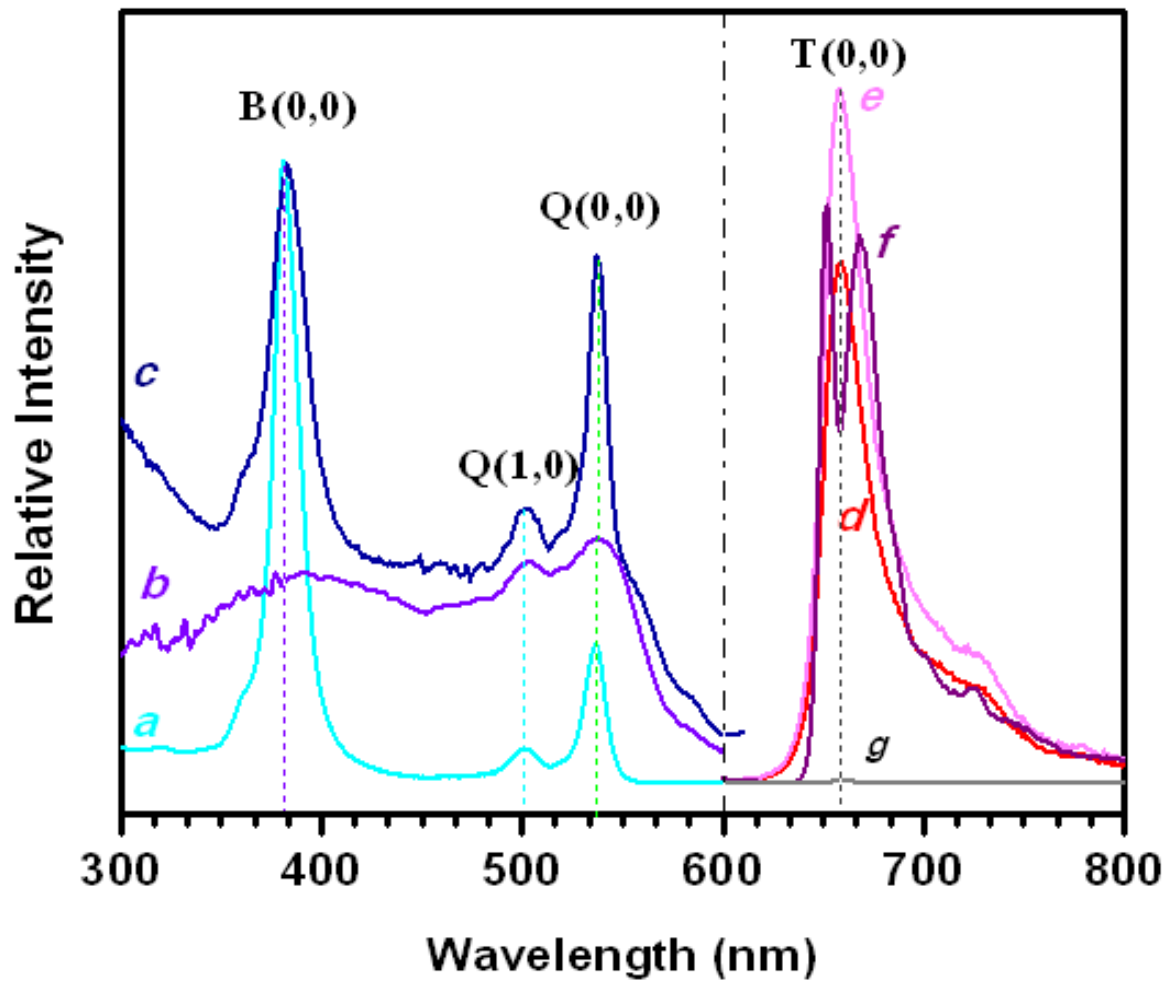


Figure 42. Solution absorption in dichloromethane (**a**) and solid-state diffuse reflectance (**b**), excitation (**c**, $\lambda_{\text{em}} = 660$ nm) and photoluminescence spectra of single crystals of $[\{[3,5-(n\text{-C}_3\text{F}_7)_2\text{Tz}]\text{Ag}\}_3\cdot\text{PtOEP}]$ ($\lambda_{\text{ex}} = 540$ nm) under: (**d**) ambient air at room temperature ($\tau = 55$ μs); (**e**) 100% N_2 at room temperature ($\tau = 64$ μs); and (**f**) at 77 K in air ($\tau = 93$ μs). The gray trace (**g**) shows the vanishing luminescence of the PtOEP solid under ambient air and room temperature, $\lambda_{\text{ex}} = 540$ nm and the same instrument settings (intensity was too low to measure a lifetime). **Reproduced with permission from Yang, C.; Arvapally, R. K.; Tekarli, S.; Gustavo, A.; Salazar, M; Elbjeirami, O.; Wang, X.; Omary, M. A. *Angew Chem. Int. Ed.* **2015**, *54*, 4842-6.**

Although this review does not emphasize luminescence sensing studies, given much of those have been included in a previous review by Rawashdeh-Omary,⁶⁴ we include one example from the recent study of the same author's group in Figure 43.

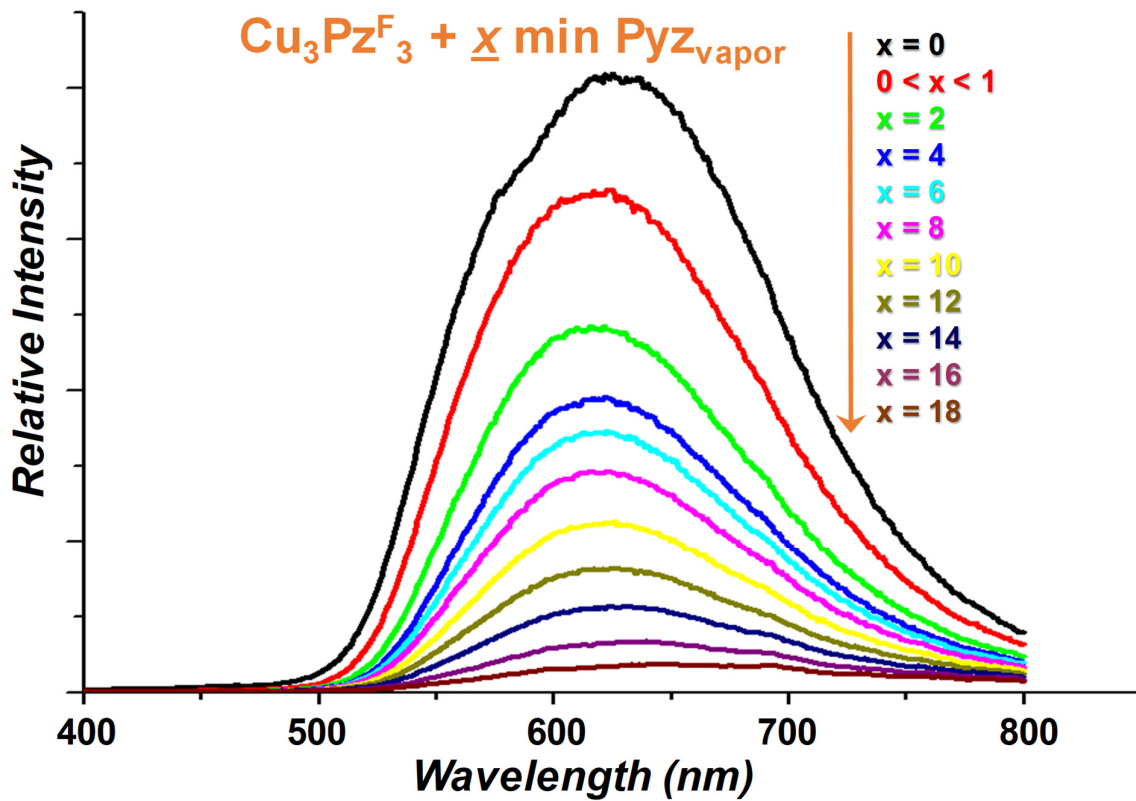
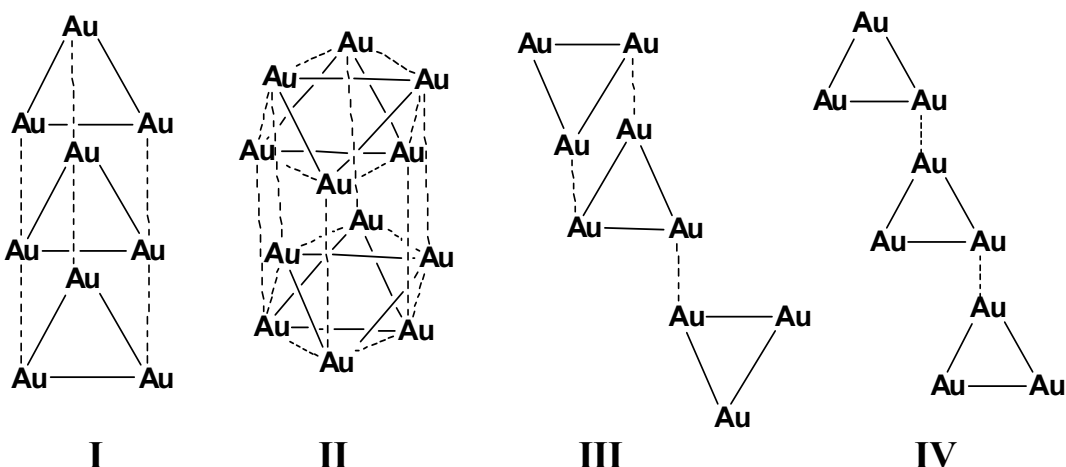


Figure 43. Quenching of the bright orange phosphorescence of $\{[3,5-(CF_3)_2Pz]Cu\}_3$ upon sublimation of solid pyrazine under ambient conditions. *Reproduced with permission from Rawashdeh-Omary, M. A. Comm. Inorg. Chem., 2012, 33, 88-101.*

Luminescent supramolecular fibres^{6a} and gels^{6b} have been also prepared, containing stacks of $[Au_3(\mu-(Me_2R')Pz)_5]_2$ trimers (R' is a lipophilic or dendritic group derived from $\{3,5$ -dihydroxyphenyl}methyl). The emission in the gels is reversibly quenched upon heating or cooling about the gel-to-sol transition temperature.^{6b} This emission is also switched from red to blue light upon addition of chloride, which intercalates within the cluster stacks. The addition of Ag^+ to the chloro gels recovers the red emission as the chloride is removed.^{6b} Several columnar mesophases containing gold(I) pyrazolide trimers with long-chain substituents have been described^{37,40} some of them are liquid crystalline at room temperature.^{41,42}

Carbeniate trinuclear derivatives show peculiar features in the field of emissive properties. As an example $[Au_3(Me-N=C-OMe)_3]$ displays an interesting solvoluminescence phenomenon: upon prior irradiation of a crystalline sample with near-UV light, a bright burst of yellow light is observed spontaneously (remaining after irradiation stops) when solvent is introduced. The intensity of the

luminescence is greatest for the best solvent for $[\text{Au}_3(\text{Me}-\text{N}=\text{C}-\text{OMe})_3]$, e.g., chloroform and methylene chloride. In the solid state, $[\text{Au}_3(\text{Me}-\text{N}=\text{C}-\text{OMe})_3]$ displays multiple crystalline polymorphs: hexagonal ($P6/m$) (which has eclipsed (I) and staggered (II) stacks), triclinic ($P\bar{1}$) (III), and monoclinic ($C2/c$).^{3a,65} Other polymorphic forms of gold carbeniate complexes, $[\text{Au}_3(^n\text{Pe}-\text{N}=\text{C}-\text{OMe})_3]$ (IV) and $[\text{Au}_3(^i\text{Pr}-\text{N}=\text{C}-\text{OMe})_3]$, with n -pentyl (^nPe) and isopropyl (^iPr) substituents on the carbeniate ligand, were recently reported.⁴¹ These polymorphs differ in the way in which the trimer moieties interact with one another. In the hexagonal form of $[\text{Au}_3(\text{Me}-\text{N}=\text{C}-\text{OMe})_3]$, which has a broad emission with a long-wavelength excitation and is the only form to display solvoluminescence, the trimers form two stack types, I and II (see Scheme 12). The hexagonal polymorph I shows an eclipsed stacking pattern with close Au—Au interactions forming a columnar extended chain, $d_{\text{Au}-\text{Au}} = 3.346 \text{ \AA}$ (intermolecular) between pairs of trimers, and $d_{\text{Au}-\text{Au}} = 3.308 \text{ \AA}$ (intramolecular) within the trimer.



Scheme 12. Possible stacking arrangements found in $[\text{Au}_3(\text{R}-\text{N}=\text{C}-\text{OR}')_3]$ complexes. Trinuclear complexes are represented by triangles, and intertrimer aurophilic interactions by dashed lines. Polymorphs are named as eclipsed (I), disordered staggered (II), chair conformation (III), and stair – step conformation (IV). *Reproduced with permission from McDougald, R. N.; Chilukuri, B.; Jia, H.; Perez, M. R.; Rabaâ, H.; Wang, X.; Nesterov, V. N.; Cundari, T. R.; Gnade, B. E.; Omary, M. A. Inorg. Chem. 2014, 53, 7485*

8.2 Semiconductor Properties

Novel complexes such as $[\text{Au}_3(\text{Me}-\text{N}=\text{C}-\text{O}^n\text{Bu})_3]$, $[\text{Au}_3(^n\text{Bu}-\text{N}=\text{C}-\text{OMe})_3]$, $[\text{Au}_3(^n\text{Bu}-\text{N}=\text{C}-\text{O}^n\text{Bu})_3]$, and $[\text{Au}_3(^c\text{Pe}-\text{N}=\text{C}-\text{OMe})_3]$, plus further investigation of the $[\text{Au}_3(\text{Me}-\text{N}=\text{C}-\text{OMe})_3]$ hexagonal polymorph⁶⁵ (where ^nBu = normal butyl and ^cPe = cyclopentyl) have been studied also for their conductive properties.^{44,66} As concern the $[\text{Au}_3(\text{Me}-\text{N}=\text{C}-\text{OMe})_3]$, it should be remarked that only

the hexagonal crystal system exhibits semiconductive properties while for the triclinic and the monoclinic polymorphs they are irrelevant as it was already ascertained for the solvoluminescence phenomenon.

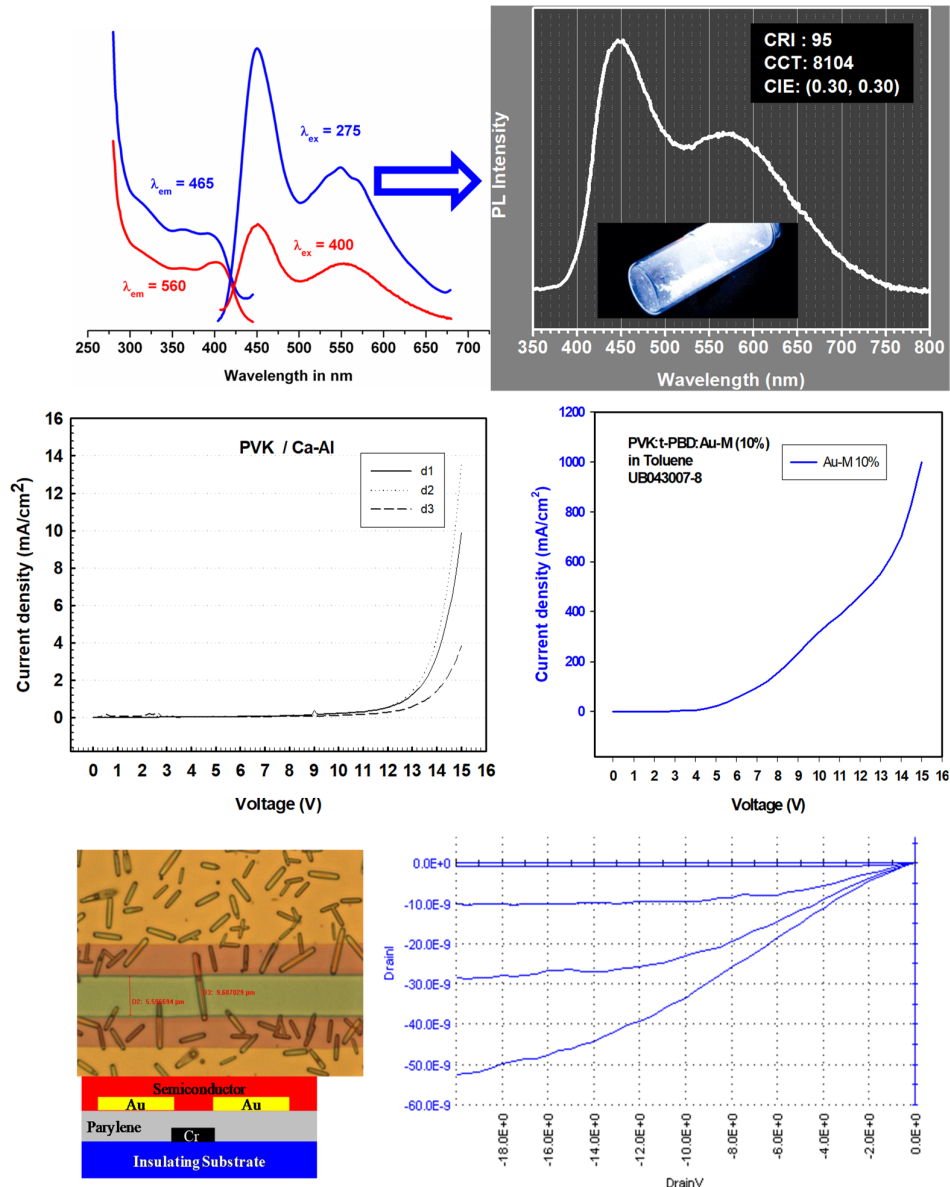


Figure 44. (a; top panel) Solid state photoluminescence spectra for the hexagonal polymorph of $[\text{Au}_3(\text{Me}-\text{N}=\text{C}-\text{OMe})_3]$ at 298 K. The photograph shows the white emission color rendered upon irradiation with 365 nm irradiation from a hand-held UV lamp. (b; middle panel) Current density-voltage (JV) curves for Schottky diodes with device structures: Left - . Right - ITO/PEDOT:PSS/10% hexagonal $[\text{Au}_3(\text{Me}-\text{N}=\text{C}-\text{OMe})_3]$: PVK/Ca-Al. Note the dramatic increase in electrical conductivity due to the hole current of the PVK thin film upon p-doping with $[\text{Au}_3(\text{Me}-\text{N}=\text{C}-\text{OMe})_3]$. (c; bottom

panel) IV curves for an organic field effect transistor (OFET) in which single needles of the trimer of hexagonal $[\text{Au}_3(\text{Me-N=C-OMe})_3]$ is the active semiconductor. The field effect shown in the right-side Figure clearly indicates that the trimer is a p-type semiconductor. Reproduced with permission from McDougald, R. N.; Chilukuri, B.; Jia, H.; Perez, M. R.; Rabaâ, H.; Wang, X.; Nesterov, V. N.; Cundari, T. R.; Gnade, B. E.; Omary, M. A. *Inorg. Chem.* **2014**, *53*, 7485

The preliminary diode and organic field effect transistor device data for the hexagonal $[\text{Au}_3(\text{Me-N=C-OMe})_3]$ complex are shown in Figure 44b and 44c, respectively.⁴⁴ The current density–voltage curves for Schottky diodes with device structures ITO/PEDOT:PSS/10% hexagonal $[\text{Au}_3(\text{Me-N=C-OMe})_3]$. PVK/Ca–Al are displayed (ITO = indium tin oxide, PEDOT:PSS = poly(3,4-ethylenedioxythiophene)- polystyrenesulfonate, PVK = poly(vinylcarbazole)).

There is a dramatic increase in electrical conductivity due to the hole current of the PVK host thin film upon p-doping with $[\text{Au}_3(\text{Me-N=C-OMe})_3]$ (Figure 44b). On the other hand, an organic field effect transistor in which single needles of the hexagonal $[\text{Au}_3(\text{Me-N=C-OMe})_3]$ trimer are the active semiconductor. The crystalline needles acted as molecular nanowires, as they have exhibited an unmistakable field effect shown on the right side of Figure 44c, clearly manifesting a p-type semiconducting behavior for this solid trimer. It was not possible to process contiguous thin films of hexagonal $[\text{Au}_3(\text{Me-N=C-OMe})_3]$ because of the solid material’s extremely low glass transition temperature ($< 50^\circ\text{C}$), insufficient solubility, and decomposition upon thermal evaporation attempts. The field effect data were reproduced several times for samples that varied in terms of numbers of needles crossing the two gold electrodes, hence the extent of current generated. However, the current magnitude in the pico–nano ampere range did not allow for quantification of the p-mobility of this material.⁴⁴ On the other hand, the conducting behavior of hexagonal $[\text{Au}_3(\text{Me-N=C-OMe})_3]$ was manifested in a different experiment by Balch and co-workers via formation of partially-oxidized long needles ascertained to have the formula $[\text{Au}_3(\text{Me-N=C-OMe})_3](\text{ClO}_4)_{0.34}$ upon electrochemical oxidation on the electrode surface.⁶⁶

Conclusions

Since the 1970s, after decades dedicated to the synthesis and characterization of elegant structures of cyclic trinuclear compounds of Au(I), Ag(I) and Cu(I) with azolate ligands (such as imidazolates, carbeniates, pyrazolates and triazolates), the investigation of this class of coordination compounds has slowly transformed into their supramolecular structure, the disruption thereof, and the concomitant optoelectronic properties and materials applications. In the development of such studies,

through sophisticated spectroscopic characterization carried out in parallel with computational studies, many aspects that are at the basis of the behavior and properties of these compounds have been comprehended. We can list as following the main noteworthy aspects:

- a) the extent of the homo- and hetero-metallophilic interactions and their implications in solid-state structures;
- b) the theoretical nature of the intra- and intermolecular metallophilic bonds;
- c) the structure and the energy of HOMO-LUMO orbitals and, therefore, the effect of metallophilic interactions for the understanding of the intriguing emissive properties; and
- d) the effect of the bridging ligands, and the substituents on them, on the metallophilic interactions.

From these studies it is clear that the energy associated with the metallophilic intermolecular interactions that often lead to the formation of dimer-of-trimers, oligomers or infinite columnar structures, estimated on a value ranging from a 10-15 kcal/mol as a hydrogen bond to a maximum value of about 43 kcal/mol for an arguably polar-covalent bond, it modulates the reactivity of these compounds and strongly affects their properties. In this review, the reactivity of the cyclic trinuclear compounds of Au(I), Ag(I) and Cu(I) with various azolate bridges have been described with respect to various types of reactant. The proposed reactions were classified according to the formation of π - π bonds, σ bonds, dipole-quadrupole or quadrupole-quadrupole moment interactions of greater magnitude than those found in starting material metallophilic interactions. In general, depending on the reactant, the breaking of the starting intermolecular metallophilic interactions is observed to give rise to a panorama of compounds where the starting triangular metal framework may be broken as well as it may be conserved. The reactivity observed in these studies is often “product favorite”, with the isolation of the products in stoichiometric yield; moreover, in some case, some reactions occur in hetero phase or in absence of solvent, making these syntheses environmental friendly. In all the cases herein overviewed, the obtained compounds exhibit novel properties with promising applications in sensing field and for the fabrication of optoelectronic devices, of which some pioneer examples have been discussed in this review.

Acknowledgments. This research has been supported by FAR of University of Camerino and CIRCSMB to R.G., the Welch Foundation (Departmental Grant for Texas Woman’s University to M.A.R.-O., Grant Y-1289 to H.V.R.D. and Grant B-1542 to M.A.O.), and the U.S. National Science

Foundation (Grant CHE-1413641, plus international supplement thereof Grant CHE-1545934 for the collaboration with R.G., to M.A.O. for research support and Departmental Grants CHE-1531468 and CHE-1726652 for equipment support).

References

1. (a) Burini, A.; Mohamed, A. A.; Fackler, J. P., Jr. *Comments Inorg. Chem.* **2003**, *24*, 253. (b) Omary, M. A.; Mohamed, A. A.; Rawashdeh-Omary, M. A.; Fackler, J. P., Jr. *Coord. Chem. Rev.* **2005**, *249*, 1372. C) Abdou, H. E.; Mohamed A. A; Fackler J. P; Burini, A.; Galassi, R.; Lopez-De-Luzuriaga, J. M; Olmos, M. E. *Coord. Chem. Rev.* **2009**, *253*, 1661.
2. (a) Tsipis, C. A.; Karagiannis, E. E.; Kladou, P. F.; Tsipis, A. C. *J. Am. Chem. Soc.* **2004**, *126*, 12916. (b) Tsipis, A. C.; Tsipis, C. A. *J. Am. Chem. Soc.* **2003**, *125*, 1136.
3. (a) Vickery, J. C.; Olmstead, M. M.; Fung, E. Y.; Balch, A. L. *Angew. Chem., Int. Ed. Engl.* **1997**, *36*, 1179. (b) Olmstead, M. M.; Jiang, F.; Attar, S.; Balch, A. L. *J. Am. Chem. Soc.* **2001**, *123*, 3260. (c) Hayashi, A.; Olmstead, M. M.; Attar, S.; Balch, A. L. *J. Am. Chem. Soc.* **2002**, *124*, 5791.
4. (a) Burini, A.; Bravi, R.; Fackler, J. P., Jr.; Galassi, R; Grant, T. A.; Omary, M. A; Pietroni, B. R.; Staples, R. J. *Inorg. Chem.* **2000**, *39*, 3158. (b) Burini, A.; Fackler J. P., Jr.; Galassi, R.; Grant, T. A.; Omary, M. A.; Rawashdeh-Omary, M. A; Pietroni, B. R.; Staples, R. J. *J. Am. Chem. Soc.* **2000**, *122*, 11264. (c) Rawashdeh-Omary, M. A.; Omary, M. A.; Fackler, J. P., Jr.; Galassi, R.; Pietroni, B. R.; Burini, A. *J. Am. Chem. Soc.* **2001**, *123*, 9689; d) Burini, A.; Fackler, J. P., Jr.; Galassi, R.; Pietroni, B. R.; Staples, R. J. *J. Chem. Soc., Chem. Commun.* **1998**, 95.
5. Yang, G.; Raptis, R. G. *Inorg. Chem.* **2003**, *42*, 261.
6. (a) Enomoto, M.; Kishimura, A.; Aida, T. *J. Am. Chem. Soc.* **2001**, *123*, 5608. (b) Kishimura, A.; Yamashita, T.; Aida, T. *J. Am. Chem. Soc.* **2005**, *127*, 179.
7. (a) Omary, M. A.; Kassab, R. M.; Haneline, M. R.; Elbjeirami, O.; Gabbaï, F. P. *Inorg. Chem.*, **2003**, *42*, 2176. (b) Haneline, M. R.; Tsunoda, M.; Gabbaï, F. P. *J. Am. Chem. Soc.* **2002**, *124*, 3737. (c) Burress, C.; Elbjeirami, O.; Omary, M. A.; Gabbaï, F. P. *J. Am. Chem. Soc.* **2005**, *127*, 12166. (d) Tsunoda, M.; Gabbaï, F. P. *J. Am. Chem. Soc.* **2000**, *122*, 8335.
8. (a) Mohamed, A. A.; Rawashdeh-Omary, M. A.; Omary, M. A.; Fackler, J. P., Jr. *Dalton Trans.* **2005**, 2597. (b) Elbjeirami, O.; Rashdan, M. D.; Nesterov, V.; Rawashdeh-Omary, M. A., *Dalton Trans.* **2010**, *39*, 9465-9468.
9. (a) Dias, H. V. R.; Diyabalanage, H. V. K.; Rawashdeh-Omary, M. A.; Franzman, M. A.; Omary, M. A. *J. Am. Chem. Soc.* **2003**, *125*, 12072. (b) Dias, H. V. R.; Diyabalanage, H. V. K.; Eldabaja,

M. G.; Elbjeirami, O.; Rawashdeh-Omary, M. A.; Omary, M. A. *J. Am. Chem. Soc.* **2005**, *127*, 7489.

10. Vaughan, L. G. *J. Am. Chem. Soc.* **1970**, *92*, 730.

11. (a) La Monica, G.; Ardizzoia, G. A. *Prog. Inorg. Chem.* (Ed. K. D. Kenneth) WILEY & Sons, Weinheim **1997**, *46*, 152. (b) Viciano-Chumillas, M.; Tanase, S.; Jos de Jongh, L.; Reedijk, J. *Eur. J. Inorg. Chem.* **2010**, *3403*. (c) Klingelea, J.; Decherta, S.; Meyer, F. *Coord. Chem. Rev.* **2009**, *253*, 2698. (d) Halcrow, M. A.; Dalton Trans. **2009**, *2059*. (e) Miras, H. N.; Chakraborty, I.; Raptis, R. G. *Chem. Commun.* **2010**, *46*, 2569.

12. (a) Masciocchi, N.; Moret, M.; Cairati, P.; Sironi, A.; Ardizzoia, G. A.; La Monica, G. *J. Am. Chem. Soc.* **1994**, *116*, 7668. (b) Büchner, E. *Chem. Ber.* **1889**, *22*, 842. (c) Barberà, J.; Lantero, I.; Moyano, S.; Luis Serrano, J.; Elduque, A.; Giménez, R. *Chem. Eur. J.* **2010**, *16*, 14545.

13. (a) Nomiya, K.; Tsuda, K.; Tanabe, Y.; Nagano, H. *J. Inorg. Biochem.* **1998**, *69*, 9. (b) Bonati, F.; Burini, A.; Pietroni, B. R.; Giorgini, E. *Inorg. Chim. Acta* **1987**, *137*, 81. (c) Bovio, B.; Bonati, F.; Burini, A. Pietroni, B. R. *Zeitschrift. Naturforschung, teil B: Anorganische Chemie.* **1984**, *39B*, 1747.

14. (a) Ardizzoia, G. A.; Brenna, S.; Castelli, F.; Galli, S.; La Monica, G.; Masciocchi, N.; Maspero, A. *Polyhedron* **2004**, *23*, 3063. (b) Masciocchi, N.; Moret, M.; Cairati, P.; Sironi, A.; Ardizzoia, G. A.; La Monica, G. *J. Chem. Soc., Dalton Trans.* **1995**, *1671*.

15. 1 (a) Kolks, G.; Lippard, S. J.; Waszczak, J. V.; Lilenthal, H. R. *J. Am. Chem. Soc.* **1982**, *104*, 717. (b) Bonati, F.; Burini, A.; Pietroni, B. R.; Bovio, B. *J. Organomet. Chem.* **1989**, *375*, 147.

16. Buchner, E. *Chem. Ber.* **1889**, *22*, 2163.

17. Raptis, R. G.; Fackler, J. P., Jr. *Inorg. Chem.* **1988**, *27*, 4179.

18. Ehlert, M. K.; Retting, S. J.; Storr, A.; Thompson, R. C.; Trotter, J. *Can. J. Chem.* **1992**, *70*, 2161.

19. Ehlert, M. K.; Retting, S. J.; Storr, A.; Thompson, R. C.; Trotter, J. *Can. J. Chem.* **1990**, *68*, 1444.

20. Dias, H. V. R.; Polach, S. A.; Wang, Z. *J. Fluorine Chem.* **2000**, *103*, 163.

21. Hou, L.; Shi, W.-J.; Wang, Y.-Y.; Wang, H.-H.; Cui, L.; Chen, P.-X.; Shi, Q.-Z. *Inorg. Chem.* **2011**, *50*, 261.

22. Zhan, S-Z.; Jiang, X.; Zheng, J.; Huang, X-D.; Chena, G-H.; Li, D. *Dalton Trans.*, **2018**, *47*, 3679.

23. Angaridis, P. A.; Baran, P.; Boca, R.; Cervantes-Lee, F.; Haase, W.; Mezei, G.; Raptis, R. G.; Werner, R. *Inorg. Chem.* **2002**, *41*, 2219.

24. (a) Boca, R.; Dlháň, L.; Mezei, G.; Ortiz-Pérez, T.; Raptis, R. G.; Telser, J. *Inorg. Chem.* **2003**, *42*, 5801. (b) Mezei, G.; Rivera-Carrillo, M.; Raptis, R. G. *Inorg. Chim. Acta* **2004**, *357*, 3721.

25. Angaroni, M.; Ardizzoia, G. A.; Beringhelli, T.; La Monica, G.; Gatteschi, D.; Masciocchi, N.; Moret, M. *J. Chem. Soc. Dalton Trans.* **1990**, *3305*.

26. Casarin, M.; Corvaja, C.; di Nicola, C.; Falcomer, D.; Franco, L.; Monari, M.; Pandolfo, L.; Pettinari, C.; Piccinelli, F.; Tagliatesta, P. *Inorg. Chem.* **2004**, *43*, 5865.

27. Ehlert, M. K., Rettig, S. J.; Storr, A. Thompson, R. C., Trotter J. *Can. J. Chem.* **1992**, *70*, 2161.

28. Ardizzoia, G. A.; Cenini, S.; La Monica, G.; Masciocchi, N.; Maspero, A.; Moret, M. *Inorg. Chem.* **1998**, *37*, 17, 4284-4292

29. Pandolfo, L.; Pettinari, C. *CrystEngComm*, **2017**, *19*, 1701.

30. Murray, H. H.; Raptis, R. G.; Fackler, J. P., Jr. *Inorg. Chem.* **1988**, *27*, 26.

31. Mohamed, A. A.; Perez, L. M.; Fackler, J. P., Jr. *Inorg. Chim. Acta* **2005**, *358*, 1657.

32. Yamada, S.; Ishida, T.; Nogami, T. *Dalton Trans.* **2004**, 898.

33. Dias, H. V. R.; Diyabalanage, H. V. K. *Polyhedron* **2006**, *25*, 1655.

34. Dias, H. V. R.; Gamage, C. S. P.; Keltner, J.; Diyabalanage, H. V. K.; Omari, I.; Eyobo, Y.; Dias, N. R.; Roehr, N.; McKinney, L.; Poth, T. *Inorg. Chem.* **2007**, *46*, 2979.

35. Chi, Y.; Lay, E.; Chou, T.-Y.; Song, Yi.-H.; Carty, A. J. *Chem. Vap. Deposit.* **2005**, *11*, 206.

36. Galassi, R.; Ricci, S.; Burini, A.; Macchioni, A.; Rocchigiani, L.; Marmottini, F.; Tekarli, S. M.; Nesterov, V. N., Omary, M. A. *Inorg. Chem.*, **2013**, *52*, 14124.

37. a) Dias, H. V. R.; Singh, S., Campana, C. F. *Inorg. Chem.* **2008**, *47*, 3943. b) Yang, C.; Wang, X.; Omary, M. A. *J. Am. Chem. Soc.* **2007**, *129*, 15454. c) Yang, C.; Arvapally, R. K. ; Tekarli, S. M.; Salazar, G. A.; Elbjeirami, O., Wang, X.; Omary, M. A. *Angew. Chem., Int. Ed.*, **2015**, *54*, 4842.

38. Hettiarachchi, C. V.; Rawashdeh-Omary, M. A.; Korir, D.; Kohistani, J.; Yousufuddin, M.; Dias, H. V. R. *Inorg. Chem.* **2013**, *52*, 13576.

39. Minghetti, G.; Bonati, F.; Massobrio, M. F. *Inorg. Chem.* **1975**, *14*, 1974.

40. Bovio, B.; Bonati, F.; Banditelli, G. *Inorg. Chim. Acta* **1984**, *87*, 25.

41. a) Barbera, J.; Elduque, A.; Gimenez, R.; Oro, L. A.; Serrano, J. L. *Angew. Chem., Int. Ed. Engl.* **1996**, *35*, 2832. Barbera, J.; b) Elduque, A.; Gimenez, R.; Lahoz, F. J.; Oro, L. A.; Serrano, J. L. *Inorg. Chem.* **1998**, *37*, 2960.

42. (a) Kim, S. J.; Kang, S. H.; Park, K.-M.; Kim, H.; Zin, W.-C.; Choi, M.-G.; Kim, K. *Chem. Mater.* **1998**, *10*, 1889. (b) Torralba, M. C.; Ovejero, P.; Mayoral, J. M.; Cano, M.C.; Campo, J. A.; Heras, J. V.; Pinilla, E.; Torres, M. R. *Helv. Chim. Acta* **2004**, *87*, 250.

43. Bonati, F.; Minghetti, G. *Angew. Chem., Int. Edit.* **1972**, *11*, 429.

44. McDougald, R. N.; Chilukuri, B.; Jia, H.; Perez, M. R.; Rabaâ, H.; Wang, X.; Nesterov, V. N.; Cundari, T. R.; Gnade, B. E.; Omary, M. A. *Inorg. Chem.* **2014**, *53*, 7485.

45. Yang, C.; Messerschmidt, M.; Coppens, P.; Omary, M. A. *Inorg. Chem.* **2006**, *45*, 6592.

46. a) Balch, A. L.; Doonan, D. J. *J. Organomet. Chem.* **1977**, *131*, 137. (b) Minghetti, G.; Banditelli, G.; Bonati, F. *Inorg. Chem.* **1979**, *18*, 658. (c) Raptis, R. G.; Fackler, J. P., Jr. *Inorg. Chem.* **1990**, *29*, 5003. (d) Bonati, F.; Burini, A.; Pietroni, B. R.; Bovio, B. *J. Organomet. Chem.* **1991**, *408*, 271. (e) Raptis, R. G.; Murray, H. H.; Fackler, J. P., Jr. *Acta Crystallogr. C.* **1988**, *44*, 970. (f) Bovio, B.; Burini, A.; Pietroni, B. R. *J. Organomet. Chem.* **1993**, *452*, 287. (g) Vickery, J. C.; Balch, A. L. *Inorg. Chem.* **1997**, *36*, 5978.

47. Burini, A.; Pietroni, B. R.; Bovio, B.; Calogero, S.; Wagner, F. E. *J. Organomet. Chem.* **1994**, *470*, 275.

48. a) Mohamed, A. A.; Ricci, S.; Burini, A.; Galassi, R.; Santini, C.; Chiarella, G. M.; Melgarejo, D. Y.; Fackler, J. P., Jr. *Inorg. Chem.* **2011**, *50*, 1014. b) Mohamed, A. A.; Burini, A.; Galassi, R.; Paglialunga, D.; Galán-Mascarós, J.-R.; Dunbar, K. R.; Fackler, J. P., Jr. *Inorg. Chem.* **2007**, *46*, 2348.

49. Dias, H. V. R.; Diyabalanage, H. V. K.; Gamage C. S. P. *Chem. Commun.*, **2005**, 1619-1621

50. Almotawa, R. M., Aljomaih, G.; Trujillo, D. V. ; Nesterov, V. N.; Rawashdeh-Omary; M. A. *Inorg. Chem.* **2018**, *57*, 9962.

51. Strelnik, I. D.; DayanovaIlya, I. R.; Kolesnikov, R. E. R. Fayzullin, I. A.; Litvinov, A.; Samigullina I.; Gerasimova, T. P.; Katsyuba S. A. Musina. E. I.; Karasik, A. A. *Inorg. Chem.* **2019**, *58*, 1048.

52. Xiao, Q.; Zheng, J.; Li, M.; Shun-Ze, Z.; Wang, J-H.; Li D. *Inorg. Chem.* **2014**, *53*, 11604.

53. Parasar, D. Almotawa, R. M.; Jayaratna, N. B.; Ceylan, Y. S.; Cundari, T. R., Omary, M. A.; Dias H. V. R. *Organometallics* **2018**, *37*, 4105-4118

54. (a) Omary, M. A.; Rawashdeh-Omary, M. A.; Gonser, M. W. A.; Elbjeirami, O.; Grimes, T.; Cundari, T. R.; Diyabalanage, H. V. K.; Gamage, C. S. P.; Dias, H. V. R. *Inorg. Chem.* **2005**, *44*, 8200. (b) Zhang, J.-X.; He, J.; Yin, Y.-G.; Hu, M.-H.; Li, D.; Huang, X.-C. *Inorg. Chem.* **2008**, *47*, 3471. (c) He, J.; Yin, Y.-G.; Wu, T.; Li, D.; Huang, X.-C. *Chem. Commun.* **2006**, 2845. (d) Dias, H. V. R.; Gamage, C. S. P. *Angew. Chem., Int. Ed.* **2007**, *46*, 2192. (e) Ovejero, P.; Mayoral, M. J.; Cano, M.; Lagunas, M.C. *J. Organomet. Chem.* **2007**, *692*, 1690. f) Omary, M. A.; Elbjeirami, O.; Gamage, C. S. P.; Sherma, K. M.; Dias, H. V. R. *Inorg Chem.* **2009**, *48*, 1784.

55. Tekarli, S. M.; Cundari, T. R.; Omary, M. A. *J. Am. Chem. Soc.* **2008**, *130*, 1669.

56. Dias, H.V. R.; Gamage C. S. P. *Angew Chem* **2007**, *119*, 2242-2244.

57. Jayaratna, N.B.; Olmstead, M.M., Kharisov, B.I.; Dias, H.V. *Inorg Chem.* **2016**, *55*, 8277-80.

58. Dias, H.V.; Singh, S.; Campana, C.F.. *Inorg Chem.* **2008**, *47*, 3943.

59. Yang, C.; Arvapally. R. K.; Tekarli; S.; Gustavo, A.; Salazar, M; Elbjeirami, O.; Wang, X.; Omary, M. A. *Angew Chem. Int. Ed.* **2015**, *54*, 4842.

60. Burini, A.; Fackler, J. P. Jr., Galassi, R.; Macchioni, A.; Omary, M. A.; Rawashdeh-Omary, M. A., Pietroni, B. R.; Sabatini, S.; Zuccaccia, C. *J. Am. Chem. Soc.* **2002**, *124*, 4570.

61. Mohamed, A. A.; Galassi, R.; Papa, F.; Burini, A.; Fackler, J. P. Jr. *Inorg. Chem.* **2006**, *45*, 7770.

62. Galassi, R.; Ghimire, M. M.; Otten, B. M.; Ricci, S.; McDougald Jr., R. N.; Almotawa, R. M.; Alhmoud, D.; Ivy, J. F.; Rawashdeh, A.-M. M.; Nesterov, V. N.; Reinheimer, E. W.; Danield, L. M.; Burini, A.; Omary, M. A. *PNAS*, **2017**, E5042.

63. Cotton, F.A., Walton, R.A. *Multiple Bonds Between Metal Atoms* **1982**, Wiley, New York

64. Rawashdeh-Omary, M. A. *Comm. Inorg. Chem.* **2012**, *33*, 88.

65. White-Morris, R. L.; Olmstead, M. M.; Jia, H.; Attar, S.; Balch, A. L. *Inorg. Chem.* **2005**, *44*, 5021.

66. Winkler, K.; Wysocka-Zołopa, M.; Rec'ko, K.; Dobrzyn'ski, L.; Vickery, J. C.; Balch, A.L. *Inorg. Chem.* **2009**, *48*, 1551-1558